ABSTRACT

Title of Dissertaion: **Role of ubiquitination in *Caenorhabditis elegans* development and transcription regulation during spermatogenesis**

Madhura Kulkarni, Doctor of Philosophy, 2008

Dissertation Directed by: Dr. Harold Smith
Center for Advanced Research in Biotechnology

Regulation of gene function can be achieved through a variety of mechanisms. In this dissertation, I present the genetic and molecular characterization of two genes involved in two distinct mechanisms of control. Each gene was initially identified by its functional role in sperm development in the model organism *Caenorhabditis elegans*. The first gene, *uba-1*, is an essential enzyme involved in protein turnover through ubiquitin-mediated proteolysis. A temperature-sensitive allele, *(uba-1)it129*^{ts}, was isolated in a classical genetic screen for mutations that cause sperm-specific sterility. The second gene, *spe-44*, encodes a putative transcription factor. Its identification by microarray screening for sperm-enriched genes led to the cytological analysis of the deletion allele *spe-44(ok1400)*, by reverse genetics approach.

it129^{ts} encodes a conditional allele of *uba-1*, the sole E1 ubiquitin-activating enzyme in *C. elegans*. E1 functions at the apex of the ubiquitin-mediated conjugation pathway, and its activity is necessary for all subsequent steps in the reaction.

Ubiquitin is covalently conjugated to various target proteins. Poly-ubiquitination typically results in target protein degradation, which provides an essential mechanism for the dynamic control of protein levels. Homozygous mutants of *uba-1(it129)* manifest pleiotropic phenotypes, and include novel roles for ubiquitination in sperm fertility, control of body size, and sex-specific development. We propose a model whereby proteins normally targeted for proteasomal degradation instead persist in *uba-1(it129^{ts})* and impair critical cellular processes.

The second gene, *spe-44*, was identified as a putative sperm gene regulator in *C. elegans* based on its up-regulated expression during spermatogenesis and its significant sequence homology to the DNA-binding SAND domain. Genetic analysis of a deletion allele of *spe-44(1400)* has revealed its functional role during sperm development. Cytological analysis of *spe-44(ok1400)* showed developmental arrest of spermatocytes prior to spermatid differentiation. *spe-44* mRNA is expressed in a narrow spatial and temporal window, just prior to spermatocyte differentiation, consistent with its functional role during spermatogenesis. Future study will be directed to find putative targets of *spe-44* and the mechanisms that regulate gene expression using microarray analysis and yeast-one hybrid screens. These studies will help to understand transcriptional regulatory aspects of spermatogenesis in *C. elegans*.

ROLE OF UBIQUITINATION IN *CAENORHABDITIS ELEGANS* DEVELOPMENT AND TRANSCRIPTION REGULATION DURING SPERMATOGENESIS

By

MADHURA KULKARNI

Dissertation Submitted to the Faculty of the Graduate School of the
University of Maryland, College Park, in Partial Fulfillment
of the Requirements for the Degree of
Doctor of Philosophy
2008

Advisory Committee:

Professor Stephen Mount, Chair
Professor Harold Smith
Professor Eric Haag
Professor Caren Chang
Professor Jonathan Dinman
Professor Douglas Julin

To

My Parents and Gurus

PREFACE

Declaration of author's intent to use own previously published text.

The main text, tables, figures and figure legends in their entirety for:

Chapter 2: E1 ubiquitin-activating enzyme UBA-1 plays multiple roles throughout *C. elegans* development

were used, and only modified to meet the formatting requirements of this dissertation. Full citation is given below:

Madhura Kulkarni and Harold Smith. E1 ubiquitin-activating enzyme plays multiple roles throughout *C. elegans* development. *PLoS Genetics*. 2008. Jul 18;4(7):e1000131

ACKNOWLEDGEMENTS

I express my profound gratitude to my advisor Dr. Harold Smith, whose guidance and constant encouragement have been a great source of inspiration in my professional life. I consider myself fortunate to have had an opportunity to work with him.

My sincere thanks to Dr. Stephen Mount, for being the chair of my dissertation advisory committee and the constant support throughout. I also would like to thank my committee members Dr. Douglas Julin, Dr. Caren Chang. Dr. Jonathan Dinman and Dr. Eric Haag for their suggestions and critical evaluation of the work throughout the duration of my graduate study.

I particularly acknowledge Dr. Todd Cooke, the ex-Graduate Director of the Department of Cell Biology and Molecular Genetics, for allowing me to work in Center for Advanced Research in Biotechnology. I'll also like to thank Dr. Zhongchi Liu, without whose support I couldn't have been in this graduate program.

I thank my lab members Dr. Daya Jirage, Dr. Antonio Del Castillo, Dr. Arun Subramanian, Sara Hapip, and Carina Nhe for their substantial contributions in terms of discussions, critique, development of the experiments, comments on my scientific writing, and encouragement during my graduate work.

The worm club members at NIH, UMBC and JHU and the worm meetings have been very helpful to keep a steady direction for my research. I need to thank especially Dr. Kevin O'Connell, Dr. Andy Golden, and Dr. Chris Richie at NIH for their valuable time during my visits to NIH for the use of their facilities.

CARB is a unique place, which provided me a very comfortable environment during the last four years. I would like to thank everyone who made me feel at home, with the specific mention of the third floor group, Dr. Zvi Kelman, Dr. Jim Ames, Jae-Ho, Gun-Young, Jennifer, Jayanti, Alexandra and Larik. I appreciate the third floor meetings for the insightful discussions and comments and regular potlucks.

I express my gratitude towards all my friends who have been part of my life in different eras during my (five year long) graduate journey. It's impossible to mention how each one of them has been important during this time. Nozomi, Rajesh, Aswani, Supratik and Tushar deserve special mention. I would like to thank my roommates Sudeshna, Uma, Sankalita, Deena, Brian, Manish and Bob for being my home away from home.

All these people will always be part of my enumerable memories from graduate school.

I take this opportunity to say how immensely grateful I am to my parents Suneeta and Dattatraya, my sister Mrunal and my fiancé Vikash, for their motivation, love and emotional support throughout.

Madhura D Kulkarni

TABLE OF CONTENTS

LIST OF TABLES

LIST OF FIGURES

Chapter 1 Regulation of gene expression in *C. elegans* development

1.1 Introduction

Development of a multicellular eukaryotic organism occurs through growth and differentiation from a single cell, the zygote. During maturation it differentiates into many cell types, each with specifically allocated function. The diversity of cell types and the co-ordination of function are determined by the differential expression of genes within each cell type. Thus, proper development depends on the precise temporal and spatial control for the differential expression of thousands of genes.

Each cell expresses only a subset of the genes from the genome. For example, muscle cells express about 7-10% (~1500) of the total genes (~19800) in *C. elegans* (Kim at al., 2001; Roy et al., 2002). Thus, at any given time, only a fraction of the genome is expressed in a cell. Because of the efforts of genome sequencing, we know the gene database for most of the eukaryotic model organisms. Yet, how the differential expression of these genes in individual cell types is regulated at a precise time and in response to environmental cues is still unclear.

Significant amounts of research effort have been directed in the past few decades towards understanding the process of gene regulation. The expression begins when a gene is transcribed into mRNA, and ends when a functional protein product is no longer needed. The studies done so far reveal that the gene function is regulated at every

possible step i.e. transcription, post-transcription (e.g. splicing), translation, post-translation (e.g. phosphorylation) and epigenetic (e.g. chromatin level).

The first level of control for any gene to be transcribed is the chromatin structure, which determines the accessibility of the DNA at a particular locus for transcription initiation. Chromatin structure is determined by various post-translational modifications of histone proteins. For example, DNA methylation is one of these factors associated with transcription repression reviewed in (Miranda and Jones, 2007).

Transcription regulation is one of the most extensively studied modes of regulation for gene expression. The regulation is achieved by one or more transcriptional activator or repressor proteins, which bind to the promoter region of the gene in a sequence-specific manner. The characteristic pattern of gene expression for a particular cell type is determined by a specific set of transcription factors contained in that cell. The activity of the transcription factor itself is controlled by co-factors and signaling molecules. How transcription is regulated will be discussed in more detail in the next section.

Once a gene is transcribed into a pre-mRNA, it is processed by RNA splicing to remove the non-coding intronic sequences. In higher eukaryotic organisms, along with the introns, alternative exons can be selected preferentially leading to more than one splice variant of a transcript. About 10% of the genes in *C. elegans* undergo alternative splicing (Kim et al., 2007a). This process of alternative splicing provides a post-transcriptional regulation for gene function. Different isoforms translated from the alternative splice variants can have tissue-specific or different sub-cellular localization, or varied kinetic performances.

A mature mRNA is regulated via untranslated regions (UTR) in the 3' and 5' regions called 3'UTR and 5'UTR, respectively. These UTRs play roles in the transport, localization, and stability of the mRNA. Significance of the spatial pattern of mRNA localization during development is well documented for *Drosophila* embryogenesis. Specific localization of mRNAs like *Oskar*, *Vasa* and *Tudor* is essential for the establishment of the primordial germ cells in the *Drosophila* embryo (reviewed in Williamson and Lehmann, 1996). AREs, AU-rich elements in the 3' UTR, play a role in stabilizing the mRNAs through recruitment of RNA-binding proteins. This stabilization can be crucial for proper development; for example, differentiation of the nervous system in *Drosophila* is achieved by stabilizing the gene *gcm* (glial cells missing) (Soustelle et al., 2008).

The sequences in the UTRs are also employed to regulate the initiation of translation from the mRNA. As mentioned earlier, *Oskar* mRNA is not translated unless it reaches the desired localization. Before its proper localization, translation is inhibited by Bruno protein, which binds to the Bruno response element in the 3'UTR of Oskar mRNA (Snee et al., 2008). The polyadenylated [poly(A)] tail at the 3' end of mRNA is also known to control translation initiation of respective RNAs. Cytoplasmic polyadenylation element binding (CPEB) protein, which binds to Cytoplasmic Polyadenylation Element (CPE), can either repress translation by binding to inhibitors or can activate translation by extending the length of the poly(A) tail (Pique et al., 2008). CPEB has been shown to be essential in various processes like germ cell development (Setoyama et al., 2007), cell division (Luitjens et al., 2000) and synaptic plasticity (reviewed in Richter, 2007). Poly(A) tail length at the 3' end of mRNA also controls the

stability of the transcript. Poly(A) tail longer than 30 As stabilizes mRNA by blocking the assembly of exonucleases involved in RNA degradation (Ford et al., 1997). The recently recognized world of small, non-coding RNAs reveal new dimensions for regulation of gene expression via RNA silencing and translation repression as reviewed by Kim, 2005.

After translation, the protein itself is subjected to regulation of its function via various post-translational modifications. There are nearly 200 different types of post-translational modifications of proteins known, which create one to two-fold diversity in the proteome compared to the genome of the organism (Walsh et al., 2005). Covalent modifications of the side chains in proteins by phosphorylation, acylation or glycosylation can regulate cellular localization and functional aspects (e.g. kinetic properties) of the proteins. For example, dual phosphorylation of MAP kinases increases their catalytic efficiency by 10^5-fold. Some of the post-translational modifications provide an 'on' or 'off' switch for the signal transduction cascade as in the classic example of the *RAS* signaling pathway involved in various functions during cellular development (reviewed by Campbell et al., 1998). *RAS* proteins belong to the superfamily of monomeric GTPases and are biologically active only when they have a farnesyl lipid modification. The lipid modification is required to anchor the protein in the membrane and to relay the switch to the downstream cascade of cytoplasmic kinases.

To achieve precise spatio-temporal regulation of gene function, the duration for which a protein remains functional in the cellular system needs to be monitored. Inactivation of the protein product once it is no longer needed, is critical for proper development. A specific type of post-translational modification is devoted to degradation

of the protein after its function is fulfilled. Covalent conjugation of ubiquitin, a 76 amino acid peptide, to the target protein marks it for degradation via the 26S proteasome. The process of ubiquitination of the target protein itself is a highly regulated enzymatic cascade as discussed in detail in section 1.3.

The regulation of gene function is further refined by the cross-talk between and within different modes of regulation. Understanding these events not only provides insights into fundamental mechanisms of gene function regulation, but also can lead to answers for curing various diseases caused by mis-regulation. The next sections will discuss transcriptional regulation and ubiquitin conjugation of proteins with respect to *C. elegans* development.

1.2 Transcriptional regulation of gene expression

The importance of regulation of gene expression in controlling the developmental programs of an organism is well appreciated. The precise pattern of gene expression determines specific developmental decisions. During development, commitment to a specific fate followed by a determined differentiation program is achieved through an interdependent network of transcription factors.

All genes require the basic transcriptional machinery known as general transcription factors (GTFs) and the spatio-temporal regulation of activation and/or repression of a gene is exerted through gene-specific factors. Eukaryotic GTF includes the RNA Polymerase II (Pol II), TBP (TATA-box binding protein) and TAFs (TBP associated factors). The role of TBP is to bind the core promoter, and TAFs assist TBP in this process (reviewed in Lee and Young, 1998).

Factors that relay the gene-specific signal to GTFs are called mediators. Generally, a specific mediator functions in a specific developmental pathway to coordinate gene-specific factors with GTFs. Mediator proteins are functionally and structurally conserved in eukaryotes and many of them have been identified in the *C. elegans* genome (Bourbon et al., 2004). For example, *med-15* functions in association with *sbp-1*, a member of the SREBP (sterol regulatory element binding protein) family of transcription activators and it is required for fatty acid homeostasis in *C. elegans* (Yang et al., 2006). Thus, mediator proteins serve an important function of integrating the regulatory signal to the basic transcription machinery as they can interact with both GTFs and gene-specific transcription factors.

The focus of this section will be on gene-specific transcriptional regulation. Many mutations have been studied so far which affect early development of invertebrates and metazoans. The majority of these mutations are encoded in transcription factors, emphasizing their importance in establishing cell commitment and pattern formation. *C. elegans* is a simple model system that has provided valuable insights into the field of transcription regulation. In *C. elegans*, 934 of the total ~ 20,000 genes encode putative transcription factors (TFs) (Reece-Hoyes et al., 2005). Recent progress in high-throughput technologies like microarray analysis and yeast-one hybrid screening is helping to understand the intricate network of these transcription factors and their target genes in the specification of tissue differentiation (Dupuy et al., 2007; Vermeirssen et al., 2007).

In *C. elegans*, transcription is silenced at the global level during oogenesis before oocytes begin maturation. Global silencing is achieved by regulating the phosphorylation

status of the carboxy-terminus domain (CTD) of the large subunit of RNA polymerase II (Seydoux and Braun, 2006; Walker et al., 2007). Oocyte maturation signals the release of transcriptional block, which aids rapid gene activation after fertilization in the zygote (Walker et. al., 2007). The transcriptional block occurs at a step after initiation but before transcription elongation. Transcription resumes in the zygote after fertilization at the four-cell stage during embryogenesis (Baugh et al., 2003; Seydoux and Fire, 1994). This transcription restart occurs only in the cells of the somatic lineage, while transcription in the germline lineage is delayed until the 100-cell stage (Martinho et al., 2004; Mello et al., 1996; Seydoux and Dunn, 1997).

Extended transcriptional silencing in the germline lineage cells is maintained by the maternally supplied protein PIE-1 (Ghosh and Seydoux, 2008; Mello et al., 1996; Seydoux et al., 1996). PIE-1 encodes a putative RNA-binding protein with two CCCH zinc-finger motifs and has been shown to repress transcription in mammalian cell culture experiments (Batchelder et al., 1999). PIE-1 inhibits transcription by competing with P-TEFb, a kinase subunit which phosporylates CTD, thus blocking transcriptional elongation (Zhang et al., 2003). *pie-1* null mutation leads to embryonic lethality due to precocious release of transcription suppression in the germline cells, which as a result adopt the somatic fate (Mello et. al., 1996). When the embryo reaches the 100-cell stage, PIE-1 levels drop in germline cells (Mello et. al., 1996) due to the action of *emb-4* via an unknown mechanism (Checchi and Kelly, 2006). Thus, the commitment of cell lineage for somatic or germline fate is determined by temporal regulation of the global transcription restart in the embryo.

1.2.1 Transcription networks for epidermal and muscle specification in *C. elegans*

As mentioned earlier, high-throughput techniques like microarray and yeast-one hybrid make it easier to study gene expression at the global level and to decipher the link between specific transcription factors and the set of target genes. RNAi knockdown of genes in *C. elegans* provides an advantageous system to validate functional significance of these targets and transcription cascades in a context of fate determination or pattern formation. A recently published study that revealed a multi-step cascade of gene activation and the interplay between the networks of transcription factors in distinguishing the cell fate of C blastomere descendents in *C. elegans* development (Yanai et al., 2008), is a very good example of these high-throughput regulation analyses.

C. elegans embryogenesis and subsequent development is a characteristic example of invariant cell lineage with a fixed pattern of cell divisions and a fixed developmental program defined for every daughter cell (Sulston et al., 1983). Through a series of asymmetric cell divisions, a founder cell population with each cell specified for a distinct lineage is generated by the 8-cell stage in the embryo. As shown in Figure 1-1, the AB lineage produces hypodermis, neurons, anterior pharynx and other cell types; MS produces the somatic gonad, muscle, the majority of the pharynx, neurons and gland cells; E produces all intestine; C produces muscle, hypodermis and neurons; D produces muscle; and the P4 cell is the germ-line precursor (Gönczy and Rose, 2005).

The C blastomere, which further differentiates into muscle, hypodermis and neuronal fates, is specified by the expression of *pal-1*, a caudal homeoprotein (Hunter and Kenyon, 1996). In the absence of maternal PAL-1 activity, the C blastomere does not

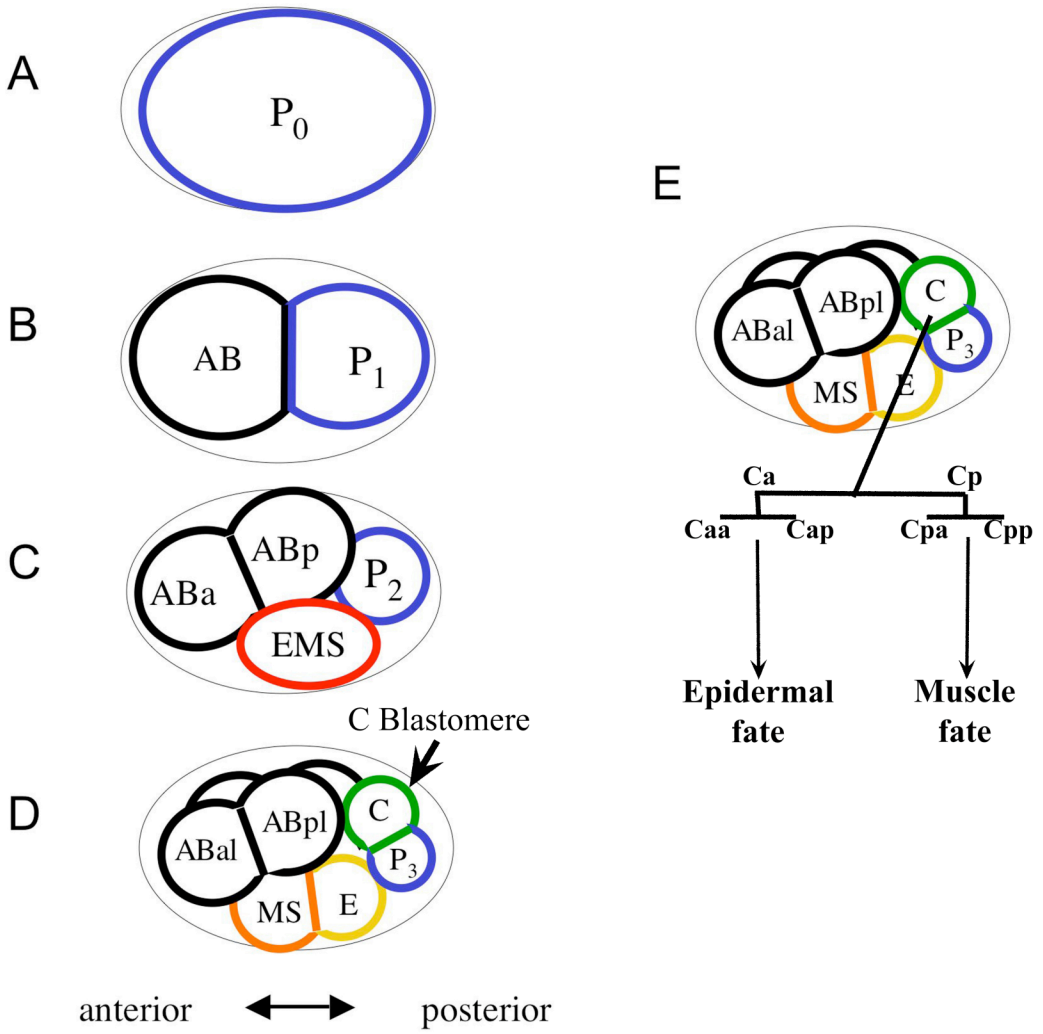

Figure 1-1: **Specification of C lineage.**

The C blastomere is born at the eight-cell embryonic stage (A-D) and divides asymmetrically to produce muscle cells and epidermal cells (E). (Figure modified from Gönczy and Rose, 2005).

develop into these fates, while ectopic *pal-1* translation causes other founder cells to produce muscle, epidermal and neuronal cells (Draper et al., 1996; Hunter and Kenyon, 1996). Initial microarray analysis for *pal-1* targets revealed 308 candidate targets (Baugh et al., 2005). Functional annotations of these targets indicated 13 putative transcription factors representing many families, including homeodomain, zinc-finger, GATA, MADS domain, bHLH and T-box proteins. So many diverse transcription factors amongst the targets of PAL-1 suggested that *pal-1* controls a transcriptional regulatory network (Baugh et al., 2005). Further, RNAi followed by microarray analysis and reporter gene expression of *pal-1* targets and putative transcription factors indicated two sub-networks of transcription regulators arranged in topological order (Yanai et. al., 2008). The interesting finding was that these two sub-networks compete with each other to specify either muscle or epidermal cell fate.

Epidermal cell fate is induced by *elt-1*, a GATA transcription factor necessary and sufficient for determining epidermal fate (Gilleard et al., 1999). Its expression is activated by *pal-1* in the epidermal lineage of C blastomere (Baugh et al, 2005). *elt-1* in turn activates expression of downstream transcription factors *elt-3*, *lin-26* and *nhr-25* (Baugh et al., 2005; Gilleard et al., 1999; Labouesse et al., 1996; Page et al., 1997). *elt-1* itself is temporally regulated, as its expression peaks during the earlier stages of epidermal fate determination and is reduced later (Baugh et al., 2003). RNAi of *elt-1* reduced target gene expression, consistent with the genetic studies, but RNAi of any of these three target genes elevated the expression of *elt-1* and the rest of the targets (Yanai et. al., 2008). Thus, the target transcription factors impart a negative feedback on their common activator, generating a transcriptional network for epidermal fate determination. This

topology of expression suggests that epidermal specification occurs via a two-step process, with a negative feedback loop.

Unlike epidermal fate, muscle fate is specified by three transcription factors; *hlh-1*, *hnd-1* and *unc-120* (Baugh et al., 2005; Fukushige et al., 2006). Out of 81 total body wall muscles, 32 are born from the C lineage, and the rest are born from the AB, MS and D lineages (Sulston et al., 1983). *hlh-1* is shown to be essential for muscle fate specification irrespective of the lineage (Krause et al., 1994). Its activation is regulated by different factors in distinct cell lineages and *pal-1* regulates its activation only in C and D cell lineages.

The three transcription factors mentioned above, *hlh-1*, *hnd-1* and *unc-120,* act redundantly in muscle specification based on genetic studies. They seem to activate each other's expression as shown by RNAi (Yanai et. al. 2008). RNAi of *hlh-1* reduces the expression of *hnd-1* and *unc-120*. RNAi of *hnd-1* or *unc-120* reduces the expression of each other, but both increase the mRNA levels of *hlh-1*, indicating negative feedback loop similar to the one observed during epidermal fate determination.

As summarized in Figure 1-2 these two networks of transcription regulators are initiated from the same cell lineage, yet specify a distinct cell fate. This distinction is achieved by antagonistic action of epidermal and muscle transcription networks on each other (Yanai et al., 2008). RNAi of any of the three muscle TFs resulted in increased expression of all four epidermal TFs, suggesting that the muscle network represses the epidermal network of transcription factors. Yeast-one hybrid analysis with the *elt-1* promoter showed that 10 out of 13 transcription factors bound the promoter, indicating that the muscle network of transcription factors directly

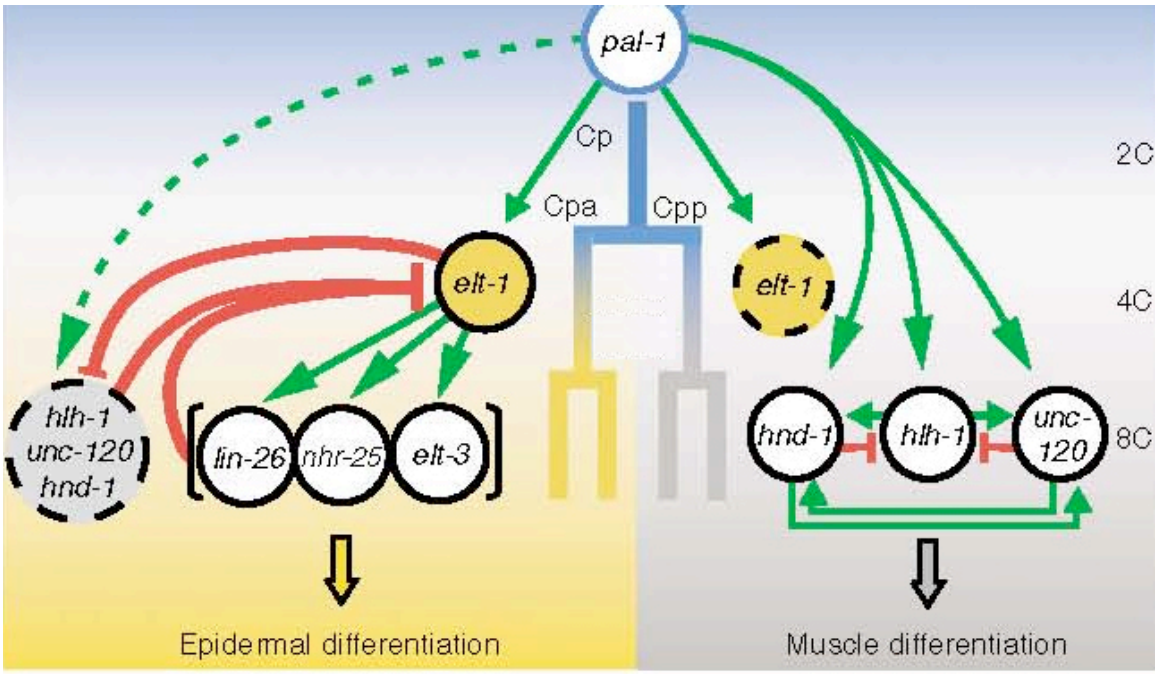

Figure 1-2: **A Cartoon of the C lineage transcriptional network.**
PAL-1 initiates C blastomere development, inducing first *elt-1* such that ELT-1 is present in all cells at the 4-cell (4C) stage embryo. At 8-cell (8C) stage, ELT-1 induces the second stage epidermal TFs and represses the muscle TF network. In the posterior daughter cell, ELT-1 expression is not maintained and all three muscle TFs are expressed, which suppress *elt-1* expression (Modified from Yanai et al., 2008).

regulates *elt-1* expression. Similar and reciprocal increase in the expression levels of muscle transcription factors was observed in *elt-1* RNAi. During development, the C blastomere expresses muscle transcription factors and *elt-1* expression in the epidermal daughter cell is essential to suppress the muscle fate (Yanai et. al., 2008).

1.2.2 Transcription regulation in *C. elegans* sex determination

C. elegans exists as two naturally occurring sexes, hermaphrodite (with two copies of the X chromosome) and male (with one copy of the X chromosome). The hermaphrodite is somatically female but produces male gametes (sperm) for a short period of time. Both sexes exhibit numerous sex-specific differences in the body plan. About 40% of male and 30% of hermaphrodite cells are sexually specialized and lead to extensive sexual dimorphism in *C. elegans* (Sulston and Horvitz, 1977). These sex-specific differences are orchestrated by differential expression of genes throughout development, as identified by the microarray analysis of global expression levels in two sexes (Jiang et al., 2001).

The master regulator, TRA-1, defines the differential expression in a sex-specific manner. It encodes a GLI family transcription factor with zinc fingers and its mRNA is expressed at similar levels in both the sexes of *C. elegans* (Zarkower and Hodgkin, 1992). Its function is required to initiate hermaphrodite fate and to suppress male fate in a tissue-specific manner. Differential accumulation of TRA-1 protein leads to distinct sexual fates as shown by Schvarzstein and Spence (2006). This differential accumulation of TRA-1 is achieved via sex-specific proteolysis regulated by intricate control of the sex-determination pathway, which is elaborated in the next section on ubiquitination

(Figure 1-6). In this section, I'll discuss its function as a global transcriptional regulator in directing sexually dimorphic development in a tissue-specific manner (Summarized in Figure 1-3).

The hermaphrodite-specific neurons (HSNs) are required for proper egg-laying behavior of hermaphrodites. They are born embryonically in both hermaphrodites and males but are retained only in hermaphrodites during the course of differentiation. The HSNs are not needed in males and undergo programmed cell death during embryonic development (Sulston and Horvitz 1977, Sulston 1983). The cell death is induced by pre-apoptotic gene *egl-1*, which encodes a protein with a BH3 domain known as cell death activator (Conradt and Horvitz, 1998). *egl-1* is directly repressed in hermaphrodites by TRA-1 (Conradt and Horvitz, 1999). As TRA-1 activity is reduced in males, *egl-1* repression is released, inducing male-specific cell death of HSNs.

Another class of neurons that show sexually-dimorphic programmed cell death in *C. elegans* is the cephalic male neuron (CEM). The CEM neurons die during hermaphrodite embryogenesis but survive in males (Sulston et al., 1983). These neurons are essential for males to respond to the hermaphrodite pheromone (Chasnov et al., 2007). Survival of CEMs in males is regulated by *ceh-30*, an anti-apoptotic Bar-homeodomain transcription factor (Schwartz and Horvitz, 2007). Sex-specific expression of *ceh-30* is directly regulated by TRA-1 as it represses *ceh-30* in hermaphrodites thereby allowing CEM death (Schwartz and Horvitz, 2007).

A homolog of DM domain transcription factors in *C. elegans*, MAB-3, promotes development of male-specific organs and male mating behavior (Shen and Hodgkin, 1988; Yi et al., 2000). For example, in development of V rays, a sensory organ required

for male mating, *mab-3* promotes activation of bHLH transcription factor *lin-32* by preventing expression of the Hes family transcription factor *ref-1* specifically in males (Ross et al., 2005). *mab-3* is also required to suppress the vitellogenin gene *vit-2* in male intestine. Thus, *mab-3* primarily appears to function at the apex of the transcriptional regulatory cascade as a repressor during male specific development. *mab-3* is a target of TRA-1 as TRA-1 inhibits *mab-3* expression in hermaphrodites thus suppressing male-specific development (Yi et al., 2000).

Along with the somatic sexual fate, TRA-1 is also required for germline sexual fate determination. The male germline continues spermatogenesis throughout its life while the hermaphrodite germline temporarily produces male gametes during L4 larval stage. In somatic tissue, TRA-1 acts as female fate-inducing factor by suppressing male-specific gene expression. Genetic studies indicate that TRA-1 activity is essential in the germline for both oogenic and spermatogenic fate determination. So far, the only known direct target of TRA-1 in specifying the germline fate is *fog-3* (Chen and Ellis, 2000). *fog-3* encodes a Tob homolog, and along with *fog-1* promotes spermatogenesis in both sexes. Both have been proposed to act as terminal regulators for sperm fate decision (Barton and Kimble, 1990; Ellis and Kimble, 1995). TRA-1 promotes oogenesis in adult hermaphrodites by transcriptional repression of *fog-1* and *fog-3* (Chen and Ellis, 2000; Jin et al., 2001; Lamont and Kimble, 2007). But TRA-1 also sustains continued spermatogenesis in males and in L4 stage hermaphrodites (Hodgkin, 1986; Hodgkin and Brenner, 1977; Kimble, 1988), most likely by positively regulating *fog-3* under special

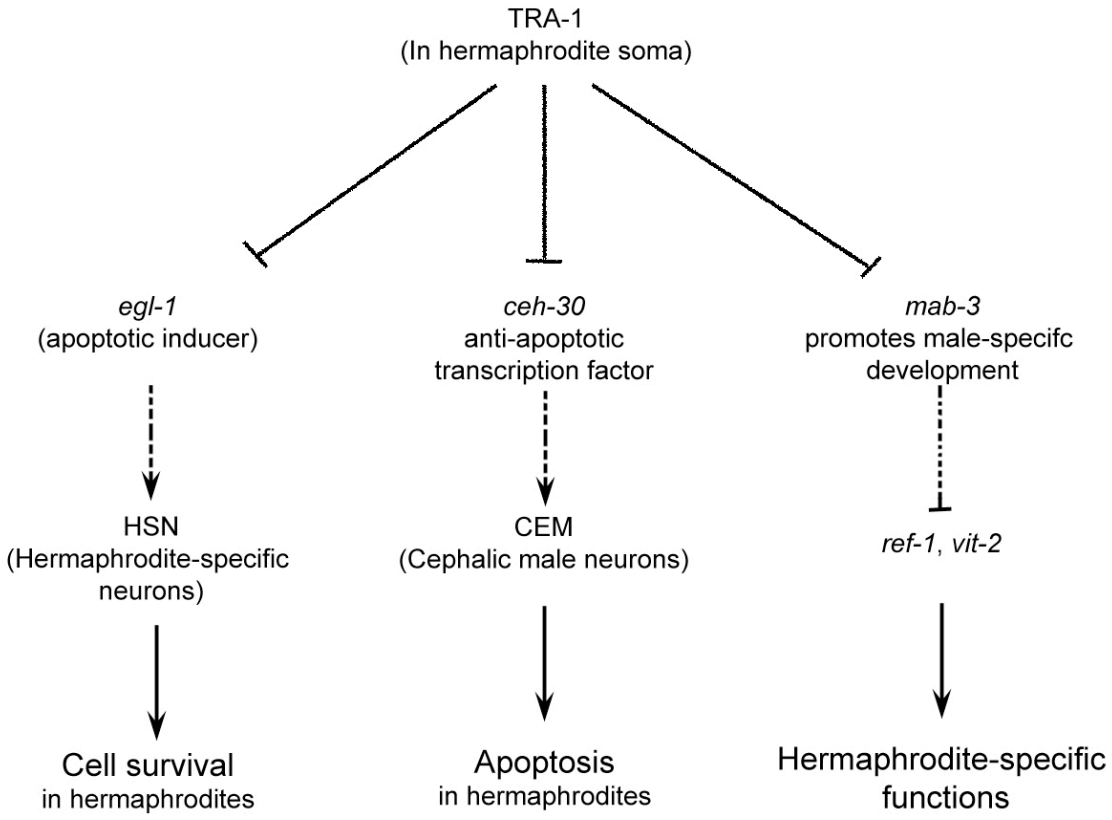

Figure 1-3: Schematic representation of cell-specific regulation of sexual fate by TRA-1.

TRA-1, a GLI family transcription factor, regulates sexually dimorphic development in a tissue-specific manner mainly by repressing male-specific target genes in the hermaphrodite soma.

circumstances (Chen & Ellis, 2000). No downstream targets of *fog-3* and *fog-1* are known as yet, and how these two genes bring about sperm differentiation is still an open question. In chapter III, I present the study of one of the putative transcription regulators that acts downstream of sperm-fate determination and is essential for sperm differentiation.

Even though transcriptional regulatory activity of TRA-1 is well established, very few direct downstream targets of TRA-1 have been identified. Sex-specific microarray experiments done by Jiang et al., (2001) identified 1,651 genes enriched in males and 520 genes enriched in hermaphrodites out of the total of 18,967 genes. These sex-regulated genes include 37 that encode putative transcription factors. Twenty-three of these mRNAs that encode sex-regulated transcription factors are enriched in hermaphrodites, and fourteen are enriched in males. Three of these 37 putative transcription factors are shown to be direct targets of TRA-1 (Jiang et. al., 2001). This set of 37 putative transcription factors could be direct or indirect targets of TRA-1 and could constitute the regulatory network that controls sexually dimorphic gene expression patterns, which needs to be studied further.

1.3 Ubiquitin conjugation as gene regulatory mechanism

Ubiquitin mediated degradation of TRA-1 has been identified recently as a critical mechanism for controlling its activity (see below). Ubiquitin, a 76 amino acid peptide, is conjugated to various proteins via a cascade of enzymatic reactions. Post-translational modification of proteins by ubiquitin conjugation regulates gene function mainly by controlling protein turnover mediated by a multisubunit 26S proteasomal complex

(Hershko and Ciechanover, 1998). More recently, ubiquitination has also been shown to regulate protein activity and their spatial sorting. Ubiquitin conjugation plays an essential role in cell fate determination and organismal development. Aberrant ubiquitin conjugation has been associated with various cell cycle defects, developmental diseases and neuropathologies (Ardley and Robinson, 2004; Nakayama and Nakayama, 2006).

Ubiquitin is translated as three different precursors: a polymeric head-to-tail concatemer (polyubiquitin) and two N-terminal fusion proteins with ribosomal polypeptides UbL40 and UbS27 (Nenoi et al., 2000). Although more variations of ubiquitin encoding exist (Catic and Ploegh, 2005), these three are the most conserved genes amongst phyla. Also, the number of polyubiquitin-encoding loci and the number of coding repeats found in the gene varies from species to species (Ozkaynak et al., 1984; Wiborg et al., 1985).

The concentration of free ubiquitin moieties in the cell is of critical importance and is monitored by regulating transcription from the polyubiquitin gene and release of ubiquitin monomers after degradation of the polyubiquitin tag from the conjugated proteins. This ubiquitin homeostasis is essential for cell survival and proper function of the proteasome, as failure to do so can lead to defects from meiotic arrest (Okazaki et al., 2000) to various diseases (Hanna et al., 2007).

The polyubiquitin gene produces the precursor polypeptide polyubiquitin. This unprocessed polyubiquitin chain has an additional amino acid residue at its C-terminus in the last ubiquitin moiety, which prevents its activation and hence conjugation to the target protein (Ozkaynak, et al., 1984). The polyubiquitin precursor is then processed by de-ubiquitinating enzyme to release monomeric ubiquitins (Johnston et al., 1999).

Regulation at both the transcriptional step and the processing step can control the availability of free ubiquitin monomers, thus maintaining homeostasis.

The monomeric ubiquitin has a Gly-Gly sequence at the C terminus, which then is activated by ubiquitin-activating enzyme. It is an ATP-dependent process carried out by the ubiquitin-activating enzyme (E1) in two steps: 1) adenylation of the C terminus of ubiquitin polypeptide through the hydrolysis of ATP, and 2) the transfer of this ubiquitin to a conserved cysteine residue within E1. As a result, ubiquitin gets covalently attached to the cysteine via a thioester linkage, generating ubiquityl-S-E1 (Haas and Rose, 1982).

The activated ubiquitin is then transferred to ubiquitin-conjugating enzyme, E2, via energy-neutral trans-esterification (Ciechanover et al., 1982; Pickart and Rose, 1985). The E2 enzyme then transfers the ubiquitin moiety to the substrate protein either directly or with an additional step of an E3 ubiquitin ligase, a process referred to as ubiquitination of the target protein. Ubiquitination of the substrate leads to branched-protein conjugates in which the C-terminal glycine residue of ubiquitin is linked by an isopeptide bond to a specific internal lysine residue (acceptor lysine) (Ciechanover and Schwartz, 1989; Hershko, 1991; Reiss et al., 1989). Multiple rounds of this cascade of enzymatic reactions lead to a polyubiquitin tag on the target protein. The majority of substrates conjugated with ubiquitin are subjected to proteolysis via the 26S proteasome (reviewed in Hershko, 1991; Jentsch, 1992; Rechsteiner, 1987). Thus, post-translational modification with ubiquitin mainly regulates half-life of the substrate protein.

Ubiquitin has seven lysine residues - K_6, K_{11}, K_{27}, K_{29}, K_{33}, K_{48} and K_{63}. Polyubiquitin chains built up on distinct lysine linkages differ in their structural and functional information. Regioselectivity for specific lysine residue of ubiquitin as an

acceptor site for the first covalent attachment to a substrate depends on the ubiquitin-conjugating enzyme, E3, and the nature of the substrate. K_{48} and K_{63} are the best-characterized residues involved in polyubiquitylation (Haglund and Dikic, 2005). A polyubiquitin chain of at least four ubiquitin molecules at K_{48} is sufficient to target a conjugated substrate for proteasomal degradation (Thrower et al., 2000). In contrast, K_{63} linkage is involved in non-proteolytic functions like regulation of cellular processes such as DNA repair, signal transduction, intracellular trafficking, and ribosomal biogenesis (Chan and Hill, 2001).

Recently, novel non-canonical functions of K_{48} and K_{63} linkages have been discovered (reviewed in Li and Ye, 2008). Met4 activates expression of genes in the methionine biosynthetic pathway in *S. cerevisiae*. Its transcriptional activity is regulated by polyubiquitination via K_{48} but in non-proteolytic fashion (Kaiser et al., 2000). Similarly, canonically K_{63} linkage is involved in non-proteolytic functions, but it has also been implicated to target substrates for proteasomal degradation (Li and Ye, 2008).

Unlike K_{48} and K_{63} linkages, which have been studied extensively, very little is known about the biological significance of other ubiquitin linkages. For example, Deltex, an E3 ligase involved in the Notch signalling pathway, itself gets polyubiquitinated by another E3 ligase, AIP4 via K_{29} likage and is then targeted for lysosomal degradation (Chastagner et al., 2006). AMPK-related kinases regulate cell polarity and proliferation. NUAK1 and MARK4 are members of this family and are regulated via K_{29}/K_{33}-linked polyubiquitin chains (Al-Hakim et al., 2008). Recent studies also report mixed ubiquitin

chains that contain more than one type of ubiquitin linkage within a single polymer (Ben-Saadon et al., 2006; Kim et al., 2007b).

Apart from the polyubiquitin tag, the E1-E2-E3 enzymatic cascade also regulates monoubiquitination and multiple monoubiquitinations of the target protein. The addition of a single ubiquitin to a substrate is referred as monoubiquitination (Reveiwed in Hicke, 2001). It plays a regulatory role in the endocytosis of plasma membrane proteins, DNA repair, histone modification and transcriptional regulation (Hicke, 2001). When multiple lysine residues in the substrate are conjugated to monoubiquitin moieties it is referred as multiple monoubiquitination (Haglund et al., 2003).

1.3.1 Enzymes involved in ubiquitin-conjugation

The enzymes involved in the ubiquitin-conjugation are described in detail from the bottom of the cascade. The substrate selectivity and type of ubiquitin linkage is determined by an E3 ubiquitin ligase. The E3s are a large, diverse group of proteins defined by different characteristic motifs. The majority of them can be grouped in two categories, the RING (really interesting new gene) class and the HECT (homologous to E6-associated protein C-terminus) class (reviewed in Jentsch et al. 1992). RING E3s function as mediators between E2 and the substrate. They interact with both simultaneously, bringing the substrate lysine in close proximity to the reactive ubiquitin-E2 thioester bond and facilitating the transfer of the active ubiquitin. Thus, RING E3s work as adaptors and do not possess catalytic activity. These RING E3s can work as stand-alone adaptors like Mdm2 or in huge complexes like APC, the anaphase-promoting complex. HECT E3s have a catalytic function. The ubiquitin is first transferred from the

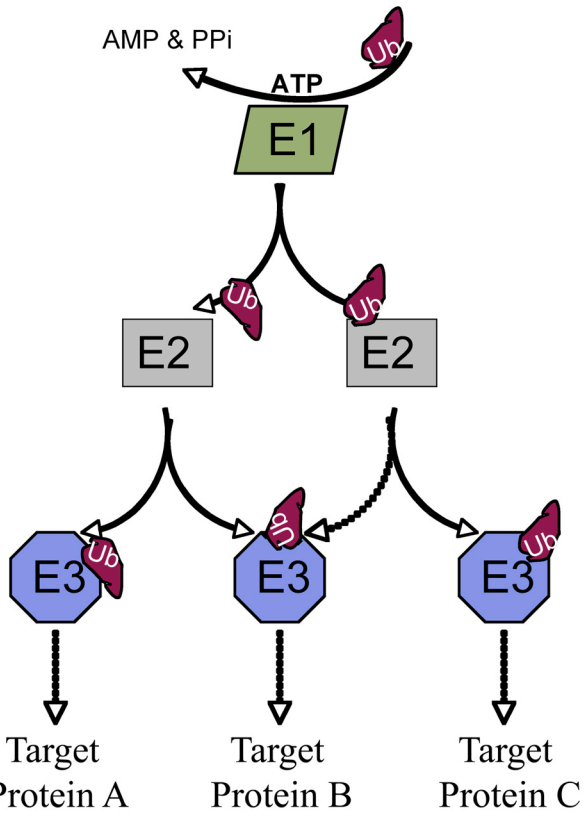

Figure 1-4: Schematic representation of ubiquitin-conjugation pathway.
Ubiquitin-activating enzyme (E1) activates ubiquitin in ATP-dependent reaction. E1 interacts with multiple ubiquitin-conjugation enzymes (E2s) to transfer the activated ubiquitin-thiolester. E2 can transfer the ubiquitin to multiple ubiquitin ligases (E3s) which then ubiquitinate specific target proteins.

E2 to an active-site cysteine in the conserved HECT domain of the E3. The thioester-linked ubiquitin is then transferred to substrate from E3 (Scheffner et al., 1995). HECTs play important roles in disease-related pathways like TGF-β signaling and p53 regulation (reviewed in Kee and Huibregtse, 2007).

Ubiquitin conjugation enzymes (UBCs) known as E2s, function at the intermediate step of the ubiquitination cascade, transferring activated ubiquitin from E1 to either E3 or directly to a substrate with the help of an E3. Recent studies suggest that E2 interacts with E1 and E3 in mutually exclusive fashion, such that E1 must be dissociated after ubiquityl transfer before E2 can bind a specific E3 (Eletr et al., 2005; Huang et al., 2005). All known E2 enzymes have a conserved 16Kd UBC domain. This domain contains a centrally located cysteine residue essential for ubiquitin-thiolester formation (Sung et al., 1991).

The cascade of ubiquitin conjugation through a series of enzymes is driven by the differential affinities of the E1-E2 and E2-E3 enzymes towards each other in ubiquitin-linked and ubiquitin-unlinked state. Ubiquitin-thioestered E1 has higher affinity for free E2. Once the E2 is coupled to ubiquitin, E1 looses its affinity for ubiquitin linked E2 (Hershko et al., 1983; Pickart and Rose, 1985). Similar affinity variations have been demonstrated for E2-E3 interactions (Kawakami et al., 2001; Siepmann et al., 2003).

Ubiquitin-dependent regulation of protein activity and degradation is an essential function of development and survival of an eukaryotic system. Vast numbers of substrate proteins are regulated by ubiquitin conjugation, and they are involved in diverse processes like DNA repair, cell cycle progression, transcriptional regulation, receptor-mediated signaling pathways, and stress response (Petroski and Deshaies, 2005;

Weissman, 2001). The diversity is achieved by ubiquitin ligases with their remarkably specialized substrate recognition, and there are over 100 different E3s known in various eukaryotic systems (Hicke et al., 2005). E2s are encoded by relatively lower number of proteins; for example, the *S. cerevisiae* genome encodes 13 UBCs while the human genome contains 30 putative UBCs (Scheffner et al., 1998).

1.3.2 Ubiquitin activating enzyme (E1), at the apex of the ubiquitin-conjugation pathway

In contrast to E3s and E2s, there is typically only one E1 protein, which serves the ubiquitin-activating function. Exceptions include an additional spermatogeneis-specific E1 in rodents, marsupials and human testis (Kay et al., 1991; Mitchell et al., 1992; Zhu et al., 2004) and multiple E1s encoded in plant genomes (Hatfield et al., 1997; Hatfield and Vierstra, 1992). The E1 enzyme contains signature motifs, two UBACT domains for ubiquitin activation and one or two Thif domains. The cysteine residue upstream of the UBACT domain is the most conserved residue as it is essential for covalent attachment of ubiquitin (Hatfield et al., 1992). Multiple forms of E1 protein have been detected in animals and plants (Cook and Chock, 1992; Hatfield et al., 1997). These different isoforms have been shown to vary in their post-translational modifications and sub-cellular localization (Trausch et al., 1993). For example, the human E1 gene encodes two isoforms, E1a of 117KDa size and E1b of 110KDa size (Cook and Chock, 1992; Cook and Chock, 1995; Handley-Gearhart et al., 1994). Only the E1a isoform is shown to be dynamically phosophorylated in human cell lines (Stephen et al., 1996), and phosophorylated E1a isoform predominantly localizes in the nucleus during G2 phase of

cell cycle (Stephen et al., 1997). Quantitative distribution studies in the nucleus and the cytosol of HeLa cells suggested that the concentration of functional E1 (presumably the phosphorylated form) is the rate-limiting step for ubiquitin conjugation in the nucleus (Stephen et al., 1997).

Although more than one isoform of E1 exists, there is essentially one functional E1 in the system. Thus, the complexity of ubiquitin conjugation realized at the level of E3 function narrows down to the single enzyme, E1, essential for ubiquitin activation. As the first enzyme in the pathway, E1 has the potential to regulate the rate of ubiquitin conjugation (Hatfield et al., 1990; Stephen et al., 1996). Blocking the E1 function can collapse the entire downstream ubiquitin conjugation cascade, as has been demonstrated in different species by various temperature-sensitive alleles of E1. Genetic studies in the yeast *S. cerevisiae* have revealed that inactivation of the yeast E1 gene, *Uba1,* blocks most of the ubiquitin conjugation (Ghaboosi and Deshaies, 2007; McGrath et al., 1991; Swanson and Hochstrasser, 2000). Chapter II of this dissertation also reports that a hypomorphic allele of *uba-1* in *C. elegans* dramatically reduces the amount of ubiquitin conjugates globally in total protein extracts (Kulkarni et al., 2008).

Since functional aberrations in E1 activity affect all possible ubiquitin conjugation reactions, conditional mutations in E1 have turned out to be extremely useful in uncovering and understanding ubiquitin-dependent functions. Mammalian cell lines containing temperature-sensitive alleles of E1 have revealed its functional role in cell cycle progression and ubiquitin-mediated proteolysis (Ciechanover et al., 1984; Ciechanover et al., 1985; Finley et al., 1984; Kulka et al., 1988; Salvat et al., 2000). A conditional E1 mutant in *S. cerevisiae* has helped elucidate the mechanism of

polyubiquitin chain recognition by proteasomal components (Ghaboosi and Deshaies, 2007). Studies with weak and strong E1 alleles in *Drosophila* show opposing effects on cell survival, revealing complexities of the ubiquitin conjugation pathway ((Lee et al., 2008). In that study, partial loss of ubiquitin conjugation caused by weak *Uba1* alleles inhibited cell death, while strong *Uba1* alleles showed high apoptotic activity. At the same time, the strong allele induced neighboring cell proliferation in non-autonomous manner due to failure to downregulate Notch signaling (Lee et al., 2008).

1.3.3 Ubiquitin-like (Ubl) modifiers and cross-talk between ubiquitin and Ubl conjugation systems

Along with ubiquitin, there is family of ubiquitin-like modifiers (Ubls), which are conjugated to target proteins in a similar E1-E2-E3 conjugation cascade. A series of Ubls (e.g. SUMO, NEDD8, UCRP, FAT10, HUB, Fau, APG12, URM1, ISG15, Atg8) are emerging from recent studies. Some of them share sequence homology with ubiquitin but the majority of them have similar 3D topology, called the β-grasp fold (reviewed by Hochstrasser, 2000; Jentsch and Pyrowolakis, 2000; Kerscher et al., 2006). They function as critical regulators of distinct cellular processes like transcription, DNA repair, signal transduction, autophagy, and cell-cycle, but via non-proteolytic mechanisms except for FAT10 (Reviewed in Kerscher et al., 2006; Schwartz and Hochstrasser, 2003).

Each of these Ubls has a dedicated E1 and E2 for its activation and conjugation as reviewed in Kerscher et. al., (2006). So far it had been thought that conjugation of distinct Ubls occurs through parallel and non-identical enzymatic cascades. But in last few years, emerging cross-talk between the components of distinct

Ubl's machinery is challenging this concept. For example, a common E2, UbcH8, is involved in conjugation of two distinct polypeptides; ISG15 and ubiquitin. The E1 enzyme transfers ubiquitin onto UbcH8, whereas the Ube1L/E1ISG15 transfers ISG15 onto UbcH8 (Zhao et al., 2004). Another example of crosstalk is Atg8 and Atg12, which are involved in autophagosome formation. Both share a single E1, Atg7, but each Ubl uses a distinct E2 (Ichimura et al., 2000). SUMO-1, 2, and 3 also share a common E1, a heterodimer of AOS1-UBA2 (Johnson, 2004). UBA6, an E1, ubiquitin-activating enzyme-like protein, is shown to activate both ubiquitin and FAT10 (Chiu et al., 2007). Even more interestingly, it transfers conjugated ubiquitin only to a specific subset of E2s, to Ubc5 and Ubc13 but not to Ubc3 and E2-25K (Chiu et al., 2007). Thus, ubiquitin-activating enzyme is not the sole activator of ubiquitin and this finding increases the complexity of ubiquitin-mediated regulation.

1.3.4 Ubiquitination in *C. elegans* development

As in other eukaryotic organisms, ubiquitin-mediated protein regulation plays important roles in multiple aspects of *C. elegans* development. Detailed lists of the known and putative components of the ubiquitin conjugation pathway are well summarized by Kipreos (2005) and by Jones et al., (2002). The *C. elegans* genome has two ubiquitin loci; *ubq*-1, a polyubiquitin locus (Graham et al., 1989), and *ubq-2*, which encodes ubiquitin fused to the L40 ribosomal large subunit protein (Jones and Candido, 1993). The *ubq-1* locus encodes 11 tandem repeats of ubiquitin as an 838 amino acid polypeptide. The genome encodes over 600 putative E3s, 22 E2s, three E2 variants without the critical catalytic cysteine, one E1, and four E1-like proteins. More than the

list of the factors, functional aspects of ubiquitin-conjugation pathway in *C. elegans* development will be discussed further.

Knock down by RNAi of *uba-1,* which encodes the sole E1 ubiquitin-activating enzyme, leads to severe phenotypes. The treated worms die earlier than wild type without producing any fertilized embryos (Jones et al., 2001). This emphasizes that ubiquitin conjugation is essential for progeny formation and functions through adult maintenance. The conditional allele of *uba-1*, reported in this dissertation, also points towards the same conclusion based on the various diverse roles uncovered in the mutant worms (chapter II and Kulkarni et al., 2008).

Only four of the 22 UBCs, *let-70* (*ubc-2*), *ubc-9*, *ubc-12* and *ubc-14,* play essential roles during early embryonic development as shown by RNAi experiments and by elevated expression in microarray experiments (Jones et al., 2001). Depletion of *ubc-20* by RNAi brings developmental arrest at the L3 larval stage, indicating its functional necessity during larval development (Jones et al., 2001). RNAi depletion of the rest of the UBCs individually does not impair any aspect of *C. elegans* development (Jones et al., 2001). This observation is most likely due to the fact that E3s can interact with more than one E2; thus, E2s could be serving redundant functions in specific developmental pathways. This notion is also implicated in yeast-two hybrid studies for interactions within the ubiquitin conjugation system of *C. elegans* (Gudgen et al., 2004).

Involvement of ubiquitin-mediated regulation in individual developmental aspects of *C. elegans* is dissected through studies of the terminal E3 ligases. Although not all predicted E3s have been studied at the genetic or biochemical level, a number of them are known to regulate various developmental roles, as reviewed in WormBook (Kipreos,

2005). Recent studies have uncovered E3s playing functional roles in aging (Li W et al., 2007), synaptic signaling and plasticity (Schaefer and Rongo, 2006; Teng and Tang, 2005), endoplasmic reticulum-associated degradation (Sasagawa et al., 2007), and sex determination (Jager et al., 2004; Starostina et al., 2007) in *C. elegans*.

1.3.5 Ubiquitination role in polarity establishment in early embryo

The role of ubiquitin-mediated degradation is evident from the first cell division of the zygote. The posterior cell generated after the first asymmetric division of the zygote is dedicated for germline, whereas the anterior cell specifies somatic fate. The asymmetry is determined and established by multiple protein and RNA factors. CCCH finger-encoding proteins, like PIE-1, POS-1 and MEX-1 bind RNA, and are known to segregate preferentially to the germline cell during the first cell division (Guedes and Priess, 1997; Tenenhaus et al., 1998). The restriction of these CCCH finger proteins to the germline lineage requires their degradation in somatic lineage cells. Degradation specifically in the somatic lineage is mediated by a zinc finger-interacting protein, ZIF-1 (DeRenzo et al., 2003). ZIF-1 acts as a substrate recruitment factor and regulates PIE-1, POS-1 and MEX-1 degradation via CUL-2-containing E3 ligase (DeRenzo et al., 2003).

The anaphase-promoting complex (APC), a multi-subunit E3 ligase, is involved in germline proliferation, cell cycle progression in early embryo, and formation of the hermaphrodite vulva and male tail of *C. elegans* (Shakes et al., 2003). Its role in the metaphase-to-anaphase transition of meiosis I in *C. elegans* is very well characterized. The APC has been shown to poly-ubiquitinate securin, the inhibitory partner of separase (Cohen-Fix et al., 1996; Funabiki et al., 1996). Once securin is degraded, separase is

relieved from the inhibition. Active separase then proteolytically cleaves cohesin, a protein that holds sister chromatids together, so that the sister chromatids can be pulled to opposing spindle poles (Buonomo et al., 2000; Nasmyth et al., 2000). Thus, the metaphase-to-anaphase transition is mediated by APC action. When any one of the subunits of APC is depleted either by RNAi or a genetic mutation, the affected embryos show a cell cycle block in metaphase of meiosis I or delayed progression through meiosis (Davis et al., 2002; Furuta et al., 2000; Golden et al., 2000; Kitagawa et al., 2002; Shakes et al., 2003). Sex determination of *C. elegans* is also regulated by ubiquitination as will be discussed in detail in the following section.

1.4 Interplay between transcriptional regulation and ubiquitin-mediated regulation

Gene function is regulated at multiple levels as discussed in the introduction. These modes of regulation do not function as stand-alone mechanisms, but they in turn regulate each other's function to create an intricate network for controlling gene expression. For example, monoubiquitination of histone H2A is required for methylation of histone H3, which relieves transcriptional repression in that locus (Kim et al., 2008). This intricate connectivity of different regulatory modes makes the eukaryotic system able to respond to the finest changes in its intra- and extra-cellular environments. Recent studies reveal the interplay between ubiquitination and transcription in regulating various developmental aspects of *C. elegans* development.

1.4.1 Interplay during the development of an early embryo of *C. elegans*

Spatial asymmetry in the early embryo of *C. elegans* is generated through interplay between ubiquitination and transcription. The single-celled *C. elegans* zygote divides asymmetrically to produce two blastomeres, each with distinct developmental potential. SKN-1, a transcription factor required for mesoendoderm specification, is one of the first proteins to be asymmetrically localized in the embryo (Bowerman et al., 1993; Bowerman et al., 1992). The protein accumulates in the posterior cell at 2-cell stage but not in the anterior sister cell. This asymmetry becomes more pronounced at the 4-cell stage. The protein is completely degraded from the embryo as it reaches the 8-cell stage (Bowerman et al., 1993). SKN-1 regulates the expression of mesoderm-determining genes like *med-1* in the anterior EMS blastomere (Maduro et al., 2001; Tenlen et al., 2006). *efl*-1, a transcription factor analogous to mammalian E2F, indirectly controls transcription of SKN-1. A HECT domain containing ubiquitin-ligase, EEL-1, targets SKN-1 for degradation in the posterior cell at 2-cell stage, thus controlling its persistence in very narrow spatial window. But, EFL-1 and EEL-1 together regulate the spatial and temporal expression pattern of SKN-1. Deletion of both of these factors eliminates SKN-1 asymmetry at the 2 and 4-cell stages, and the protein can be detected until the 28-cell stage (Page et al., 2007).

1.4.2 Interplay during sex determination of *C. elegans*

The sex determination program is one of the pathways well-studied at the molecular level. It integrates the ubiquitin-mediated regulation at TRA-1, the global

transcription regulator of sex-specific differentiation. *C. elegans* develops either as XX hermaphrodite or as XO male (Madl and Herman, 1979). The X-to-autosome (X:A) ratio determines the expression levels of transcription regulators such as *sex-1* (a nuclear hormone receptor) and *ceh-39* (a ONECUT homeodomain protein), which are encoded on the X chromosome (Gladden and Meyer, 2007), and a T-box transcription factor *sea-1* encoded on an autosome (Powell et al., 2005). These transcription factors together regulate the expression of the gene *xol-1* (XO lethal) (Figure 1-5), which integrates two downstream pathways: dosage compensation and sex determination (Luz et al., 2003).

xol-1 in-turn regulates the complex of transcription factors SDC (*sdc-1*, *sdc-2*, *sdc-3*), essential to repress *her-1* expression in hermaphrodites (Perry et al., 1993; Zarkower, 2006). The *her-1* gene encodes a secreted protein, which is a primary sex-determining signal. It promotes male development by inhibiting the function of a transmembrane protein TRA-2 (Hunter and Wood, 1992). TRA-2, together with proteins FEM-1, 2 and 3, regulate the activity of TRA-1, the terminal transcription factor in the sex-determination cascade. TRA-1 then brings about sex-specific differentiation through downstream targets as discussed in the previous section (1.2.2).

TRA-1 promotes female fate by suppressing transcription of male-specific genes in the hermaphrodite. TRA-1 is expressed in both the sexes and is primarily localized in the nucleus (Segal et al., 2001). But the overall TRA-1 levels are higher in hermaphrodites compared to males, implying that TRA-1 is regulated at the post-translational level (Schvarzstein and Spence, 2006). Recent studies report that TRA-1 protein is downregulated by a CUL-2-based E3 complex via ubiquitin-mediated

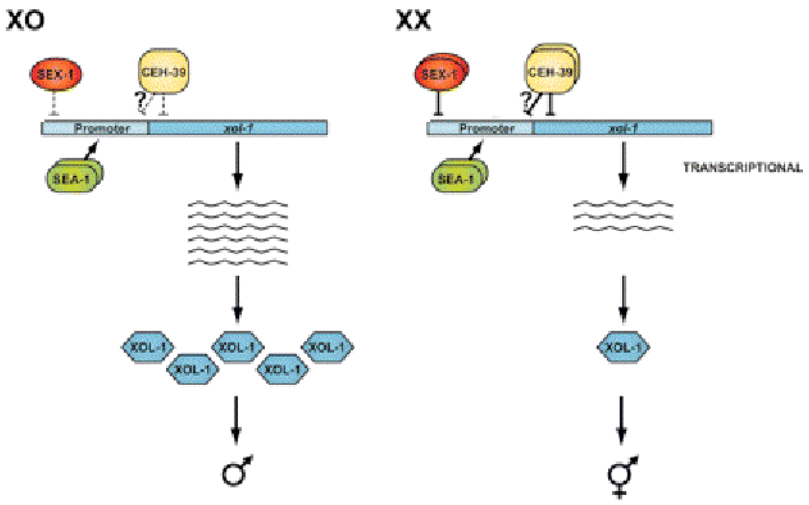

Figure 1-5: Sex-specific regulation of *xol-1*.

xol-1 integrates both X and autosomal components to determine sexual fate. The molecular diagram indicates that CEH-39 and SEX-1 (nuclear hormone receptor) act to repress *xol-1*, whereas SEA-1 (T-box protein) functions to activate *xol-1*. In XX worms, X-encoded factors out-compete to inactivate *xol-1*, but in XO animals, auotosomal factors outcompete to activate *xol-1*. The high level of XOL-1 protein present in XO animals then induces the male fate whereas the lower level of XOL-1 in XX animals permits the hermaphrodite fate (Adopted from Gladden et al., 2007).

proteolysis, and that the FEM proteins are in fact part of this E3 complex (Starostina et al., 2007). FEM-1 functions as the substrate-recognition subunit while FEM-2 and FEM-3 function as cofactors for CUL-2 ubiquitin ligase activity. CUL-2 negatively regulates somatic TRA-1 levels in males and in L4-stage hermaphrodites to promote masculine fate in the soma and the germline, respectively (Starostina et al., 2007). FEM-1 and FEM-3 proteins themselves are also indicated to be proteolytically degraded through the ubiquitin conjugation pathway. *sel-10* (also known as *egl-41*) encodes a F-box protein that directly interacts with FEM-1 and FEM-3, targeting them for proteolytic degradation (Jager et al., 2004). The sex-determination pathway is illustrated in the following Figure 1-6.

The sex-determination cascade is regulated at each level though various mechanisms like translational regulation of *tra-2* and *fem* mRNAs, receptor-mediated signaling via *her-1* and *tra-2,* and stability of TRA-2 and TRA-1 proteins. As one can notice, *tra-2* is subjected to complex and intricate regulation at all possible levels. TRA-2 promotes female fate via TRA-1 activity. During L4 larval stage of hermaphrodite, TRA-2 activity needs to be transiently suppressed to allow sperm development. This transient downregulation of TRA-2 depends on *rpn-10*, which encodes a ubiquitin-binding protein, and *ufd-2*, which encodes an E3 ubiquitin ligase (Shimada et al., 2006). Sexual fate of *C. elegans* is thus regulated by the interplay between transcription and ubiquitin-mediated regulation at multiple levels.

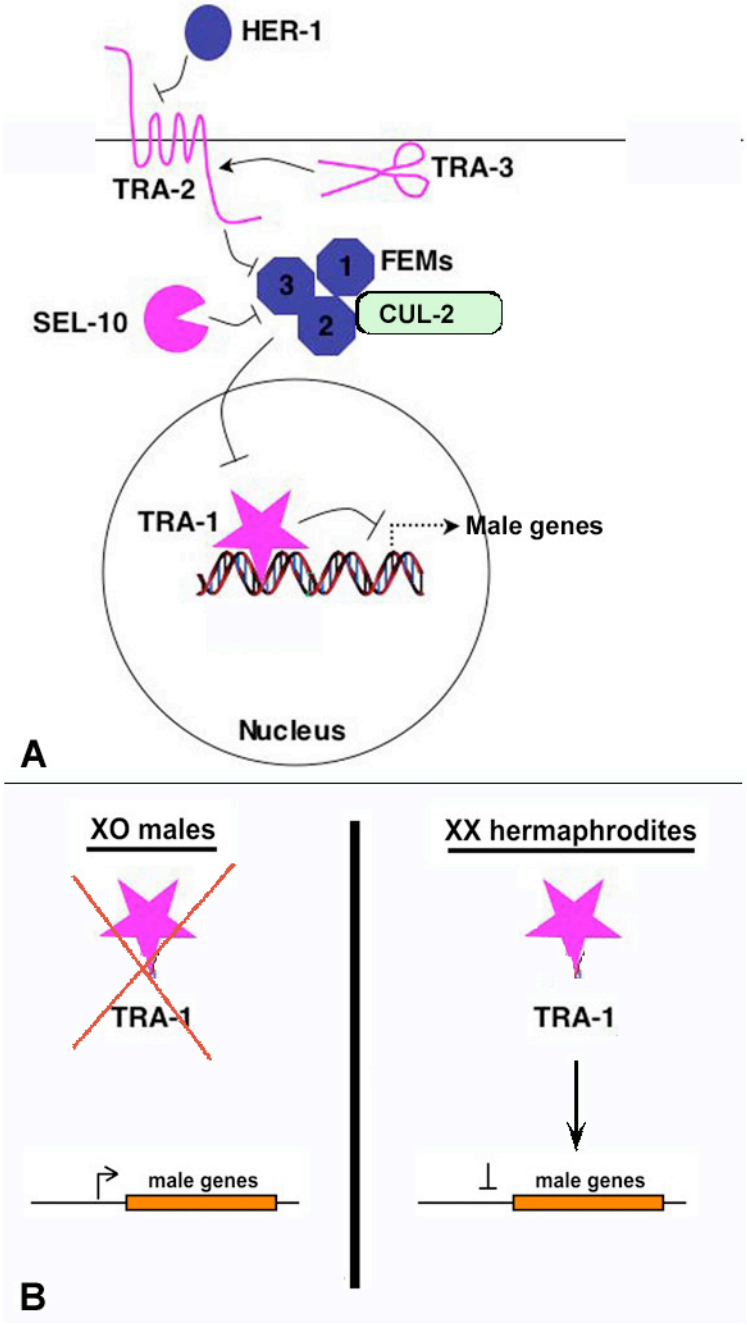

Figure 1-6: Illustration of sex determination pathway components.

A) HER-1 is present only in males. It binds the transmembrane receptor TRA-2. TRA-2 in turn interacts with the FEM complex, which together with CUL-2 ubiquitinates TRA-1. The FEM proteins are also ubiquitnated by the F box protein SEL-10 (Modified from

Zarkower 2005). B) Left, in males, TRA-1 gets degraded due to polyubiquitination by FEM and CUL-2 complex. In the absence of TRA-1, genes promoting the male fate are expressed. Right, in hermaphrodites, TRA-1 degradation is inhibited; as a result, it can suppress the male genes promoting hermaphrodite fate.

This dissertation reports the study of two genes involved in regulation of gene function in the context of *C. elegans* development. The first gene, *uba-1*, encodes the E1 ubiquitin-activating enzyme, which is essential to initiate ubiquitination and hence to regulate protein turnover during *C. elegans* development. The second gene, *spe-44*, encodes a putative transcription factor that is required for the regulation of sperm-specific gene expression in *C. elegans*.

Chapter 2 E1 ubiquitin-activating enzyme UBA-1 plays multiple roles throughout *C. elegans* development

2.1 Abstract

Poly-ubiquitination of target proteins typically marks them for destruction via the proteasome, and provides an essential mechanism for the dynamic control of protein levels. The E1 ubiquitin-activating enzyme lies at the apex of the ubiquitination cascade and its activity is necessary for all subsequent steps in the reaction. We have isolated a temperature-sensitive mutation in the *C. elegans uba-1* gene, which encodes the sole E1 enzyme in this organism. Manipulation of UBA-1 activity at different developmental stages reveals a variety of functions for ubiquitination, including novel roles in sperm fertility, control of body size, and sex-specific development. Levels of ubiquitin conjugates are substantially reduced in the mutant, consistent with reduced E1 activity. The *uba-1* mutation causes delays in meiotic progression in the early embryo, a process that is known to be regulated by ubiquitin-mediated proteolysis. The *uba-1* mutation also demonstrates synthetic lethal interactions with alleles of the anaphase-promoting complex, an E3 ubiquitin ligase. The *uba-1* mutation provides a sensitized genetic background for identifying new *in vivo* functions for downstream components of the ubiquitin enzyme cascade, and is one of the first conditional mutations reported for the essential E1 enzyme in a metazoan animal model.

2.2 Introduction

Post-translational modification of proteins performs a critical role in regulating protein activity, and ubiquitin-mediated proteolysis has emerged as the key player in the control of protein turnover. Ubiquitin, a highly conserved small protein, is covalently attached to a target protein through an enzymatic cascade, and the assembly of a poly-ubiquitin chain typically specifies that protein for rapid degradation via the 26S proteasome (Hershko and Ciechanover, 1998). Ubiquitin-mediated proteolysis thus provides an "off" switch for governing the spatial and temporal distribution of proteins that are no longer needed. This mode of regulation is essential for normal cellular processes (e.g., cell cycle progression and differentiation), and defects have been implicated in human diseases such as cancers and neurodegenerative disorders (Ardley and Robinson, 2004; Nakayama and Nakayama, 2006).

Ubiquitination of target proteins can also regulate function by mechanisms other than proteasome-mediated degradation. Mono-ubiquitination serves a signal for endocytosis and trafficking of various cell surface proteins, and is also implicated in histone and transcription factor regulation (Haglund and Dikic, 2005; Mukhopadhyay and Riezman, 2007; Schnell and Hicke, 2003). The assembly of poly-ubiquitin chains can occur at different lysines within ubiquitin, which promotes different outcomes for the labeled protein. Conjugation at lysine 48 typically leads to proteasomal degradation, while linkage through lysine 63 can modulate protein activities in processes as diverse as nuclear localization, DNA repair, or inclusion formation in neurodegenerative diseases (Chiu et al., 2006; Geetha et al., 2005; Lim et al., 2005).

A trio of enzymes mediates the attachment of ubiquitin to substrate protein: the E1 ubiquitin-activating enzyme, E2 ubiquitin-conjugating enzyme, and E3 ubiquitin ligase (Hershko et al., 1983). Repeated cycles of ligation to the initial ubiquitin lead to poly-ubiquitination. Substrate specificity is conferred by the selective binding of individual E3 ligases to one or a few target proteins (Jackson et al., 2000). Eukaryotes typically possess a single gene encoding the E1-activating enzyme, tens of E2-conjugating enzymes, and as many as several hundred E3 ligases. Some E3 ligases are themselves multi-subunit complexes, in which a substrate recognition subunit specifies the protein targeted for ubiquitination.

In vivo roles for ubiquitination in organismal development have been determined primarily through the characterization of specific E3 ligases. In the nematode *Caenorhabditis elegans*, E3 ligases regulate processes as diverse as sex determination, cell cycle progression, and synaptic signaling (Burbea et al., 2002; Feng et al., 1999; Juo and Kaplan, 2004; Schaefer and Rongo, 2006; Starostina et al., 2007). Studies of E2 conjugating enzymes indicate interactions with multiple E3s, as their relative numbers would predict. For example, inactivation of *ubc-2* produces a broader range of phenotypes than inactivation of its known E3 partner *apc-11* (Frazier et al., 2004).

One of the best-characterized functions for ubiquitination and proteasomal degradation in *C. elegans* is the coordination of early events of embryogenesis (Bowerman and Kurz, 2006). The anaphase-promoting complex (APC) is a multi-subunit E3 ligase that is essential for completion of meiosis immediately after fertilization of the oocyte by the sperm (Davis et al., 2002; Golden et al., 2000). Ubiquitin-mediated proteolysis also plays a role in the degradation of several proteins that are involved in

establishment of anterior-posterior (A-P) polarity in the early embryo. These proteins become asymmetrically localized at the first cell division, and failure to degrade these components correlates with developmental defects such as changes in cell fate specification and embryonic lethality. Formation of the A-P axis and progression of the embryonic cell cycle requires the activities of a class of E3 complexes known as Cullin-RING ligases (Bosu and Kipreos, 2008; DeRenzo et al., 2003; Kemphues et al., 1986; Liu et al., 2004; Pintard et al., 2003; Sonneville and Gonczy, 2004; Xu et al., 2003). Mutations in components of the APC also affect A-P polarity, possibly as a consequence of defects in meiosis (Rappleye et al., 2002; Shakes et al., 2003).

The E1 ubiquitin-activating enzyme lies at the apex of the enzymatic cascade, and manipulation of its activity might provide a crucial entry point for identifying the myriad roles performed by ubiquitin during development. Temperature-sensitive alleles of E1 have been identified in mammalian cell lines as cell cycle mutations that exhibit reduced ubiquitination and degradation of substrate proteins (Ciechanover et al., 1984; Finley et al., 1984). Similarly, a temperature-sensitive allele of E1 in yeast dramatically reduces ubiquitin conjugation and also leads to cell cycle arrest (Ghaboosi and Deshaies, 2007). Conditional alleles have also been isolated in *Drosophila* in a screen for suppressors of *hid*-induced apoptosis during eye development (Lee et al., 2008). Detailed characterization demonstrated the complexity of ubiquitin regulation in this system. Whereas weak alleles of the E1-encoding *Uba1* gene block apoptosis, strong alleles promote cell cycle arrest and death. Furthermore, these pro-apototic alleles promote non-autonomous proliferation in adjacent cells via elevated levels of Notch signaling.

We report here the isolation of a temperature-sensitive mutation in the *C. elegans uba-1* gene, which encodes the sole E1 enzyme in this organism. Prior results for RNAi of *uba-1* reported maternal sterility and embryonic lethality, with defects in meiotic progression (Jones et al., 2002; Kamath et al., 2003; Sonnichsen et al., 2005). The *uba-1(it129)* mutation recapitulates these phenotypes and also reveals several novel functions, including roles in sperm fertility, body size, and sex-specific development. The *uba-1(it129)* mutation reduces *in vivo* levels of ubiquitin conjugates and causes a delay in meiotic progression in the early embryo, consistent with a reduction in E1 activity. The *uba-1(it129)* mutation also demonstrates synthetic lethal interactions with known components of the anaphase-promoting complex and, as such, provides a sensitized genetic background for identifying new *in vivo* functions for other components of the ubiquitin cascade.

2.3 Materials and methods

2.3.1 Genetics

C. elegans strains were derived from the wild-type isolate N2 (Bristol) and contained one or more of the following mutations: *uba-1(it129)IV, uba-1(ok1374)IV, dpy-20(e1282)IV, fem-1(hc17)IV, fem-3(q20)IV, him-5(e1490)V, mat-3(or180)III*, *fzy-1(h1983)II*, *spe-26(it112),* or chromosome IV deficiencies *eDf19* or *mDf7*. A linked *uba-1(it129) dpy-20(e1282)* double mutant strain was generated to facilitate discrimination of homozygous and heterozygous lines in some experiments. The integrated *oma-1::GFP* transgenic line was constructed by Reuyling Lin (Lin, 2003). Strains were maintained on nematode growth medium (NGM) plates seeded with *E. coli* strain OP50. Age-

synchronized populations of embryos were obtained by sodium hypochlorite treatment of gravid hermaphrodites. Strains were maintained at 15˚C and shifted to 25˚C as indicated for phenotypic analysis. Genetic manipulations were carried out according to Brenner (Brenner, 1974).

2.3.2 Microscopy

Microscopy was performed with an Olympus BX51TF or Zeiss Axio Imager equipped with Nomarski DIC objectives and appropriate filter sets for fluorescent imaging and cooled CCD camera for image capture. Images were processed using the AxioVision (release 4.6) package and prepared for publication using Adobe Photoshop CS v. 9.0.2. Intact animals were typically mounted on 2% agarose pads for imaging. Body length was measured from captured images using ImageJ software v. 1.38.

2.3.3 Sperm assays

Sperm morphology was assessed by dissection of gonads from adult hermaphrodites or males in SM medium (Shakes and Ward, 1989a). Nuclear DNA morphology was visualized by 4'-6-Diamidino-2-phenylindole (DAPI) staining of sperm from dissected gonads. *In vitro* activation of male spermatids was by treatment with monensin on poly-lysine-coated slides (Shakes and Ward, 1989a). Motility and localization of hermaphrodite sperm were determined in intact animals by fixation and staining with DAPI, then counting the number of sperm nuclei in the spermathecae and uterus. Sperm transfer was ascertained by vital staining of males (Hill and L'Hernault, 2001) with the mitochondrial dye MitoTracker Red CMXRos (Molecular Probes), then mating to unstained hermaphrodites anesthetized with tricaine and tetramisole. After 12

or 24 h, fluorescently-labeled male sperm within the hermaphrodite reproductive tract were visualized by microscopy using rhodamine filters. Self-fertility of hermaphrodites was assessed by shifting individual L3 animals to 25˚C and counting the entire brood size. Cross-fertility of males was determined by mating with individual wild-type hermaphrodites or *fem-1(hc17)* females, then counting the number of male and hermaphrodite progeny produced by each animal after mating.

2.3.4 Cloning and molecular analysis

The *uba-1(it129)* mutation was localized to chromosome IV between *elt-1* and *dpy-20* by three-factor crosses. Single nucleotide polymorphisms that affect restriction sites (snip-SNPs) were employed as physical mapping markers of individual *uba-1(it129) dpy-20(e1282)* recombinants with Hawaiian strain CB4856 (Wicks et al., 2001). Deficiency mapping was performed by complementation testing in *uba-1(it129)/Df* heterozygous strains. RNAi of candidate genes was performed by feeding (Timmons and Fire, 1998) and assessed by phenocopy of F1 embryonic lethality for treated adult hermaphrodites and by defects in adult tail morphology for treated L3 males. Complementation of the *uba-1(ok1374)* deletion allele was determined by generating *it129/ok1374* heterozygous animals and performing temperature-shift assays as described for phenotypic characterization. Transformation rescue (Mello et al., 1991) was obtained by germ line microinjection of a 6.0 kb genomic fragment of the wild-type *uba-1* gene mixed with plasmid pRF4, which contains the dominant roller marker *rol-6(su1006)*, and linearized N2 genomic DNA at concentrations of 1, 50, and 100 µg/ml, respectively. Stable roller transgenic lines were generated from *uba-1(it129)* hermaphrodites

maintained at 15˚C, then rescue of sperm-specific sterility and embryonic lethality was scored after shifting to 25˚C.

The molecular lesion of the *uba-1(it129)* allele was identified by PCR amplification of the 6.0 Kb *uba-1* genomic interval from mutant worms followed by sequence determination. *In situ* hybridization for *uba-1* germ line expression was performed on dissected gonads following fixation (Lee and Schedl, 2005). Digoxigenin-labeled, single-stranded sense and antisense probes were generated from a 1 kb cDNA fragment by linear amplification according to the manufacturer's protocol (Roche, Indianapolis, IN). Following hybridization, probe detection was by colorimetric assay with alkaline phosphatase (AP) conjugated anti-digoxigenin antibodies and nitro blue tetrazolium (NBT) and 5-bromo-4-chloro-3-indolyl phosphate (BCIP) substrate.

Western blot analysis was performed on soluble worm lysates from age-synchronized young adult hermaphrodites shifted to 25˚ as L2 larvae. Lysates were obtained by one freeze-thaw cycle, homogenization, and centrifugation for 10 minutes at 10,000 RCF. Protein concentration of the soluble fraction was quantified by Bradford assay. 10 µg samples were fractionated by SDS-PAGE and transferred to PVDF membranes. Ubiquitin-conjugated proteins were detected by mouse anti-ubiquitin monoclonal antibody (1˚) followed by HRP-conjugated goat anti-mouse IgG polyclonal antibody (2˚; both Stressgen, Ann Arbor, MI). Duplicate gels were stained with Gelcode Blue (Pierce, Rockford, IL) to visualize total protein.

2.4 Results

2.4.1 Phenotypic characterization

The temperature-sensitive *it129* allele was isolated by Diane Shakes and, on the basis of sperm sterility and larval lethality, was provisionally designated as *spe-32* (S. Ward, pers. comm.). We have determined that *spe-32* is allelic to *uba-1* (see below), the sole E1 ubiquitin-activating enzyme in *C. elegans*, and have adopted the latter gene name for the sake of clarity. Our detailed characterization of *uba-1(it129)* demonstrates a number of phenotypes, some of which are sex-specific, in addition to those mentioned above.

Different phenotypes are manifested at different developmental stages (summarized in Table 1). To facilitate characterization, temperature-shift experiments were performed with age-synchronized populations of *uba-1(it129)* hermaphrodites. Adults shifted to the restrictive temperature produce dead embryos, and the number is equal to the number of progeny produced by wild-type animals at this temperature (Figure 1A). Embryonic arrest is heterogeneous, based on the variable morphology of the embryos and the broad range in the number of nuclei observed with DAPI staining (Figure 1B). Temperature shift at any stage of embryogenesis leads to normal hatching, but 100% of the resulting larvae die at the L2 stage (data not shown). Thus, the *uba-1* gene product is essential for both embryonic and larval development.

Larvae that are shifted to the restrictive temperature at the L3 stage exhibit normal

Table 1. Summary of *uba-1(it129)* phenotypes	
Stage shifted	**Phenotype(s)**
Adult	F1 embryonic lethality Paralysis (male only)
Embryo	Larval lethality
L2/L3 larva	Sperm-specific sterility Change in body size Tail defect (male only) Paralysis (male only)

Table 2-1: Summary of *uba-1(it129)* phenotypes

Divers phenotypes manifested by the temperature sensitive allele of *uba-1* based on the life stage of the temperature shift. Every life stage of the mutant worms is affected by the temperature shift.

somatic development. However, reproduction is adversely affected in the adult hermaphrodite. These sterile animals lay only unfertilized oocytes instead of embryos, but produce viable progeny when mated to wild type males, indicating that the sterility is sperm-specific (Figure 1C). Viability of these outcross progeny is high (96%), suggesting that oocyte development (which occurs subsequent to sperm production in the hermaphrodite) is largely unaffected by the mutation. Detailed characterization of the spermatogenesis defect (described below) indicates that these hermaphrodites produce appropriate numbers of morphologically normal sperm, but that the sperm are incapable of fertilization.

All of the above phenotypes are fully recessive, as heterozygous hermaphrodites are indistinguishable from wild type. These phenotypes are largely though not completely rescued in *uba-1(it129)* homozygous animals at the permissive temperature. There is an increase in embryonic lethality as well as a decrease in the number of embryos produced (Figure 1A), which indicates that the *uba-1(it129)* gene product is not fully functional at 15˚C. In addition, temperature causes a small but significant ($p < 0.001$ by Student's t-test) difference in body size between wild-type and *uba-1(it129)* adults (Figure 1D). When reared at 15˚C, *uba-1(it129)* hermaphrodites are 16% longer than wild type. The opposite phenotype is observed at 25˚C, with the *uba-1(it129)* mutants being 16% shorter than the wild type adults.

In the course of generating heterozygous strains for phenotypic characterization, we observed strong maternal effect rescue of the early developmental defects. Homozygous *uba-1(it129)* progeny derived from *+/uba-1(it129)* hermaphrodites reared at the restrictive temperature exhibited little embryonic or larval lethality (Table 2).

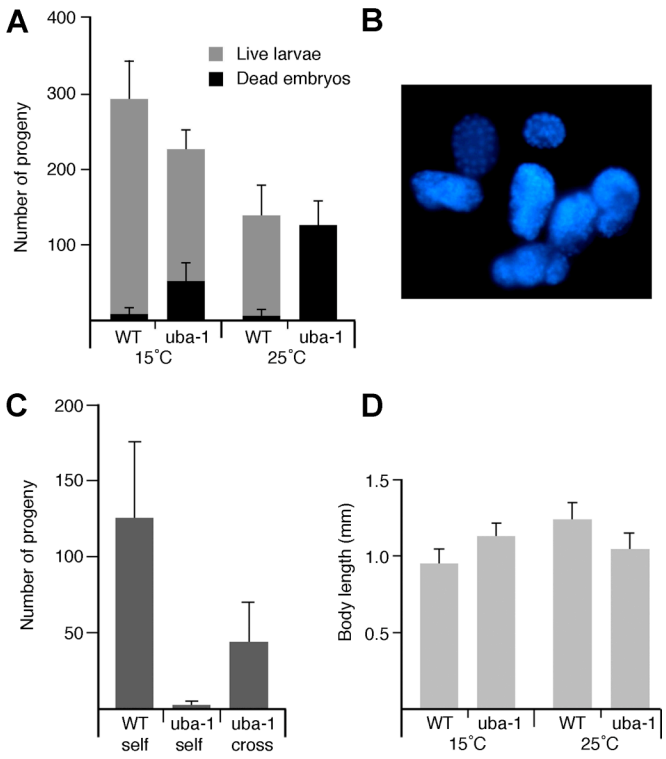

Figure 2-1: Defects in *uba-1* hermaphrodites.

A) Number of viable and inviable progeny produced by wild type (WT) or *uba-1(it129)* hermaphrodites at 15˚C or 25˚C. Shown are mean values and standard deviations (N=6) of total progeny. B) DAPI staining of *uba-1(it129)* embryos from adults shifted to 25˚C. C) Sperm-specific sterility. Number of viable progeny produced at 25˚C by wild type or *uba-1(it129)* hermaphrodites, either unmated (self) or mated with wild-type males (cross). Shown are mean values and standard deviations (N=6) of progeny produced in 48 h. D) Body length. Mean body length and standard deviations (N=20) of age-synchronized adult hermaphrodites.

Table 2. Maternal and paternal rescue of lethality			
Rescue	**Hermaphrodite genotype**	**Male genotype**	**Lethality (predicted)**
Maternal	*uba-1(it129) /* +	none (self-fertile)	3.8% (25%)
Paternal	*uba-1(it129) / uba-1(it129)*	*uba-1(it129) /* +	7.2% (50%)
Data are from five (maternal) or six (paternal) hermaphrodites. Mean total progeny numbers with s.d. are 123 ± 11 (maternal) and 73 ± 35 (paternal).			

Table 2-2: Maternal and paternal rescue of lethality

The lethality in the homozygous progeny is rescued by the wild type copy of the *uba-1* gene from either parent.

Maternal rescue was not complete for all phenotypes; although the homozygous hermaphrodites developed normally into adulthood, sperm-specific sterility was still observed in these animals. We also tested for paternal rescue by mating *uba-1(it129)/+* heterozygous males to *uba-1(it129)* homozygous hermaphrodites. Again, embryonic and larval lethality (though not sperm sterility) were largely rescued (Table 2). Because the presence of a single wild-type copy of *uba-1* in either the hermaphrodite or male parent effectively suppresses embryonic and larval lethality in homozygous mutant progeny, it suggests that the maternal or paternal contribution of UBA-1 protein is sufficient to allow somatic development to proceed normally until adulthood.

2.4.2 Male-specific phenotypes

To facilitate the phenotypic characterization of males, we constructed a *uba-1(it129) him-5(e1490)* strain [the *him-5(e1490)* mutation produces males via nondisjunction of the X chromosome] (Hodgkin et al., 1979). Temperature-shift experiments were performed with age-synchronized populations, and the same phenotypes were observed in males as above: embryonic and larval lethality and a reduction in body size (data not shown). Sperm-specific sterility of mutant males was assessed by crossing to *fem-1(hc17)* hermaphrodites, which lack sperm but produce oocytes that can be fertilized by mating. Experiments described below indicate that mating was successful but no cross-progeny were produced, demonstrating that male sperm are incapable of fertilization. Thus, the same array of defects are produced by the *uba-1(it129)* mutation in males and hermaphrodites.

We also observed additional phenotypes in *uba-1(it129)* males. The most conspicuous phenotype in the adult was constitutive protraction of the spicules (Figure 2A, first vs. second panel). These structures are part of the reproductive apparatus of the male tail, and are normally extended only during insertion into the vulva for sperm transfer. A defect in spicule retraction was apparent in adult males at both the permissive and restrictive temperatures. Constitutively protracted spicules were observed in approximately one-third of *uba-1(it129)* males reared at 15˚C and nearly all of those reared at 25˚C. In some cases the spicules, gubernaculum, and surrounding tissues were everted, suggestive of structural defects in the integrity of the male reproductive tract as well.

Additional abnormalities in the male copulatory apparatus were observed in animals reared at the restrictive temperature. The tail of the wild-type male possesses a cuticular fan containing nine pairs of sensory rays (Figure 2A, first panel), which are involved in mate detection and the behavioral responses necessary for locating the hermaphrodite vulva. The size of the fan is greatly diminished in *uba-1(it129)* homozygous males raised at 25˚C, which results in shortening of the tail tip and sensory rays as well (Figure 2A, third panel). The number of rays is not affected, and other male reproductive structures appear superficially normal by light microscopy. The shortened fan phenotype is semi-dominant: the fan expanse in heterozygous *+/uba-1(it129)* males is less than in wild-type but greater than in homozygous animals (data not shown). Therefore, proper formation of the male copulatory structures appears to be quite sensitive to the dosage of UBA-1 protein.

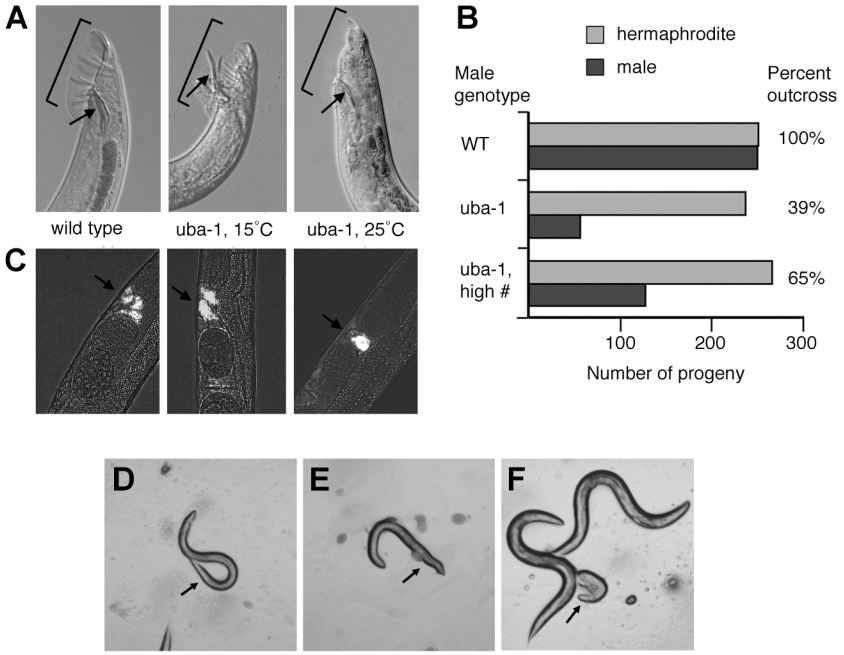

Figure 2-2: Defects in *uba-1* males.

A) Male tail defects. Shown are DIC photomicrographs of the male tail from wild type or *uba-1(it129)* animals grown at the indicated temperature. Bracket indicates the fan and sensory rays. Arrow indicates the spicules. B) Reproductive success of male mating. Graph indicates the mean number of male and hermaphrodite progeny produced by wild type hermaphrodites (N=6) mated to wild type or *uba-1(it129)* males grown at 15˚C. Only the first 500 progeny were counted for wild type. Matings combined one hermaphrodite with five males, or three hermaphrodites with 12 males (high #) for 24 h. Percent outcross is calculated by multiplying the number of male progeny by two, then dividing by the total number of progeny. C) Sperm transfer. Arrow indicates fluorescently-labeled sperm from wild type or *uba-1(it129)* males localized within the spermatheca of unlabeled hermaphrodites after mating. D-F, male-specific paralysis. D) Young adult *uba-1(it129)* male. Arrow indicates normal sinusoidal curve of tail. E) Older

adult *uba-1(it129)* male. Arrow indicates flaccid posture of tail. F) Dead *uba-1(it129)* male (arrow) and two *uba-1(it129)* hermaphrodites.

The male tail structures are critical for mating behavior and sperm transfer, so aberrations in the fan or in spicule function might adversely affect male reproductive success. Sperm from wild-type males take precedence over hermaphrodite sperm such that only outcross progeny are produced until the male sperm are depleted, at which time the production of self progeny continues (Ward and Carrel, 1979). Male sperm produce male and hermaphrodite progeny in equal numbers, while hermaphrodite sperm produce exclusively hermaphrodite progeny. Therefore, the number of outcross progeny, an indicator of male reproductive success, can be readily calculated by determining the number of males produced.

Reproductive success was ascertained for homozygous *uba-1(it129)* males grown at the permissive temperature. Some of these animals have protruding spicules, which might be predicted to impair sperm transfer. The fertility of *uba-1(it129)* hermaphrodites at 15˚C demonstrates that sperm function is normal at this temperature, so the production of outcross progeny was used as an indicator of successful mating. Mating to wild-type males produced males and hermaphrodites in the expected 1:1 ratio, indicating that all of the offspring in the measured time interval resulted from fertilization by male sperm (Figure 2B, WT). In contrast, mating with *uba-1(it129)* males produced an average of only 56 male vs. 236 hermaphrodite progeny (Figure 2B, *uba-1*), suggesting that the number of outcross progeny is reduced. The same data could be explained if the nullo-X sperm, which produce male progeny, are less competent for fertilization than the X-bearing sperm that produce hermaphrodites. This explanation seems unlikely, because the percentage of male progeny is elevated if the density of males for mating is increased (Figure 2B, *uba-1,* high #). To eliminate conclusively this possibility, *uba-1(it129)* males

were mated to *fem-1(hc17)* adult hermaphrodites that lack sperm. Only outcross progeny are produced in this experiment and, although the numbers were low, males and hermaphrodites were observed in a ratio of 1:1 (data not shown). Therefore, the protruding spicule phenotype observed in *uba-1(it129)* males at the permissive temperature decreases the successful transfer of sperm for fertilization.

Reproductive success was also characterized in the same manner for *uba-1(it129)* males shifted to the restrictive temperature at L3. No outcross progeny were observed from matings to either wild-type or *fem-1(hc17)* hermaphrodites. This failure might arise from the inability of sperm to fertilize the oocytes (as is true for hermaphrodite sperm at 25˚C), or might be a consequence of the severe morphological defects in the male copulatory apparatus that occur at the restrictive temperature. A direct assessment of sperm transfer was performed to discriminate between the two possibilities. Males from *him-5(e1490)* strains that are wild-type or mutant for *uba-1(it129)* were raised at both 15˚C and 25˚C, stained with a fluorescent dye, then mated to *fem-1(hc17)* hermaphrodites that lacked sperm. Wild-type males reared at either temperature and mutant males reared at 15˚C were successful in mating 50-70% of the time, as revealed by the presence of labeled sperm in the *fem-1(hc17)* hermaphrodites (Figure 2C, first two panels). In contrast, *uba-1(it129)* males raised at 25˚C successfully transferred sperm in only two out of 10 instances. Although the efficiency of mating is reduced at 25˚C, defects in the male copulatory structures arising from the *uba-1(it129)* mutation do not completely abrogate sperm transfer (Figure 2C, third panel). However, even those relatively rare successful matings do not give rise to outcross progeny, indicating that *uba-1(it129)* sperm from males are incapable of fertilization at the restrictive temperature.

An additional, sex-specific phenotype was observed *in uba-1(it129)* males: a late onset, progressive paralysis in two-thirds of the animals (Figure 2, D-F). The paralysis initiates at the posterior of the male and proceeds anteriorly as the worm ages, culminating in a completely paralyzed animal with a significantly shortened lifespan. Progressive paralysis is restricted to males, as *uba-1(it129)* hermaphrodites exhibit normal motility and lifespan (Figure 2F). The phenotype is not a consequence of aberrant somatic development but instead occurs post-developmentally, since delaying the temperature shift until adulthood still results in paralysis. Therefore, the *uba-1* gene product is required for the maintenance of neuromuscular function in the adult male.

2.4.3 Sperm-specific defect of *uba-1* mutation

Sperm development in *C. elegans* has been described in detail (Ward et al., 1981; Wolf et al., 1978), which allows the identification of specific cytological and functional defects in the developmental program that occur as a consequence of mutation. Normal spermatogenesis initiates from a mitotically dividing population of germ line stem cells. Primary spermatocytes separate from a syncytial cytoplasmic core and undergo a coordinated program of meiosis and differentiation. The two meiotic divisions give rise to four haploid spermatids with highly condensed nuclei. These small round cells separate from a larger residual body, which contains components not needed for subsequent steps in development. Activation by an extracellular signal converts the immotile spermatids into mature crawling spermatozoa capable of fertilization, and several compounds that promote activation *in vitro* have been identified (Nelson and Ward, 1980; Shakes and Ward, 1989a; Ward et al., 1983). Activation in hermaphrodites

occurs in the spermatheca, where the mature spermatozoa are stored. Activation of male spermatids occurs at the time of insemination, and the male spermatozoa crawl from the uterus into the spermatheca. Fertilization takes place within the spermatheca as the oocyte squeezes into this chamber of hermaphrodite reproductive tract, and the newly formed zygote then passes into the uterus. Most of the spermatozoa are dislodged and must crawl back into the spermatheca to await the next oocyte.

Sperm-specific sterility caused by the *uba-1(it129)* mutation was characterized in greater detail, beginning with the early events leading to spermatid formation. DAPI staining of L4 and young adult hermaphrodites and males revealed no differences in meiotic progression, the number of sperm produced, or (for hermaphrodites) their initial localization to the spermathecae (Figure 3, A-B and data not shown). Activation of spermatids was normal *in vivo* and *in vitro* and produced crawling spermatozoa with no discernible defect in pseudopod movement or cell motility (Figure 3C). Since motility and localization appear normal and yet no zygotes are formed, the *uba-1(it129)* mutation produces mature spermatozoa that are nonetheless incapable of fertilization.

A secondary defect in sperm function was detected later in adult hermaphrodites. Spermatozoa are displaced from the spermatheca into the uterus by each passing oocyte, and must return to the spermatheca and await the next egg. Fertilization efficiency is essentially 100% in wild type animals, with nearly every sperm being utilized for reproduction (Ward and Carrel, 1979). Thus, the number of sperm in the spermatheca decreases in concordance with an increase in the number of progeny produced. Because *uba-1(it129)* spermatozoa are motile but incapable of fertilization, one might predict that numbers within the spermatheca would remain high throughout oocyte production.

Instead, the opposite phenomenon was observed, as sperm counts declined more rapidly in *uba-1(it129)* hermaphrodites than in wild type (Figure 3B). Furthermore, significant numbers of spermatozoa were detected in the uterus instead of the spermatheca (Figure 3A, *uba-1*). These cells are swept from the spermatheca by the unfertilized oocyte but are unable to return, and instead are expelled through the vulva when oocytes are deposited. Thus, although sperm motility and localization initially appear normal, these processes are clearly impaired in older animals. This observation may indicate a defect in the maintenance of sperm quality over time, which adversely impacts either motility or sperm-spermatheca interaction.

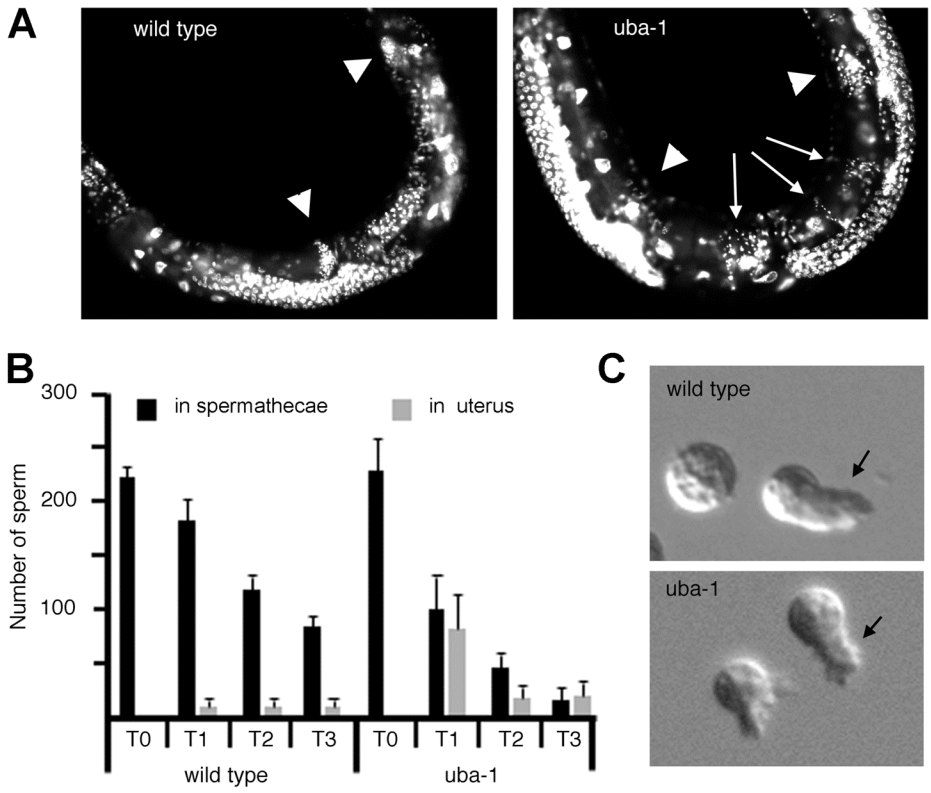

Figure 2-3: Sperm defects.

A) Sperm localization in the hermaphrodite reproductive tract. Wild type and *uba-1(it129)* adults at 25˚C were fixed and stained with DAPI to count sperm nuclei. Arrowheads, location of spermathecae; small arrows, sperm displaced into the uterus. B) Summary of sperm localization data. Shown are mean values and standard deviations per hermaphrodite (N=6). T0, before egg-laying commences; T1, after 1-2 ovulations; T2, 8 h post-T1; T3, 8 h post-T2. C) *In vitro* activation. Spermatids from wild type and *uba-1(it129)* males at 25˚C were activated with monensin. Arrow indicates pseudopod of crawling spermatozoon.

2.4.4 Identification of *it129* as *uba-1*

The identity of the *it129* allele was determined through a combination of genetic and physical mapping strategies (Figure 4A). Three-factor crosses placed this allele on chromosome IV between *elt-1* and *dpy-20* (F. Fell and S. Ward, pers. comm., and our own results; mapping data available at www.wormbase.org). Single nucleotide polymorphisms that overlap restriction sites (snip-SNPs) were analyzed in recombinant lines (Wicks et al., 2001). Strains containing the deficiency *eDf19* or *mDf7* failed to complement *it129*, further limiting its position to the overlapping 310 kb interval. A total of 80 candidate genes within the interval were available from a large-scale RNAi feeding library (Kamath et al., 2003). All were tested for the ability to replicate two of the *it129* phenotypes: F1 embryonic lethality of treated adult hermaphrodites, and tail deformation in adult males treated as larvae. Only one of the plasmids tested reproduced both phenotypes. That plasmid contains a fragment of the gene encoding the ubiquitin-activating enzyme E1, which in *C. elegans* is known as *uba-1*.

Complementation tests confirmed that *it129* is an allele of *uba-1*. The Gene Knockout Consortium (http://celeganskoconsortium.omrf.org) has generated a deletion allele, *uba-1(ok1374),* that removes much of the third and fourth exons and is predicted to be a null mutation (Figure 4B). Mutants homozygous for *uba-1(ok1374)* exhibit embryonic lethality or early larval arrest, so *ok1374/it129* animals were obtained from crosses at the permissive temperature to allow recovery of viable lines. Complementation between the two alleles was tested by temperature shift at various developmental stages as described above. The identical phenotypes reported for *it129* homozygotes were observed for *ok1374/it129* double heterozygotes: embryonic lethality, larval lethality,

sperm-specific sterility, defects in male tail formation, and male-specific progressive paralysis (Figure 4C, and data not shown). Thus, *ok1374* and *it129* fail to complement each other and are both alleles of *uba-1*.

The *ok1374* deletion is a putative null allele, while the *it129* mutation is probably hypomorphic (i.e., reduction of function; see Discussion). Therefore, we sought to ascertain whether *it129/ok1374* heterozygotes were more adversely affected than *it129* homozygotes. Most of the phenotypes observed in the *it129* homozygous animals are highly penetrant, making enhancement difficult to detect. However, data from the complementation assay for sperm-specific sterility strongly suggest a more severe defect in *it129/ok1374* animals. Cross-fertilization of sterile *it129* homozygous hermaphrodites by wild type males yields progeny with high viability (96%; see Figure 1C). In contrast, cross-fertilization of sterile *it129/ok1374* hermaphrodites produces embryos with very low viability (6%; Figure 4C). Furthermore, the same data demonstrate that the number of fertilized embryos is significantly lower for *it129/ok1374* heterozygotes than *it129* homozygotes (10 vs. 48, respectively). Sperm are normally the limiting gamete for fertilization in *C. elegans*, but these results suggest that oocyte production might be defective in *it129/ok1374* hermaphrodites. Therefore, we examined the gonads of these strains directly by DAPI staining.

Germ cell development in *C. elegans* proceeds distally to proximally within the gonad, and is most readily distinguishable by changes in nuclear morphology (Hirsh et al., 1976). In hermaphrodites, the proximal arm of the wild-type adult gonad contains a

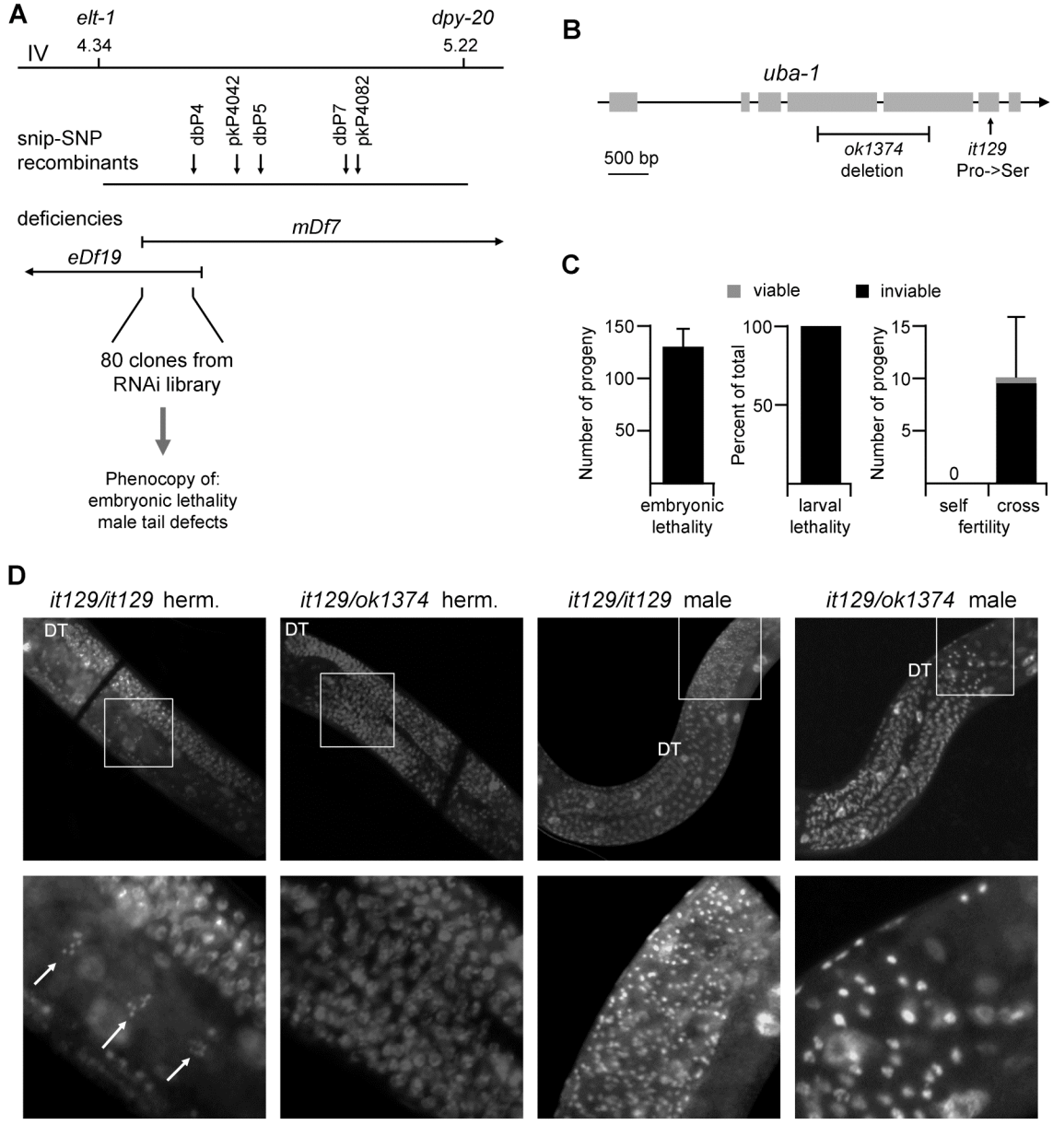

Figure 2-4:Cloning and complementation.

A) Schematic of cloning strategy. Shown at top is the interval of chromosome IV from *elt-1* to *dpy-20*. Line two indicates the position of snip-SNPs identified in recombinant lines from N2 *uba-1(it129) dpy-20(e1282)* crossed with Hawaiian strain CB4856. The next two lines indicate the endpoints and overlapping regions of chromosomal deficiencies *eDf19* and *mDf7*, which failed to complement *uba-1(it129)*. Eighty genes

within the 0.31 Mb overlap were screened by RNAi feeding for two *uba-1(it129)* phenotypes: embryonic lethality and male tail defects. B) Predicted gene structure of *uba-1*. Shown are position of the Pro1024Ser missense mutation identified in the *it129* allele and extent of the deleted region of the *ok1374* allele. C) Complementation data for *it129/ok1374* heterozygotes. Assay conditions for F1 embryonic lethality (N = 6 hermaphrodites), larval lethality (minimum 500 embryos), and sperm-specific sterility (N = 10 hermaphrodites) were identical to those used to characterize *it129* homozyogotes; see Figure 1 and accompanying text. D) Germ line defects in *it129/ok1374* heterozyogotes. Germ line nuclei were visualized by DAPI staining of fixed adult animals. The distal tip (DT) of the gonad is indicated for orientation. Top row shows a single gonad arm from (left to right) an *it129* homozygous hermaphrodite, *it129/ok1374* heterozygous hermaphrodite, *it129* homozygous male, and *it129/ok1374* heterozygous male. Bottom row shows a high-magnification image of the boxed region of the proximal gonad. Arrows, oocyte nuclei in diakinesis.

row of individual oocytes whose nuclei are arrested at diakinesis of meiosis I. Our analysis indicates that the germ lines of *it129* homozygotes are similar to wild type hermaphrodites, and the proximal gonad contains morphologically normal oocytes whose six diakinetic bivalents are easily seen (Figure 4D, top and bottom left panels). In contrast, the germ lines of *it129/ok1374* animals show an increased population of germ cells and a concommitant reduction in the number of oocytes in the proximal arm of the gonad. This defect in oogenesis is variable; some germ lines appear largely normal, while in other examples oocytes are absent and have been completely supplanted by an excess number of germ cells (as in Figure 4D, top and bottom second panels). A similar phenotype has been reported for mutations in a number of genes that govern the proliferation vs. meiosis decision, such as *glp-1* (Berry et al., 1997).

In addition, we also observed a spermatogenesis defect in the germ line of males. Wild-type adult males accumulate large numbers of highly condensed spermatid nuclei within the seminal vesicle. The *it129* homozygous males likewise contain an abundance of compact spermatid nuclei (Figure 4D, top and bottom third panels). However, the seminal vesicle of *it129/ok1374* males contain relatively few nuclei that also appear larger or less condensed than spermatid nuclei (Figure 4D, rightmost top and bottom panels). In both hermaphrodites and males, the mitotic and pachytene regions of the germ line in the distal gonad appear normal (albeit occasionally reduced in size). These results suggest that the differentiation of gametes in both sexes is impaired in the *it129/ok1374* heterozygous mutants, but with opposite effects depending upon the type of gamete: males possess fewer spermatids than normal, while hermaphrodites contain an excess of germ cell nuclei rather than oocytes. Gamete-specific differences in

proliferation and differentiation have been reported previously. For example, loss of *gld-1* causes germ line overproliferation only in hermaphrodites undergoing oogenesis (Francis et al., 1995), while loss of *puf-8* causes overproliferation only in sperm-producing germ lines (Subramanian et al., 2003).

Transgene rescue of *it129* with the wild type *uba-1* gene further confirmed its identification. Initial attempts at rescue by germ line microinjection indicated that worms might be exquisitely sensitive to the dosage of this gene. Control injections with the *rol-6* marker (Mello et al., 1991) produced numerous F1 rolling progeny with stable transmission in subsequent generations. In contrast, coinjection of *uba-1* with *rol-6* at typical concentrations resulted in low brood sizes with very few F1 rollers and no stably transmitting lines, suggestive of transgene toxicity. To reduce the gene dosage, the concentration of *uba-1* DNA was decreased relative to *rol-6* and genomic N2 DNA was also included in the injections. At the lowest concentration tested, four of sixteen stably transmitting lines exhibited partial rescue of both sperm-specific sterility and embryonic lethality at the restrictive temperature. Therefore, the wild type *uba-1* transgene is able to complement the *it129* mutation.

Expression of a *uba-1::GFP* reporter transgene has been reported in a variety of somatic tissues but not the germ line (McKay et al., 2004), although a functional role for UBA-1 in this tissue is indicated by the mutant phenotype. Transgenes are often silenced within the germ line, so *in situ* hybridization was employed to detect transcription of the endogenous *uba-1* gene within the gonad. Abundant expression was detected in germ cells that had initiated meiosis in wild type hermaphrodites (during sperm and oocyte production) and males (Figure 5). Signal intensity appeared to be higher during oocyte

production; this observation was confirmed by comparing *fem-1(hc17)* hermaphrodites, which make only oocytes, to *fem-3(q23)* hermaphrodites, which make only sperm. Peak expression occurs at pachytene of the first meiotic division, is absent immediately afterwards, and is detected again in late oogenesis. This pattern is more apparent in the *fem-1(hc17)* gonad, which is from an older adult than the wild type hermaphrodite.

Sequence determination of the *uba-1* coding region from the *it129*-bearing strain revealed the molecular lesion. A single nucleotide substitution was detected that converts the proline at position 1024 to serine (Pro1024Ser, Figure 4B). The complete structure of E1 ubiquitin-activating enzyme has not yet been determined, but X-ray crystal structures of the activating enzymes for ubiquitin-like proteins SUMO and NEDD8 are available (Lois and Lima, 2005; Walden et al., 2003). The proline residue that is mutated in *uba-1(it129)* maps near the active site where the ubiquitin moiety is predicted to be covalently attached to the E1 protein. On the basis of the structural data, the Pro1024Ser mutation might be expected to alter catalytic activity of the enzyme.

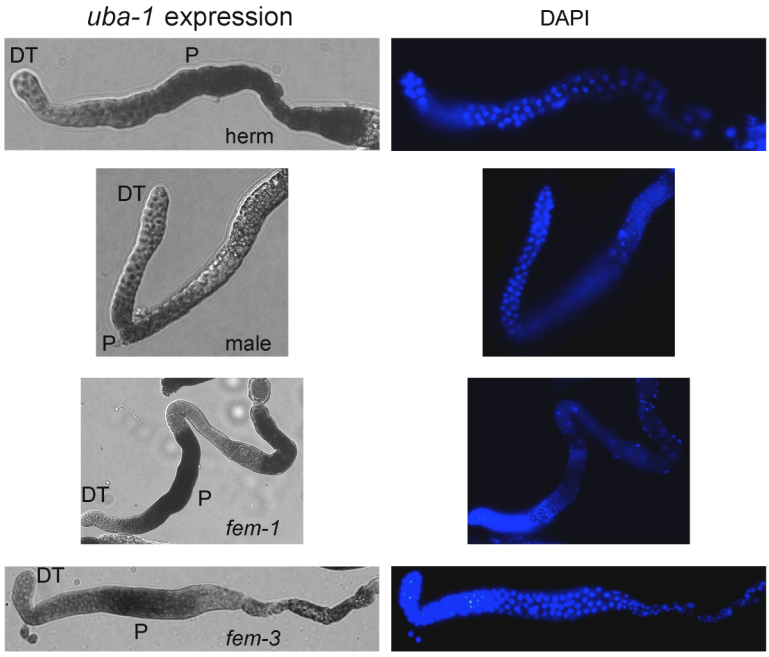

Figure 2-5: *In situ* hybridization of gonads.

Panels on the left show the *uba-1* expression pattern in dissected gonads. Panels on the right show nuclear morphology by DAPI staining. From top to bottom, gonads are from adult hermaphrodites during oogenesis, adult males during spermatogenesis, *fem-1(hc17)* adult hermaphrodites that produce only oocytes, and *fem-3(q23)* adult hermaphrodites that make only sperm. At least 20 gonads were examined for each genotype or sex. DT, distal tip of gonad; P, pachytene region.

2.4.5 *In vivo* defects in ubiquitination and embryogenesis

The *uba-1* gene encodes the only known E1 ubiquitin-activating enzyme in *C. elegans*, so a defect in its activity is predicted to impair subsequent steps in the enzymatic cascade and cause an overall decrease in the level of ubiquitination on substrate proteins. We tested this hypothesis directly by using ubiquitin-specific antibodies to assess the amount of ubiquitination in worm protein lysates. To control for variations in ubiquitination activity at different stages of development, we extracted protein from age-synchronized young adult hermaphrodites shifted as L3 larvae. Since these *uba-1(it129)* animals are infertile due to sperm-specific sterility, we included as an additional control a strain containing *spe-26(it112)* (a temperature-sensitive, sperm-specific sterile mutation). Western blots show a significant reduction in the amount of ubiquitin signal in *uba-1(it129)* protein extracts compared to wild-type and *spe-26(it112)* controls (Figure 6). Note that the level of ubiquitin in the high molecular weight region of the blot is particularly diminished, presumably reflecting a substantial reduction in the amount of poly-ubiquitinated substrates. Therefore, the *uba-1(it129)* mutation exhibits an *in vivo* decrease in protein ubiquitination.

Reduced ubiquitination is predicted to adversely impact proteasomal degradation of target proteins. Well-characterized roles for ubiquitin-mediated proteolysis in *C. elegans* occur during the early events of embryogenesis. The anaphase-promoting complex (APC) is an E3 ligase that is required for degradation of the meiotic inhibitor securin (Kitagawa et al., 2002). Complete loss of APC activity results in metaphase arrest of the one-celled embryo (Golden et al., 2000).

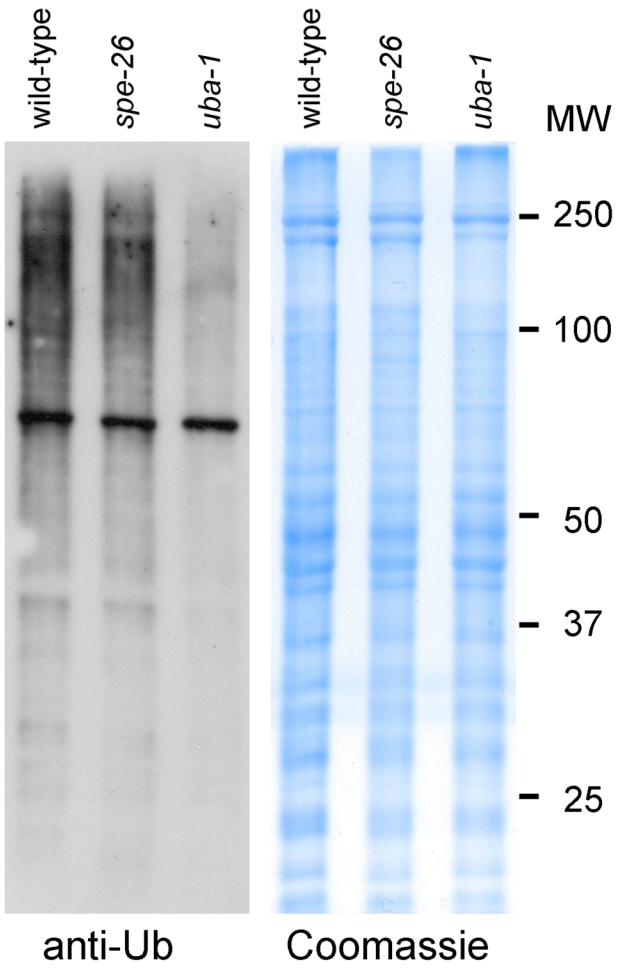

Figure 2-6: Western blot for ubiquitin.

Panel on the left (anti-Ub) shows the overall level of ubiquitin conjugates from wild-type, *spe-26(it112),* or *uba-1(it129)* young adult hermaphrodites. Equal amounts of soluble protein extracts were detected with ubiquitin-specific monoclonal antibody. Panel on the right (Coomassie) shows the same extracts stained for total protein. Size standards (MW) are indicated to the far right.

The *uba-1(it129)* mutation does not produce the one-celled arrest caused by loss of APC activity, but instead mimics the multicellular embryonic lethality resulting from reduced APC function. This phenotype is produced by hypomorphic mutations in APC components or by synthetic interactions between some pairs of temperature-sensitive alleles (i.e., each single mutation has no effect at the permissive temperature, whereas the combination of both mutations causes maternal embryonic lethality) (Shakes et al., 2003). Since UBA-1 and APC function in the same enzymatic cascade, mutations in both might likewise exhibit a synthetic interaction. Therefore, we tested the *uba-1(it129)* allele in combination with APC components. Double mutants of *uba-1(it129)* with either the APC subunit *mat-3(or180)* (Golden et al., 2000) or the APC activator *fzy-1(h1983)* (Kitagawa et al., 2002) resulted in maternal embryonic lethality at the permissive temperature (Table 3).

Early embryogenesis was examined in *uba-1(it129)* adult hermaphrodites shifted to 25˚ for defects in meiotic progression or A-P polarity in the first cell division. An *oma-1::GFP* transgene was used to allow visualization of embryonic polarity (Lin, 2003). In wild-type hermaphrodites, OMA-1::GFP protein is evenly distributed throughout the cytosol and excluded from the intact pronuclei of the one-celled embryo. Our observations at 25˚C indicate that the protein is also concentrated on the sperm centrioles and mitotic spindle. Ubiquitin-mediated proteolysis at the first cell division degrades the bulk of OMA-1::GFP. The protein is absent in the anterior (A) cell of the two-celled

Table 3. Synthetic interactions between double mutants			
Genotype	+	*mat-3(or180)*	*fzy-1(h1983)*
+	WT	WT	WT
uba-1(it129)	WT	Mel	Mel
WT, wild type; Mel, maternal embryonic lethality. Data are from a minimum of ten hermaphrodites for each genotype reared at the permissive temperature of 15˚C.			

Table 2-3: Synthetic interactions between double mutants

Worms double heterozygous for *uba-1* and weak alleles of APC mutants show synthetic maternal embryonic lethality at permissive temperature.

embryo, and the remaining OMA-1::GFP becomes associated with P granules in the posterior (P) cell. In *uba-1(it129)* animals, the pattern of OMA-1::GFP in one-celled embryos is indistinguishable from wild-type. OMA-1::GFP degradation during the first cell division is likewise identical, and the protein persists only in the P cell. However, progression of the zygote through the first division is slower than normal for *uba-1(it129)* embryos. The delayed progression leads to an increase in the number of one-celled embryos within the uterus, which is easily visualized by the presence of OMA-1::GFP (Figure 7A). Wild-type hermaphrodites typically contain a single one-celled embryo in each arm of the gonad; in contrast, *uba-1(it129)* mutants possess an average of three one-celled embryos per gonad arm (Figure 7B). In addition, 35% of the *uba-1(it129)* hermaphrodites contained a crushed zygote within the uterus. Formation of the rigid eggshell is completed late in meiosis, so these crushed zygotes might be either an indirect consequence of the observed meiotic delay or indicate a structural requirement for ubiquitination in the embryo immediately following fertilization.

The delay in progression through the first embryonic division was examined in greater detail. Upon fertilization, the oocyte nucleus completes the first and second meiotic divisions. The oocyte and sperm pronuclei meet and fuse, then undergo the first mitotic division. The percentage of embryos observed at each of these stages (meiosis, pronuclear migration and fusion, and mitosis) was determined for wild-type and *uba-1(it129)* animals. The fraction of one-celled embryos in the meiotic and pronuclear stages was equivalent in wild type, but approximately two-fold higher in the meiotic stage for *uba-1(it129)* embryos (Figure 7C), suggesting that meiosis is acutely sensitive to UBA-1.

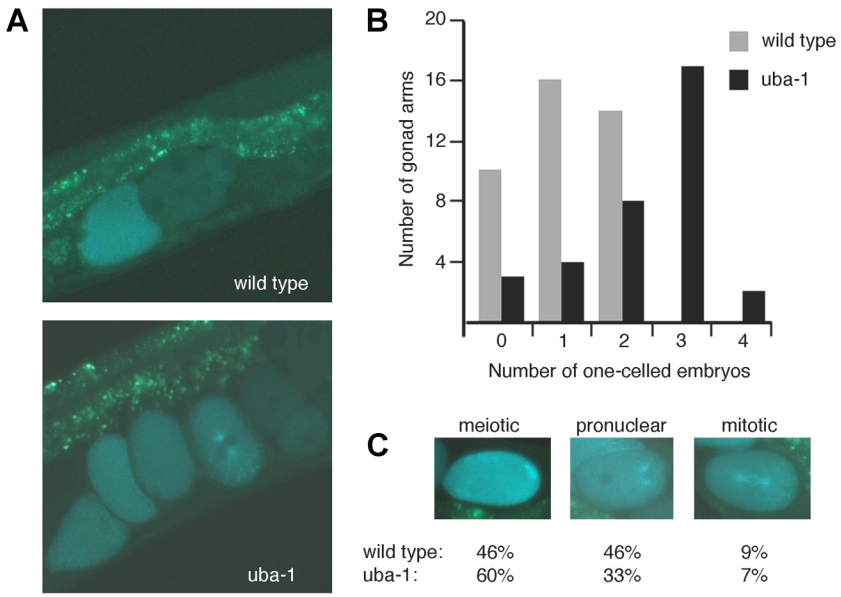

Figure 2-7: OMA-1::GFP expression.

A) Adult hermaphrodites expressing the *oma-1::GFP* integrated transgene. Shown are examples of wild type and *uba-1(it129)* animals that contain one and four one-celled embryos, respectively. B) Frequency of one-celled embryos in the uterus. The number of one-celled embryos per gonad arm were counted for wild type (N=40) and *uba-1(it129)* (N=34) hermaphrodites. C) Distribution of one-celled embryos in the meiotic, pronuclear, and mitotic stages of development, as visualized by OMA-1::GFP.

Despite this significantly skewed distribution ($p < 0.001$ by Pearson's chi-square test), there were no gross defects in nuclear or cellular morphology or OMA-1::GFP distribution as embryonic development progressed.

2.5 Discussion

We report here the isolation and characterization of a temperature-sensitive mutation of the *uba-1* gene, which encodes the E1 ubiquitin-activating enzyme of *C. elegans*. Activation by E1 is the first step in the enzymatic pathway that leads to the conjugation of ubiquitin to target proteins. Manipulation of E1 activity by temperature shift provides a mechanism for identifying the many roles for ubiquitination throughout development. Effects of the *uba-1(it129)* mutation are manifested at both the organismal (i.e., embryonic and larval lethality, reduction in body size) and cellular (sperm-specific sterility) levels, and also result in sex-specific differences of developmental (formation of the male copulatory apparatus) and post-developmental (late-onset male paralysis) processes. The *uba-1(it129)* mutation causes a substantial reduction of *in vivo* levels of ubiquitin-conjugated substrates, exhibits synthetic embryonic lethality with components of the anaphase promoting complex (an E3 ubiquitin ligase), and produces delays in early embryonic events known to be regulated by ubiquitin-mediated proteolysis.

Taken together, the data indicate that the *uba-1(it129)* mutation results in a temperature-sensitive reduction in its ubiquitin-activating enzymatic activity. Since the *uba-1* gene product is the only E1 enzyme in *C. elegans*, a reduction in its activity is predicted to negatively impact the function of E2 and E3 enzymes globally. This reduction would extend the half-life of proteins normally targeted for the proteasome, as

well as altering the localization and/or activities of other ubiquitin-conjugated substrates. Some of these downstream pathways will be more or less sensitive to a reduction in E1 activity, but the result will be a decrease in the rate of ubiquitination for a wide variety of substrate proteins. In support of this model, Western blotting with anti-ubiquitin antibodies demonstrated an overall reduction in ubiquitin labeling of extracts from the *uba-1(it129)* mutant strain (Figure 6). Also, structural data from related E1 enzymes predict that the Pro1024Ser mutation in *uba-1(it129)* might alter its catalytic activity. Finally, the model is consistent with our results in the candidate gene screen (in which reduced levels of UBA-1 by RNAi reproduced both the embryonic lethality and male tail defects) as well as the phenocopy of APC hypomorphic alleles rather than strong loss-of-function mutations (i.e., multicellular vs. one-celled embryonic arrest).

An alternative hypothesis, that the *uba-1(it129)* mutation blocks only one or a few E2/E3 pathways, is less likely. The observed reduction of *in vivo* ubiquitination in the mutant would require that the bulk of ubiquitin conjugation be mediated by one or a few E3 ligases; however, the hundreds of E3s that are present in *C. elegans* argue against this model. Furthermore, the range of phenotypes produced by the *uba-1* mutation is much broader than those reported for inactivation of any single E2 or E3 enzyme (Kipreos ET, 2005), consistent with its participation in multiple E2/E3 pathways. We clearly demonstrate genetic interactions between *uba-1(it129)* and one E3 pathway, the APC, via synthetic embryonic lethality with *mat-3* or *fzy-1* alleles. However, the sperm-specific fertilization defect appears to involve a different E3 pathway. This phenotype is not observed in APC mutants but has been reported for mutations in *spe-16*, which has

recently been determined to encode an E3 ubiquitin ligase homolog (Steve L'Hernault, personal communication).

Some effects of the *uba-1* mutation can be interpreted in light of the variety of phenotypes that arise from the loss of individual E2 or E3 activities. For example, embryonic and larval lethality have been reported for a number of E2 and E3 homologs in large-scale RNAi screens (Jones et al., 2002; Kamath et al., 2003; Sonnichsen et al., 2005). However, the majority of these genes have not been further characterized and, absent additional knowledge of which proteins are substrates for particular E2 and E3 enzymes, it's difficult to speculate on the molecular mechanisms responsible for the observed lethality.

In other instances, the *uba-1* mutant phenotype suggests a previously unidentified role for ubiquitination. Body size in *C. elegans* is governed by a canonical TGF-ß signal transduction pathway that initiates with the DBL-1 ligand (Savage et al., 1996; Suzuki et al., 1999). Components of the TGF-ß pathway in other organisms are known to be regulated by ubiquitin conjugation (Itoh and ten Dijke, 2007). Different ubiquitin modifications produce antagonistic effects on signal transduction: mono-ubiquitination of Co-Smad stabilizes the protein and promotes signaling, while poly-ubiquitination of R-Smad leads to its proteasomal degradation and down-regulation of signaling. Given the effects of the *uba-1* mutation on *C. elegans* body size, it seems likely that components of the DBL-1/TFG-ß pathway are similarly regulated by ubiquitin.

The sperm-specific sterility of *uba-1(it129),* coupled with the recent identification of *spe-16* as an E3 ubiquitin ligase homolog (Steve L'Hernault, personal communication), indicate a previously uncharacterized role for ubiquitin in *C. elegans*

spermatogenesis. Ubiquitination is known to be essential for sperm function in a wide variety of organisms, and roles in mammalian spermatogenesis include regulation of the meiotic cell cycle, histone modification and chromatin remodeling, protein sorting during sperm differentiation, and quality control for defective sperm (Baarends et al., 1999a; Guardavaccaro et al., 2003; Morokuma et al., 2007; Sutovsky et al., 2001). In *C. elegans*, early events like meiosis appear unaffected by the *uba-1(it129)* mutation, suggesting that the infertility of these morphologically normal spermatozoa is due to a later defect in sperm development. In a manner analogous to mammalian sperm, ubiquitination in *C. elegans* might function in protein sorting as the spermatids divide from the residual body. Errors in this process are known to adversely affect sperm function: mutation of *spe-15*, which encodes a myosin homolog, impairs the asymmetric segregation of proteins during spermatid budding and causes sperm-specific sterility (Kelleher et al., 2000). Alternatively, ubiquitination might promote proteasomal degradation of a protein that inhibits fertilization, and decreased activity of UBA-1 would lead to inappropriate persistence of the proposed inhibitor. Spermatid activation and downstream events occur in the absence of new protein synthesis, so degradation of pre-existing component(s) is a plausible mechanism of regulation. Another possibility is that *uba-1(it129)* infertility might reflect a role for ubiquitin-mediated proteolysis in the sperm-oocyte interaction. Fertilization in ascidians is mediated by an extracellular enzyme from sperm that conjugates ubiquitin to a sperm receptor on the egg surface, leading to its degradation via the proteasome (Sawada et al., 2002). Ongoing analysis is designed to determine if one (or more) of these hypotheses is correct.

Multiple E3 ligases are involved in formation of the reproductive structures of the male tail, so the defects observed in *uba-1* mutant males might arise from impairment of one or more known ubiquitination pathways. Mutation of *mat-1*, which encodes the CDC27 subunit of the APC, causes a diminution in the size of the fan and sensory rays similar to the defect produced by *uba-1(it129)* (Shakes et al., 2003). The heterochronic gene *lin-41*, which encodes a homolog of the RING finger subclass of E3 ligases, is also required for proper formation of the male tail. A decrease in LIN-41 function causes precocious retraction of the male tail so that the fan and rays are reduced or absent (Del Rio-Albrechtsen et al., 2006; Slack et al., 2000). The DBL-1/TGF-ß pathway (mentioned above) that determines body size also plays a role in formation of the spicules (Baird and Ellazar, 1999), and might be implicated in the protruding spicule phenotype of *uba-1(it129)* males.

The late-onset paralysis and associated lethality produced by the *uba-1(it129)* mutation is unusual in two regards: it is sex-specific, affecting only males, and can be induced after all somatic development is complete. There are few reports of such post-developmental phenotypes for *C. elegans*, and this property suggests a defect in the maintenance of neuronal and/or muscle function rather than its establishment. Roles for ubiquitination in *C. elegans* neuromuscular activity have been reported previously. Multiple E2 conjugating enzymes have been implicated in polyglutamine protein aggregation in muscle (Howard et al., 2007). E3 ligase complexes that have been demonstrated to affect either muscle or neuronal function include CHN-1/UDF-2, APC, KEL-8/CUL-3, SCF/FSN-1/RPM-1, SCF/LIN-23, and SCF/SEL-10 (Ding et al., 2007; Hoppe et al., 2004; Juo and Kaplan, 2004; Liao et al., 2004; Mehta et al., 2004; Schaefer

and Rongo, 2006). However, the paralysis of *uba-1(it129)* males is distinct from the more subtle neuromuscular defects reported for other ubiquitin pathway components such as APC (decreased duration of forward movement) or KEL-8/CUL-3 (changes in nose touch response and spontaneous reversal frequency) (Juo and Kaplan, 2004; Schaefer and Rongo, 2006). Furthermore, functional roles for all of these enzymes have been demonstrated in hermaphrodites, so the sex-specific ubiquitination that is responsible for male paralysis remains to be elucidated.

Why are male-specific processes, including the fertility defect of the male gamete (i.e., sperm), so acutely sensitive to the level of UBA-1 activity? One intriguing possibility involves the recently discovered role for ubiquitin-mediated proteolysis in the sex determination pathway. The TRA-1 transcription factor is the critical regulator of somatic and germ line sex determination and acts primarily as an inhibitor of male sexual fate (Hodgkin, 1987). Three FEM proteins negatively regulate TRA-1 activity and thereby promote male cell fates, including sperm development in hermaphrodites (Hansen and Pilgrim, 1999). Starostina et al. (Starostina et al., 2007) demonstrate that the FEM proteins form an E3 ubiquitin ligase complex with CUL-2 that binds to and promotes proteasome-dependent degradation of TRA-1. Impairment of UBA-1 function by mutation would be predicted to decrease activity of the FEM/CUL-2 E3 complex, leading to an increase in TRA-1 levels that would inhibit male developmental processes. This weakly feminizing effect might act synergistically with one or more of the E3 pathways described above. If this hypothesis is correct, then some of the sex-specific defects of the *uba-1* mutation might be suppressed by a decrease in TRA-1 activity.

The observation of synthetic embryonic lethality between *uba-1(it129)* and mutations in components of the APC suggests a powerful approach for identifying new functions for downstream components of the ubiquitin pathway. A number of E2 and E3 homologs exhibit detectable phenotypes in genome-scale RNAi screens, but the majority are indistinguishable from wild type (Jones et al., 2002; Kamath et al., 2003). One possible explanation is that many of these enzymes are functionally redundant, and that the determination of their roles will require inactivation of multiple E2s or E3s. Alternatively, in some instances the reduction of E2 or E3 levels by RNAi might be insufficient to disrupt function. However, the *uba-1* mutation provides a sensitized genetic background for detecting decreased activity of downstream enzymes. Reanalysis by RNAi screening of the E2 and E3 homologs in the *uba-1* mutant strain is likely to reveal novel functions for a number of those genes whose roles are currently unknown.

ACKNOWLEDGMENTS

We wish to thank Diane Shakes for isolating and Sam Ward for providing the *uba-1(it129)* allele, Michael Stitzel of Geraldine Seydoux's lab for providing the *oma-1::GFP* strain, the Caenorhabditis Genetics Center and *C.elegans* Gene Knockout Consortium for providing strains, Andy Golden for providing strains and suggesting the synthetic lethal experiment, Eugene Melamud for assistance with the structural prediction, Sara Hapip for assistance with the RNAi candidate screen, and members of the lab and the Baltimore/Washington worm community for fruitful discussions.

Chapter 3 *spe-44*, a putative transcription regulator of sperm gene expression

3.1 Introduction

Development of an organism is achieved through cellular differentiation into specialized cell types. How cells differentiate and develop into specific cell types is a fundamental question in developmental biology, and an important wealth of work has already been done to understand this phenomenon (Lewis et. al., 1998). The cell type is determined by the specific set of genes that govern the process towards the terminal differentiation stage. The expression of genes is precisely regulated in a spatial and temporal manner to restrict the 'message' passed on to the cell, which then gets determined to be of specific fate. As discussed in Chapter 1, transcriptional control is one of the modes for regulating gene expression in a cell-specific context. Studying the transcriptional control of gene expression can help understand how cells control a particular order of gene expression in spatial and temporal context.

Spermatogenesis in *Caenorhabditis elegans* provides a good model system to study stem cell differentiation and cell fate specification. The germline in *C. elegans* changes its fate during hermaphrodite development. The proliferative germline initially differentiates into sperm, but later in life the fate switches to oocyte. The spermatogenic germline goes through series of changes at the single cell level that are morphologically dramatic yet at the same time essentially similar to universal processes such as asymmetric cell division and signal transduction. Studying the transcriptional regulation

of the genes necessary for sperm differentiation and development can give insights about the fundamental mechanisms of cellular differentiation and development in a complex eukaryotic system.

3.1.1 Sperm development in *C. elegans*

The process of development of the haploid spermatozoon from undifferentiated germline nuclei is referred to as spermatogenesis (Figure 3-1). The germline nuclei divide meiotically, generating four haploid spermatids plus a residual body that contains components not needed for subsequent steps of development. The residual body eventually gets degraded or absorbed. The spermatid differentiates from a single spherical cell into a motile spermatozoan through the process of activation or spermiogenesis. The terminally differentiated spermatozoon in *C. elegans* is an asymmetric cell with an amoeboid pseudopod for motility instead of a flagellum (Ward et al., 1981)..

Although sperm development is essentially the same in both hermaphrodites and males, there are three major differences. First, spermatozoa in males are larger in size compared to hermaphrodite spermatozoa, which gives them a competitive advantage during mating (LaMunyon and Ward, 1998). Second, the male germline continues to differentiate into spermatids, whereas the hermaphrodite germline switches to oogenesis at the onset of adulthood. The third difference is in the storage form and timing of activation for the spermatids (Figure 3-3). The spermatids are stored in the proximal region of the gonad in hermaphrodites and get activated after being transferred to the spermatheca. In males, spermatids are stored in the seminal vesicle and spermiogenesis

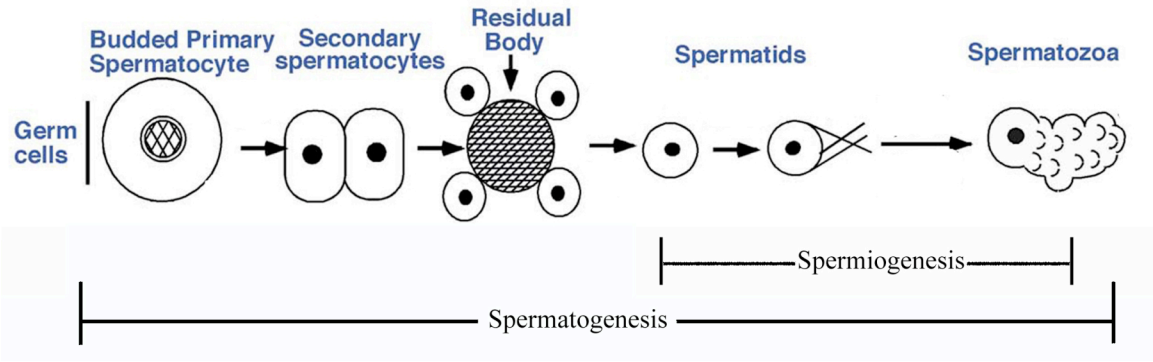

Figure 3-1: Sperm development in wild type worm.

Schematic diagram of stages during sperm development in *C. elegans*. The process of sperm development is referred to as spermatogenesis and the activation of spermatids into spermatozoa is called spermiogenesis. (Modified from L'Hernault, 2005)

occurs in the hermaphrodite uterus after mating (Ward et al., 1983).

During sperm development, germline differentiation proceeds from the distal to proximal region of the gonad, so that the spatial distribution reflects temporal stages of development (Figure 3-2). In the distal region of the gonad, the germline proliferates mitotically. It goes through a transition zone (Figure 3-2B) and enters the meiotic cycle (Figure 3-2C). Nuclei in distinct phases of meiotic prophase I can be observed with their characteristic chromosomal patterns. Crescent-shaped nuclei (Figure 3-2B) are transitioning from mitosis to meiosis, while chromosomes in pachytene stage form a "bowl of spaghetti" as shown in Figure 3-2C. Nuclei are held together in a cytoplasmic core called the rachis until this point (Hirsh and Vanderslice, 1976). As the nuclei progress through meiosis, they start budding off from the rachis as primary spermatocytes. As the primary spermatocytes complete meiosis I, the 4N nuclei condense giving a characteristic pattern of the paired file of nuclei (arrows in Figure 3-2) in the proximal gonad.

After meiosis I, primary spermtocytes can either enter meiosis II directly without going through cytokinesis or separate into two secondary spermatocytes, each with a 2N nucleus (Ward et al., 1981). Meiosis II produces 4 haploid nuclei from one primary spermatocyte or 2 haploid nuclei from a secondary spermatocyte. These haploid nuclei bud off in an asymmetric cytokinesis event as round spermatids from a central anucleate mass of cytoplasm called the residual body (Figure 3-1).

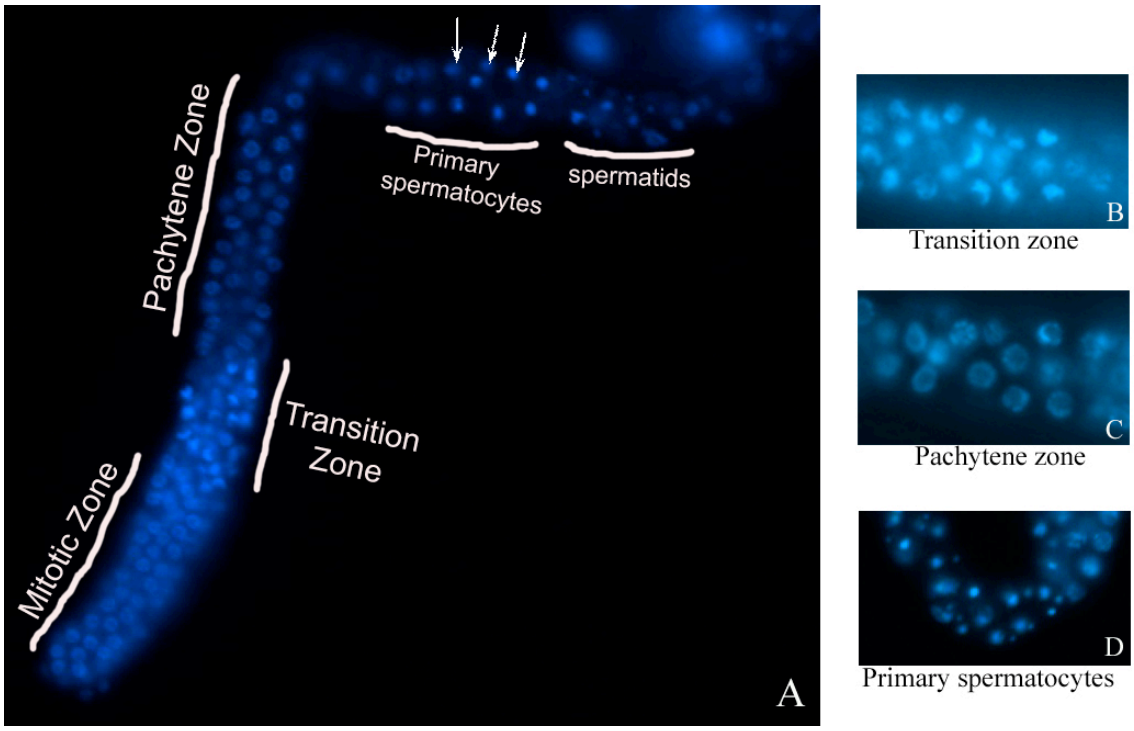

Figure 3-2: Progression of germline differentiation in the gonad during spermatogenesis.

(A) The distal tip of the gonad with mitotic nuclei progress further into meiotic cycle (C) at the gonad bent through the transition zone (B). The proximal region of the gonad illustrated the characteristic pattern of the primary spermatocyte nuclei in paired file. Spermatocytes complete the meiotic division budding off four haploid condensed sperm nuclei (D).

Terminally differentiated spermatids contain a haploid nucleus, many mitochondria, and fibrous body-membranous organelles (FB-MOs) described in detail in Ward et al., (1981) and Wolf et al., (1978). Components like ribosomes, tubulin and actin are left behind in the residual body, which is degraded or reabsorbed (Figure 3-1) (Machaca et al., 1996).

The spermatids are stored in the spermathecae within proximal region of the gonad in hermaphrodites and in the seminal vesicle of males as shown in Figure 3-3. Spermiogenesis, activation of spermatids into motile spermatozoa, occurs after mating for male sperm (Ward et al., 1983) and after entering the spermathecae for hermaphrodite sperm. The entire process of spermiogenesis is initiated and completed without any new protein synthesis. The *in vivo* signal for sperm activation is not yet known, but spermatid can be activated *in vitro* using chemical agents that elevate the pH of sperm cytoplasm, e.g. the ionophore monensin or the weak base triethanolamine (Argon and Ward, 1980; Ward et al., 1983).

The pseudopod is essential for motility in *C. elegans* sperm. Motility is achieved by continuous polymerization and depolymerization of the major sperm protein (MSP) in the pseudopod region (Roberts and Ward, 1982; Ward and Klass, 1982). MSP is synthesized very early as the primary spermatocytes cellularize and then MSP polymers are stored in the FB-MOs as spermatocytes mature into spermatids. FB-MOs and MSP go though dynamic spatial redistribution as the sperm cell differentiates into the motile spermatozoon (details in Roberts et al., 1986).

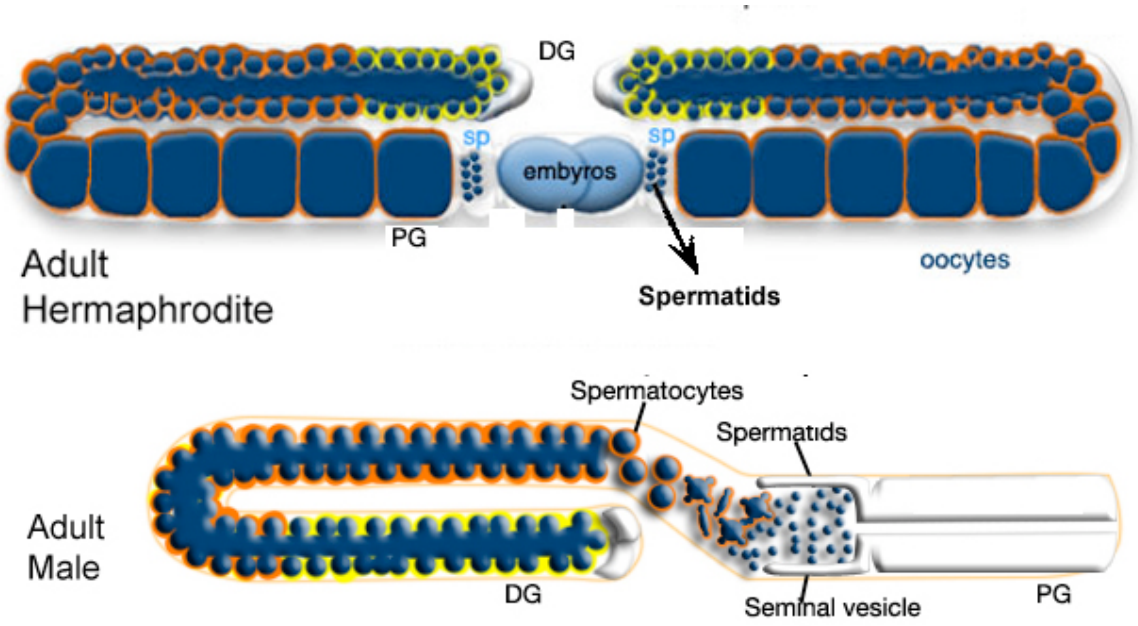

Figure 3-3: Germline distribution and morphology of hermaphrodite and male gonad.

Two armed gonad from hermaphrodite (top) and single armed male gonad (bottom) showing the distribution of germline. In hermaphrodites, spermatozoa are stored in spermathecae (sp) on each side of the uterus, while in males, spermatids are stored in the seminal vesicle in the proximal gonad (PG). DG: Distal gonad. Image adopted from Schedl et al., (1997).

The pseudopod is also required to maintain adherence to the spermathecal wall (Shakes and Ward, 1989; Ward and Carrel, 1979). As the mature oocyte enters the spermatheca, the spermatozoa release themselves from the wall and one of them fertilizes the oocyte (Ward and Carrel, 1979). The sperm are swept out of the spermatheca as the egg passes through the spermatheca and they need to crawl back with the help of pseudopod to position themselves again in the spermathecal wall invasions.

3.1.2 Mutational analysis of spermatogenesis in *C. elegans*

The hermaphroditic system of reproduction in *C. elegans* makes it easy to isolate and study spermatogenesis-defective (Spe) mutations. The Spe mutation can be maintained by mating sperm-sterile hermaphrodites to wild type males. The combination of genetics of *C. elegans* and cytological analysis of sperm development offers an easy tool to track the functional role of these Spe mutations in spermatogenesis.

Microarray analysis has been used to identify the genes expressed in *fem-1(h17)* hermaphrodites, which produce only oocytes, and *fem-3(q20)* hermaphrodites, which produce only sperm. Comparison of these two expression sets revealed 1343 genes enriched during spermatogenesis (Reinke et al., 2004, described in detail in the result section). Approximately sixty of these genes have been genetically characterized within the last two decades, but only half of them have been identified at the molecular level. These mutations are generally categorized in three types (Figure 3-4). The *spe-8* class affects spermiogenesis in hermaphrodites only ans comprises of 4 genes. The *spe-9* class, which affects sperm-oocyte interaction and thereby fertilization, comprises seven genes

and most of them encode transmembrane proteins (Chatterjee et al., 2005; Kroft et al., 2005; Singson et al., 1999; Xu and Sternberg, 2003).

The third class of mutations affects various stages of the development and leads to aberrant sperm. This class has helped to elucidate the spermatogenesis pathway based on their arrest points as explained in Figure 3-4. A few mutations like *cpb-1* and *wee-1.3* affect more general functions like translation or cell cycle control and arrest spermatogenesis during early stages of development (Lamitina and L'Hernault, 2002; Luitjens et al., 2000). Mutations that affect asymmetric distribution of components like *spe-26* and *spe-15* cause developmental arrest before completion of meiosis (L'Hernault et al., 1988; Varkey et al., 1995). One subset of this class produces 'terminal spermatocyte' arrest. These mutations impair FB-MO morphogenesis (e.g. *spe-4*, *spe-5*) affecting either spermiogenesis or maturation into spermatids (L'Hernault and Arduengo, 1992; P. Hartley and S.W. L'Hernault, unpublished results). This subclass is discussed in more detail in the discussion section.

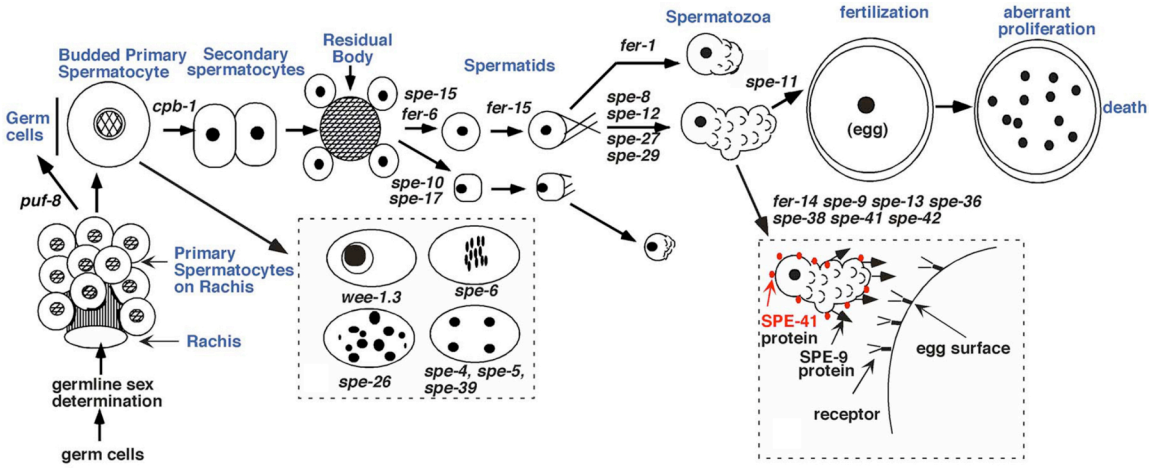

Figure 3-4: Schematic representation of mutations at their respective arrest points during spermatogeneis.

The diagram is taken from L'Hernault 2005. It shows the spatial positioning where the specified gene product is required based on their mutational analysis.

3.1.3 Putative transcriptional regulators expressed during spermatogenesis

Gene ontology annotation for the genes from the microarray analysis of germline-enriched genes (Reinke et. al., 2004) revealed about 4% of the sperm-enriched genes with predicted nucleic acid-binding domain. Only ten of those show significant homology to known DNA-binding domains (Table 3-1). These ten are important candidates to study gene expression regulation during spermatogenesis.

One of these ten is an established GATA transcription factor (Gilleard and McGhee, 2001; Page et al., 1997). *elt-1*, which encodes this GATA transcription factor, is well studied for its role in specifying hypodermal cell fate during embryogenesis (Smith et al., 2005). Mutant phenotypes during embryogenesis and further development have been characterized using genetic mutations and RNAi studies. The microarray experiment revealed up-regulation of this gene in during spermatogenesis, suggesting a novel function for ELT-1 during sperm development. ELT-1's role as a transcription regulator was confirmed when it was identified as a DNA-binding factor for a sperm-specific promoter sequence in yeast-one hybrid analysis (Smith HE, unpublished). *In situ* hybridization confirmed its expression in the spermatogenic germline (refer to Appendices).

We requested deletion alleles for the remaining nine putative transcription factors from *C. elegans* Knockout Consortium. The deletion allele for C25G4.4 was the first one to be available for study. This chapter will present genetic and cytological analysis of C25G4.4. The

Gene	Homology	Domain	Identity
ceh-1	Slouch	homeodomain	81%
elt-1	GATA binding protein GATA3	zinc finger	44%
nhr-43	retinoic acid receptor RRG1	zinc finger	26%
C17H12.9	hepatocyte nuclear factor HNF6	homeodomain	67%
C25G4.4	glucocorticoid modulatory element binding GMEB	SAND domain	37%
C44F1.2	glucocorticoid modulatory element binding GMEB	SAND domain	41%
F44D6.2	PRK1 associated protein AWP1	zinc finger	36%
F56F3.4	PRK1 associated protein AWP1	zinc finger	38%
F26F4.8	shavenbaby-ovo	zinc finger	28%
T20H4.2	Kruppel associated box KRAB	zinc finger	30%

Table 3-1: Putative sperm-gene regulators in *C. elegans* genome

Predicted transcription factors form the genome which show differential expression in the spermatogenic germline of *C. elegans*.

predicted protein sequence of C25G4.4 contains a SAND domain, a recently identified DNA-binding domain (Bottomley et al., 2001). According to the microarray data, it is expressed at two-fold higher level in spermatogenic germline than in oogenic germline (Reinke et al., 2000). *In situ* hybridization revealed specific spatial and temporal expression of the gene immediately prior to sperm production. Genetic analysis of a deletion allele of C25G4.4 has revealed its functional role during sperm development as indicated by the Spe phenotype, hence now it is called *spe-44*. Cytological analysis of this deletion allele of C25G4.4 showed a 'terminal spermatocyte' phenotype similar to the one observed in *spe-4*, *spe-5*, *spe-26* and *spe-39* mutations. Each of these genes has a distinct function in the spermatogenesis pathway, yet they produce the same mutant phenotype. If C25G4.4 is necessary for the expression of one or more of these genes and loss of C25G4.4 would lead to loss of expression of the downstream gene(s). This could be a possible explanation for the similar phenotype observed in these mutants. Thus, these genes could be the downstream targets of the putative transcription factor encoded by C25G4.4, functioning in the same regulatory cascade. The detailed analysis of the deletion allele of *spe-44* using cell biological and genetic tools and its functional role during sperm development is presented in this chapter.

3.2 Materials and Methods

3.2.1 Strains

C. elegans var. Bristol, N2 strain, was used as wild type. The strains used in this study were obtained from *Caenorhabditis* Genetics Center (CGC), unless otherwise mentioned. The alleles used were *dpy-20(e1282)IV*, *fem-1(hc17)IV* (Nelson, 1978), *fem-*

3(*q20*)*IV*, *him-5(e1490)V* (Hodgkin et. al., 1979). The deletion allele *ok1400* of C25G4.4 was obtained from *C. elegans* Knockout Consortium (http://celeganskoconsortium.omrf.org) as a heterozygous strain. The deletion strain has been assigned the name *spe-44* following the CGC nomenclature standards. The *spe-44(ok1400) dpy-20(e1282)IV* homozygous strain was created in the lab. Heterozygous strains of *spe-44(ok1400)IV* and *spe-44(ok1400) dpy-20(e1282)IV* over rearrangement *nT1* were created in the lab. This rearrangement is a translocation of chromosome IV and V that also contains an integrated transgene *qls51* with the green fluorescent protein (GFP). All strains were maintained on NGM plates seeded with *E. coli* (OP50) at permissive temperature of 15^0C unless otherwise mentioned. Genetic manipulations were carried out according to Brenner (1974).

3.2.2 Single Worm PCR

Individual heterozygous and homozygous *spe-44(ok1400)* and *spe-44(ok1400)dpy-20(e1282)* hermaphrodites were isolated based on the sterility phenotype at adulthood. Multiplex single-worm PCR was performed on 6 replicate samples of each genotype using the primers as diagramed in Figure 3-5.

For each reaction, a single worm was picked in a 2.5µl drop of worm lysis buffer (50 mM KCl, 10 mM Tris pH 8.3, 2.5 mM $MgCl_2$, 0.45% NP-40, 0.45% Tween 20, 0.01% gelatin and 60 µg/ml proteinase K) in the cap of 0.5µl PCR tube. The tube was spun briefly and frozen at -80^0C at least for 10 minutes. Before setting up the PCR, the

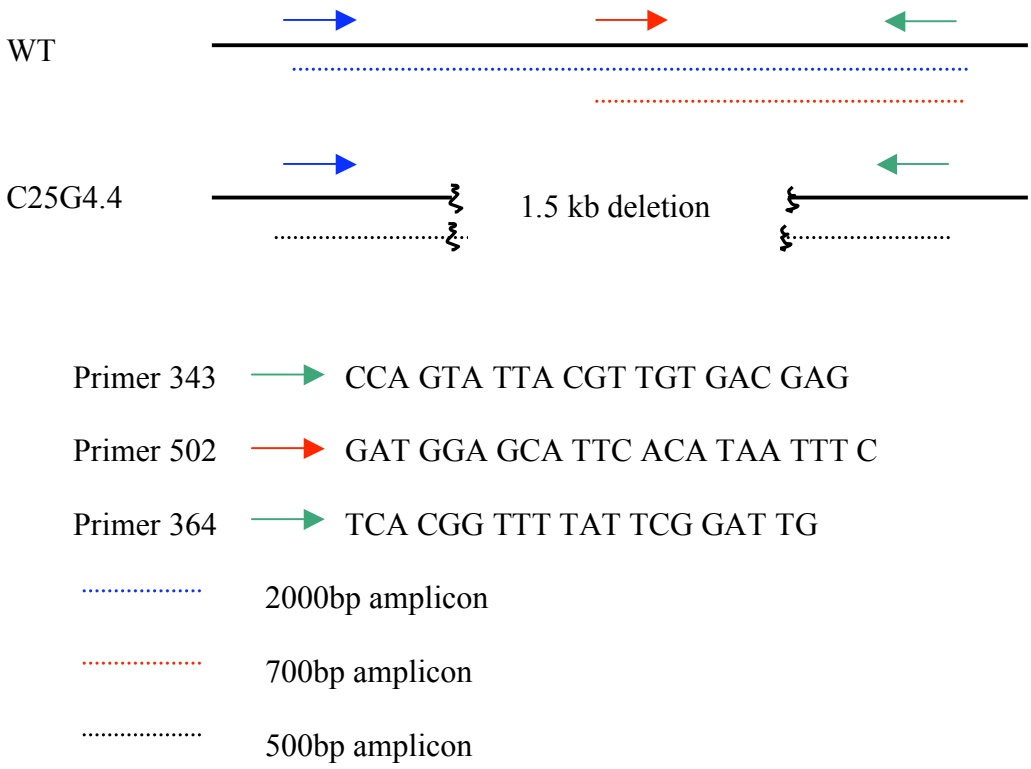

Figure 3-5: Cartoon of the primers used to detect C25G4.4 deletion.

Schematic diagram of the primers used to detect the deletion in *spe-44(ok1400)* strain compared to wild type worms.

worm was lysed at 65^0C for 1 hr 15 minutes and then at 95^0C for 15 minutes. After lysis, each tube was added with the multiplex PCR mix (with additional 1.5 mM $MgCl_2$) with primers 343, 502 and 364. The PCR was run at 37 cycles of 94^0C for 30 sec, 55^0C for 30 sec, 72^0C for 2 min with final extension of 3 minutes at 72^0C.

3.2.3 Worm microscopy

DIC microscopy was performed on staged worms and dissected gonads. The samples were mounted on 2% agar pads in M9 buffer (22 mM KH_2PO_4; 42 mM Na_2HPO_4, 85.5 mM NaCl, 1 mM $MgSO_4$). Nuclear morphology was visualized using DAPI stain. Worms were fixed in a series of 30%-65%-95% ethanol at 65^0C followed by acetone and then incubated with 100ng/ml DAPI in 1X phosphate buffered saline (PBS) (1.8 mM KH_2PO_4; 10 mM Na_2HPO_4; 137 mM NaCl; 2.7 mM KCl, pH 7.4) in the dark for 20-30 minutes. Dissected gonads were incubated in the dark with 100ng/ml DAPI in 1X PBT (PBS-Tween 20 0.1%) for 5-15 minutes. Images were taken with appropriate filters using Ziess AxioCam HRc and processed using software AxioVision Rel 4.6.

3.2.4 RNAi for C25G4.4

RNAi construct (TF1) was generated by cloning a 637bp region amplified from wild type genomic DNA into pPD129.36 between inverted T7 promoters using HinDIII and XbaI sites. The primers used were CCC AAG CTT ATG TTC GGT GGA GAC GTG and GC TCT AGA TCG TAG AAG TCG ATG GTC. The clone was then transformed in *E. coli* strain HT115.

Synchronized populations of N2 (wild type) hermaphrodites were grown until L2-L3. Sets of 20 hermaphrodites shifted to NGM + isopropyl-beta-D-thiogalactopyranoside

(IPTG) + ampicillin plates expressing *spe-44* RNAi construct or control (pPD129.36 in HT115 strain) in triplicate. The worms were maintained on RNAi plates until late adulthood and then were examined for unfertilized oocytes or sterility. Secondary *spe-44* RNAi was performed in the same manner on the F1 progeny from treated P0 hermaphrodites.

3.2.5 *In situ* hybridization

fem-3(q20) and *fem-1(hc17)* worm populations were bleached and hatched on NGM plate overnight at 15^0C. The hatched L1 larvae were shifted to NGM plates with food at 25^0C until appropriate stages. *fem-3(q20)* hermaphrodites produce only sperm while *fem-1(hc17)* produce only oocytes at 25^0C

3.2.5.1 Worm dissections

Synchronized populations of worm strains were obtained at L3, L4 and adult stages. The worms were collected in PBS with 0.25 mM leavamisole. 200-300 worms were dissected with a 20-gauge needle to extrude the gonad arms and then collected in sterile 3ml glass culture tube with the conical bottom.

3.2.5.2 ssDNA probe synthesis

spe-44 cDNA was amplified (1.3 kb fragment) from the clone pHS589B using anti-sense primer HES-539 (ACG ATC TTC TTT CTC CGA AG) and sense primer HES-540 (CTT TCT ATT ATC ATC ATT ATC CGC). Using this cDNA as a template, single-strand DNA was linearly amplified using either 3' anti-sense or 5' sense primer with a Digoxigenin (DIG) labeled mix according to the manufacturer's protocol (Roche). Amplified ssDNA was run on a denaturing agarose gel to confirm the single band and

size. ssDNA was then precipitated with 0.2M NaCl and ethanol and resuspended in 250µl hybridization buffer. The probe was boiled for 1hr and stored at -20^0C until use.

The probe concentration was determined by dot-blotting on a nitrocellulose membrane along with a marker of known concentration. The probe was detected using colorimetric assay with alkaline phosphatase (AP) conjugated anti-DIG antibody and nitro blue tetrazolium (NBT) and 5-bromo-4-chloro-3-indolyl phosphate (BCIP) called NBT/BCIP substrate by comparing the dot intensity to the control fragment. Both the sense and anti-sense probes were at 4ng/µl concentration. Prior to use, each probe was diluted 1:2 with the hybridization buffer and boiled for 5 minutes.

3.2.5.3 Gonad fixation and hybridization

This process was carried out according to the protocol by Min-Ho Lee and Tim Schedl (http://www.wormbook.org/toc_wormmethods.html) with minor modifications. After fixation, the gonads were treated with proteinase K for 1hr at the concentration of 100 µg/ml in PBT. Hybridization with the DIG-labeled ssDNA probe (150 pg/µl) was carried out at 48^0C for 36 hrs. Subsequent washes were also carried out at 48^0C. After blocking with bovine serum albumin (BSA), the DIG probe was detected by colorimetric assay of AP-conjugated anti-DIG antibody with NBT/BCIP substrate. Finally, gonads were mounted on an agar pad in PBS with 100 ng/ml 4'-6-Diamidino-2-phenylindole (DAPI) and the images were taken with Ziess AxioCam HRc and processed using software AxioVision Rel 4.6.

3.2.6 Western analysis

Homozygous and heterozygous *spe-44(1400)dpy-20(e1282)* adult males were maintained on food without hermaphrodites for 24 hrs. 50 adult males of each genotype were washed with 1X PBS and resuspended in 20 μl homogenization buffer with 1 μl of 1M DTT and 1 μl of protease inhibitor mix. The pellet was stored frozen at -80^{0}C. Immediately prior to SDS-PAGE, the pellet was boiled with equal volume of 2X sample buffer for 10 min. Equal volumes of the supernatants were loaded on the 10% SDS-PAGE gel after spinning at 6000 g for 10 minutes.

After running, the gel was equilibrated with 1X transfer buffer (25 mM Tris-HCl, 0.2 M Glycine) without methanol. The nylon membrane was activated in 100% methanol, washed with water and equilibrated with 1X transfer buffer for 20 minutes. The gel and the membrane were sandwiched between 2 sheets of 3MM Whatman papers soaked in 1X transfer buffer. The entire assembly was sandwiched in a cassette between 2 sponges soaked in 1X transfer buffer and the cassette was immersed in an electroblot tank containing 1.5 liters of 1X transfer buffer keeping the membrane towards the anode side. The transfer was carried out at 100V for 60 minutes. After transfer, the membrane was blocked in 5% milk (nonfat powdered milk) in TBST (20 mM Tris pH 8, 150 mM NaCl, 0.05% Tween-20) for 1hr at room temperature. The membrane was washed in TBST for 3 times at 15 minutes interval. It was then incubated overnight at 4^{0}C with polyclonal anti-MSP (a gift from Dr. David Greenstein, Kosinski et al., 2005) at 1:2000 dilution in 5% milk-TBST. The next morning, the membrane was washed and then incubated with horseradish peroxidase-conjugated anti-rabbit IgG (Pierce) 1:25000 diluted in 5% milk-TBST for 1 hr at room temperature. The membrane was washed 3 times with TBST and

then developed using Supersignal substrate (Pierce). The membrane was exposed to X-ray film in the dark for 1 to 40 minutes. The film was developed using AFP imaging system.

3.2.7 Microinjection rescue

Genomic region of 6449bp of *spe-44* amplified from N2 genomic DNA was cloned in pHS584 using SOEing PCR (Horton et al.1990). The primers used were HES-502+515 (GAT GGA GCA TTC ACA TAA TTT C and AAA AGG ATC CTT CGT CTA AAA AAC TCT ATT TTA AAG) and HES-364+516 (TCA CGG TTT TAT TCG GAT TG and AAA ACG GCC GTG AAA TTG TTA TGA AGT AAA TAT ATA TTT). Heterozygous *spe-44(ok1400)dpy-20(e1282)* worms were microinjected with a mixture of purified pHS584 and *pRF4* plasmid with *rol-6(su1006)* at concentrations of 4 and 200 μg/ml, respectively . Standard microinjection protocol (Mello et al., 1991) was followed. Stable roller transgenic lines were obtained by maintaining the injected worms at 15^0C. The rescue of sterility was scored by maintaining individual L3 dumpy roller hermaphrodite from F4 generation to a separate plate.

3.3 Results

Reinke et.al. (2004) performed microarray analysis to identify genes expressed specifically during spermatogenesis or oogenesis by comparing transcriptional profiles in *fem-3*(*q20*)*IV* and *fem-1(hc17)IV* strains. These mutations are both temperature-sensitive: the gain-of-function allele *q20* of *fem-3* causes only sperm production in the hermaphrodite germline (Barton et al., 1987) and loss-of-function allele *hc17* of *fem-1* causes only oocyte production in the hermaphrodite germline (Nelson et al., 1978). Out of 18,010 total genes on the microarray, 4245 genes showed differential expression between *fem-3(q20)* and *fem-1(hc17)* with 2 to 71 fold difference in the expression levels. Out of those genes, 1343 were overexpressed in *fem-3(q20)* compared to *fem-1(hc17)* and 702 showed significant enrichment in spermatogenic germline over oogenic germline (http://wormgermline.yale.edu).

Out of these 702 genes, 10 showed significant homology to reported DNA-binding domains based on the BLAST searches of NCBI nonredundant protein database, indicating their potential role in regulating gene expression specifically during sperm development. C25G4.4 is one of the genes that shows upregulation (2.215 fold) in *fem-3(q20)* worms compared to *fem-1(hc17)* and also 3.7 fold upregulation in wild type worms at L4 stage (when the worm germline is spermatogenic) compared to *glp-4(bn2)* which lack germ cells (Beanan and Strome, 1992). C25G4.4 is predicted to encode a 424-amino acid protein with a region from 65 to 150th amino acid homologous to the SAND domain (Figure 3-6). The SAND domain is a recently identified DNA-binding domain with KDWK conserved motif essential for DNA binding (Bottomley et. al., 2001). Strong

homology (37% identity to the SAND domain in GMEB protein with e-value of 1.2e-12) to this DNA-binding domain and overexpression in sperm-producing worms suggest that C25G4.4 is a putative regulator of sperm gene expression.

3.3.1 C25G4.4 RNAi produces no phenotype

To determine if C25G4.4 indeed plays a role during sperm development, RNAi was performed on wild type L2 larvae by feeding at 15^0C. Individual worms were maintained until late adulthood on the RNAi plates expressing C25G4.4 dsRNA or control RNAi with vector alone. Adult hermaphrodites were scored for the presence of unfertilized oocytes on the plates. This experiment was performed in triplicates with 20 individual worms in each. In all of these triplicate runs, all the adult hermaphrodites laid healthy brood and in normal numbers. None of the hermaphrodites laid any unfertilized oocytes during the first 4 days of the progeny-laying period.

In *C. elegans*, sperm-specific genes are particularly resistant to RNAi for unknown reasons. There are at least 11 genes on chromosome I known to play a functional role during spermatogenesis (L'Hernault et al., 1988). A large-scale RNAi feeding screen for genes on chromosome I, including all 11 known SPE genes, did not show any sperm-specific sterility (Fraser et al., 2000). Because of similar resistance to RNAi, it is possible that C25G4.4 RNAi did not reveal any sperm-specific fertility defects.

Figure 3-6: Alignment of SAND domain from homologous proteins.

Protein sequence alignment of pfam SAND domain with the SAND domain encoded in C25G4.4, DEAF-1 and GMEB proteins. The red box indicated the four most conserved residues, KDWK of the SAND domain.

3.3.2 Deletion in C25G4.4 causes sperm-specific sterility

We requested a deletion allele of C25G4.4 from the *C. elegans* Gene Knockout Consortium. The allele *ok1400* was created by the Knockout Consortium by trimethylpsoralen treatment with UV-crosslinking to induce deletion mutations and the mutation was identified by PCR screening using gene-specific primers (Barstead R.J. 2000). The allele contains a 1577bp deletion leaving only 150bp in the first exon and 71bp in the last exon and is predicted to encode a null mutation.

The strain carrying the *ok1400* deletion segregated worms that lay only unfertilized oocytes. These sterile hermaphrodites were able to produce viable progeny after mating with wild type males, which confirmed that the sterility is sperm-specific. The sterile hermaphrodites were backcrossed to N2 males a total of 6 times, selecting for sterile hermaphrodites each generation to eliminate other mutations from the genome. Heterozygous hermaphrodites were indistinguishable from wild type and segregated 24.6% sterile hermaphrodites of the total progeny further indicating that the allele is recessive. Single worm PCR was performed on the sterile and fertile hermaphrodites with multiplex PCR using a primer set external to the deleted region and one primer within the deleted region as shown in Figure 3-5. When the wild type copy of C25G4.4 is present in the worm, the primer sets would amplify two products of 2kb and 700bp. In a multiplex PCR, the shorter amplicon takes precedence and the 2kb product is never observed. A heterozygous worm, carrying a wild type copy and a deletion copy of C25G4.4 would give two products of 700bp and 500bp. A worm homozygous for the deletion would amplify only a 500bp product as shown in Figure 3-7.

In every reaction, the sterile hermaphrodites amplified only the 500bp product (Figure 3-7, Lane 1-6) demonstrating that these hermaphrodites were homozygous for the C25G4.4 deletion. Fertile hermaphrodites amplified either only 700bp (lane 7) or both 700 and 500bp products (lane 8-10) being either wild type or heterozygous for the deletion, respectively. Thus, sperm-specific sterility always segregated with homozygous deletion allele *ok1400* and is tightly linked to the C25G4.4 locus. Therefore, C25G4.4 was provisionally named *spe-44* according to the *Caenorhabditis* Genetics Center (CGC) nomenclature standards.

3.3.3 Balancer and marker linked strains for *spe-44*

For easy screening of sterile *spe-44(ok1400)* worms, the mutation was linked with the phenotypic marker, *dpy-20(e1282)*. The strain *spe-44(ok1400 dpy-20(e1282)IV* was created by crossing sterile *spe-44(ok1400)* hermaphrodites with *dpy-20(e1282)* males and then screening for sterile, dumpy recombinants. Mating these recombinants to wild type yield heterozygous *spe-44(ok1400) dpy-20(e1282)* hermaphrodites that segregate one quarter sterile-dumpy progeny as expected.

A balancer strain was created to maintain a population of homozygous sterile worms. *spe-44(ok1400)* was balanced over *nT1*, a translocation of chromosome IV and V, which has an integrated *qls51* transgene. The transgene expresses GFP in the pharynx of the worms carrying the *nT1* chromosome. Since worms homozygous for the

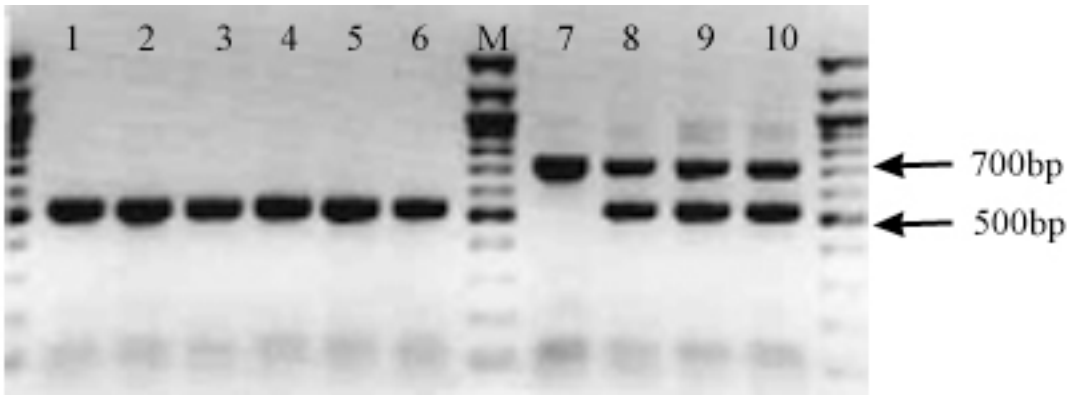

Figure 3-7: *ok1400* deletion is linked with sperm-specific sterility.

Multiplex PCR amplicons from sterile worms (Lanes 1-6) and fertile worms (Lanes 7-10). All the sterile worms show only 500bp amplicon while the rest amplify both, 700 and 500bp products (except lane-7).

translocation cannot survive, a population of heterozygous *spe-44(ok1400)/nT1* worms with glowing pharynx and homozygous *spe-44(ok1400)* worms with non-glowing pharynx is maintained. Segregation of total progeny of *spe-44(ok1400)/nT1* and *spe-44(ok1400) dpy-20(e1282)/nT1* balanced lines at 15^0C and 25^0C was tested. Proportion of homozygous *spe-44(ok1400)* or *spe-44(ok1400) dpy-20(e1282)* to heterozygous over *nT1* in the F1 progeny was 1:2 as expected, but no dead embryos for homozygous *nT1* were observed in both the strains tested.

3.3.4 Sperm-specific defect

In *C. elegans*, more than 60 mutations have been reported to affect spermatogenesis, which could be broadly categorized into developmental and functional defects. To determine which stage during sperm development is affected by the *spe-44(ok1400)* deletion, microscopic analysis was performed. Both wild type and heterozygous hermaphrodites showed normal sperm in their spermathecae (Figure 3-8A). To our surprise, the spermathecae of homozygous worms were without any sperm, as shown in Figure 3-8B.

There could be two possible explanations for the lack of sperm in the spermathecae of homozygous *spe-44(ok1400)* hermaphrodites. One possibility is that the germline in mutant worms never initiate sperm fate as observed for *fem-1* loss of function allele *hc17* (Nance et al., 1999). The other possibility is that the sperm development is defective in *spe-44(ok1400)* worms and as a result they get swept out of spermathecae as the hermaphrodites reach adulthood.

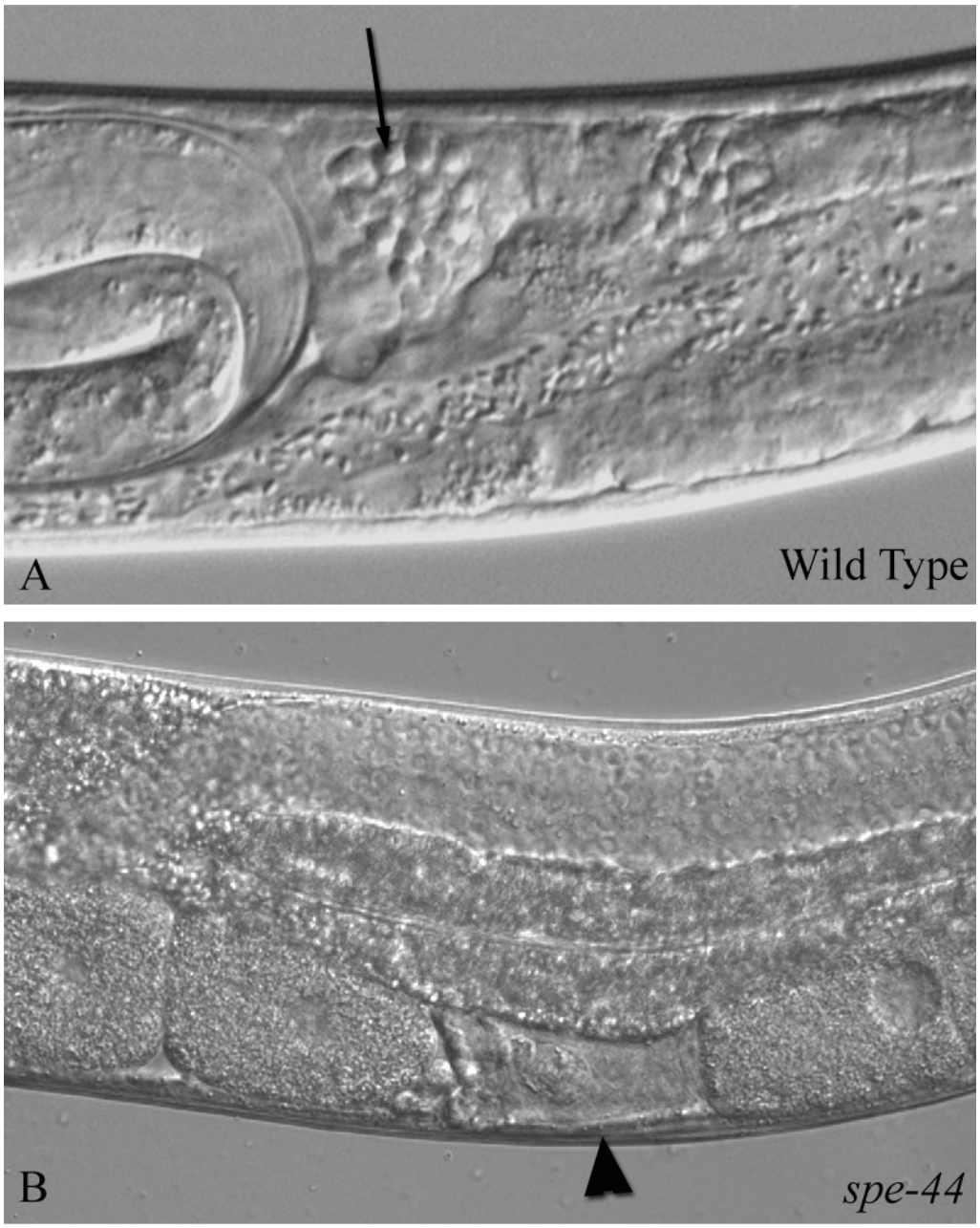

Figure 3-8: Adult hermaphrodite spermatheca.

Wild type (A) and homozygous *spe-44(ok1400)* (B) spermathecae. Arrow indicates mature spermatozoa and arrowhead indicates absence of spermatozoa. (100X magnification).

The hermaphrodite germline initiates sperm development during the L4 larval stage. To determine if homozygous *spe-44(ok1400)* worms initiate spermatogenesis or not, hermaphrodites were examined at the L4 larval stage. In heterozygous *spe-44/+* hermaphrodites, the germline contains a mixture of spermatocytes and differentiated spermatids in the most proximal region of the gonad (circle in Figure 3-9A). Spermatocytes also were observed in the homozygous *spe-44(ok1400)* hermaphrodites, but no spermatids were present. Even after the germline had switched to oocyte differentiation in these worms, only spermatocyte like cells were observed in the proximal-most part of the gonad Figure 3-9B. These spermatocyte-like cells are referred to as 'terminal spermatocytes' hereafter. Microscopic analysis of homozygous *spe-44(ok1400)* adult males also showed similar terminal spermatocytes in the germline with no differentiated spermatids.

3.3.5 Sperm development is arrested in meiosis

The *spe-44(ok1400)* mutant germline does not form functional spermatids. Cytological analysis of the germline was performed to check the developmental progression of the germline through spermatogenesis. Young adult hermaphrodite and adult male gonads were dissected and observed under DIC microscopy. Wild type gonads showed typical spermatids (arrows Figure 3-10, A-B) whereas *spe-44* gonads contained cells of spermatocyte size but no spermatids were observed (Figure 3-10, C-D). Some of the spermatocytes from the adult male gonad had a clover-leaf like structure (Figure 3-10D, inset), indicating that some of the cells attempted to divide.

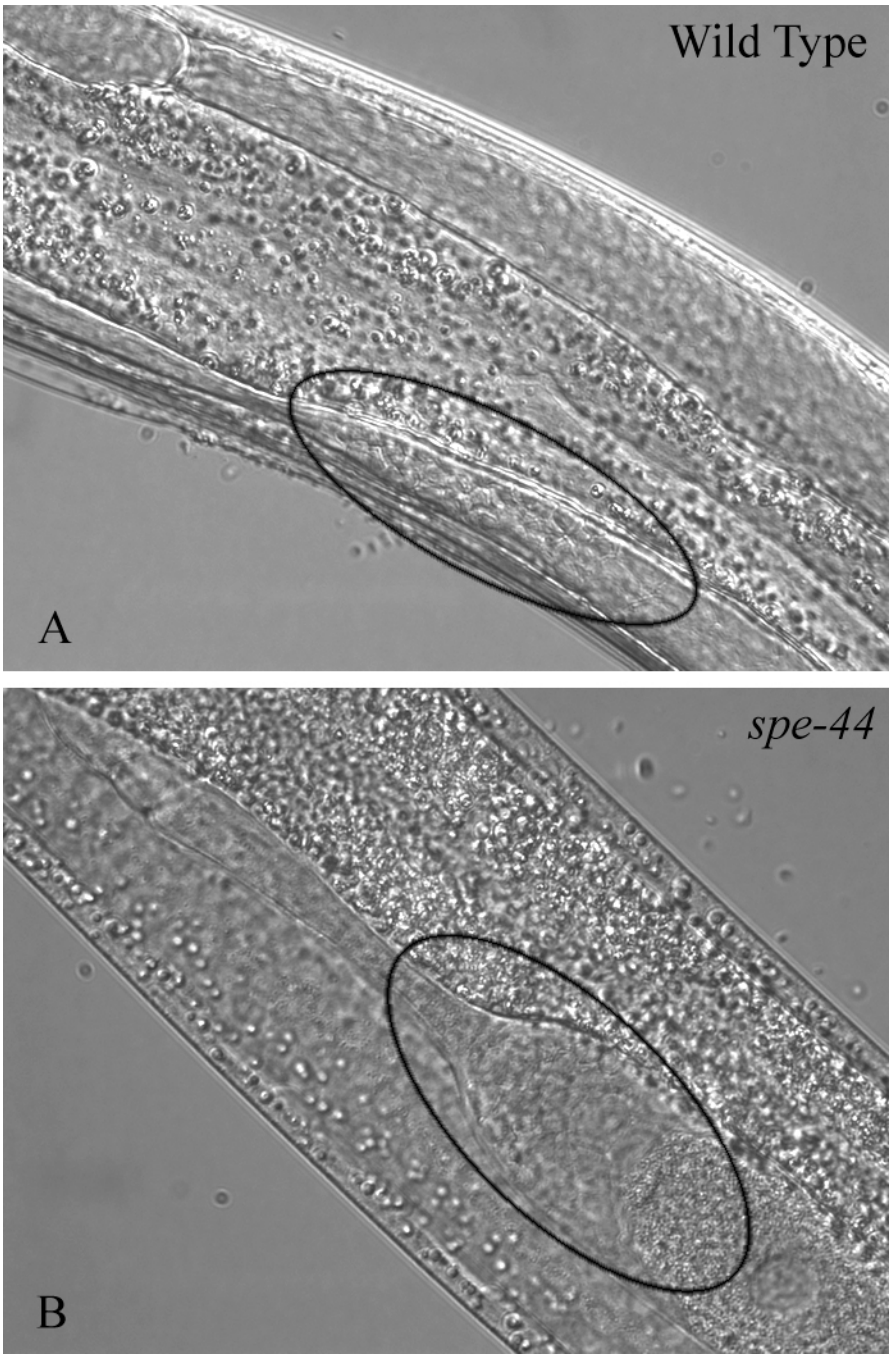

Figure 3-9: Proximal region of L4 hermaphrodite gonad.

DIC micrograph showing mature spermatids in wild type (A) and spermatocyte-like cells in *spe-44* (B) proximal region of the gonad. (100X magnification).

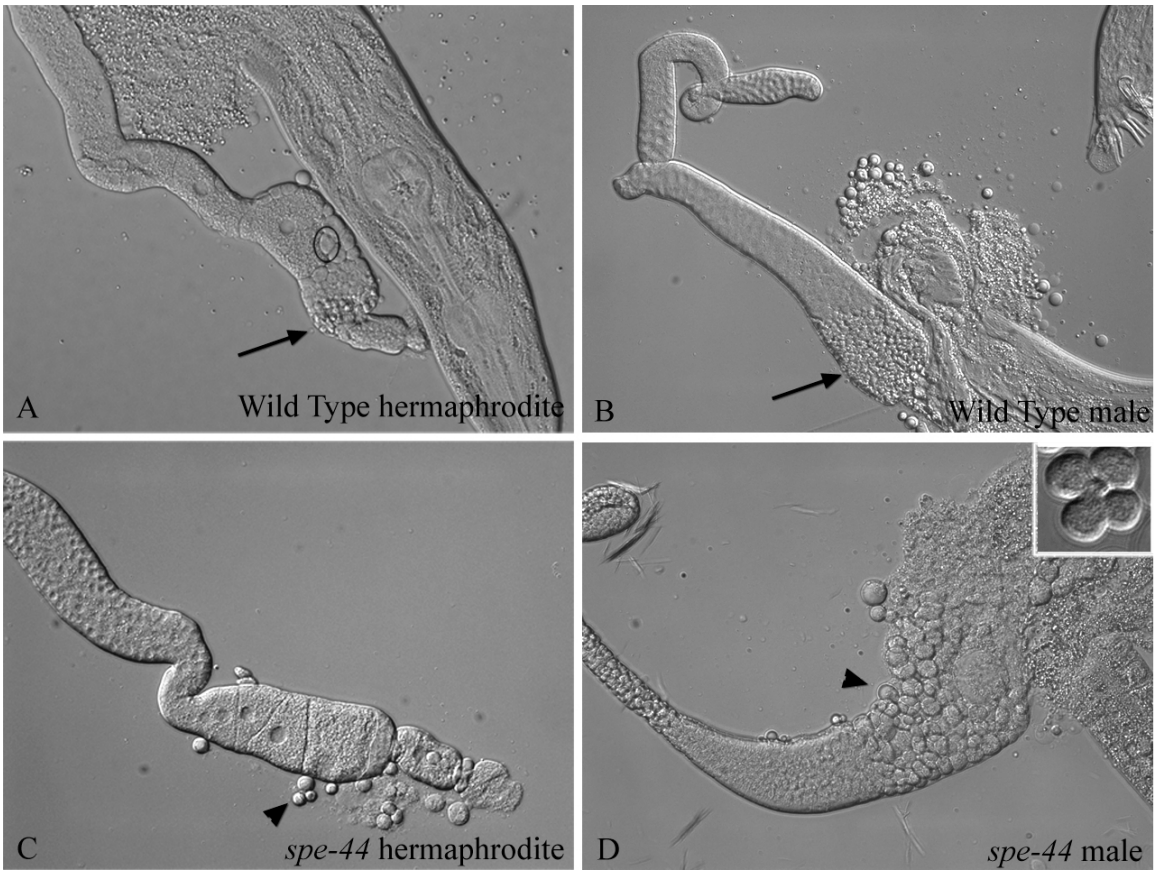

Figure 3-10: DIC micrograph of dissected gonads.

Dissected gonad from wild type hermaphrodite (A) and male (B) with spermatids (arrow) at the proximal region. The proximal region of the *spe-44* dissected gonads (C and D) show only spermatocyte like "terminal spermatocytes" (arrowheads) in the proximal region instead of mature spermatids. The inset in panel D shows one of the rare events when terminal spermatocyte attempts to divide.

DAPI staining of these dissected gonads revealed that the terminal spermatocytes typically contained 4 condensed nuclei (Figure 3-11, C-D). The morphology of the condensed nuclei within the cell is very similar to the nuclear morphology of mature wild type spermatids (Figure 3-11B). The presence of 4 condensed nuclei within the cell indicates that the spermatocyte completed karyokinesis during both meiosis I and II. However, the spermatids never separate from the residual body, although some do initiate the attempt (Figure 3-10D, inset). Thus, the *spe-44* mutant fails at cytokinesis, and sperm development in both male and hermaphrodite germlines arrests as a terminal spermatocyte just prior to the separation of haploid spermatids. Earlier progression of the germline through pachytene until the primary spermatocyte stage appears normal in *spe-44* worms (Figure 3-12) compared to the wild type germline (Figure 3-2A).

The motile pseudopod is necessary for maintaining localization to the spermatheca. As sperm development is not completed in the *spe-44* hermaphrodites, crawling spermatozoa are never formed and the terminal spermatocytes get swept away from the spermatheca with the passing oocytes (Figure 3-13). This phenomenon leads to empty spermathecea as the hermaphrodite reaches adulthood as shown in Figure 3-8B.

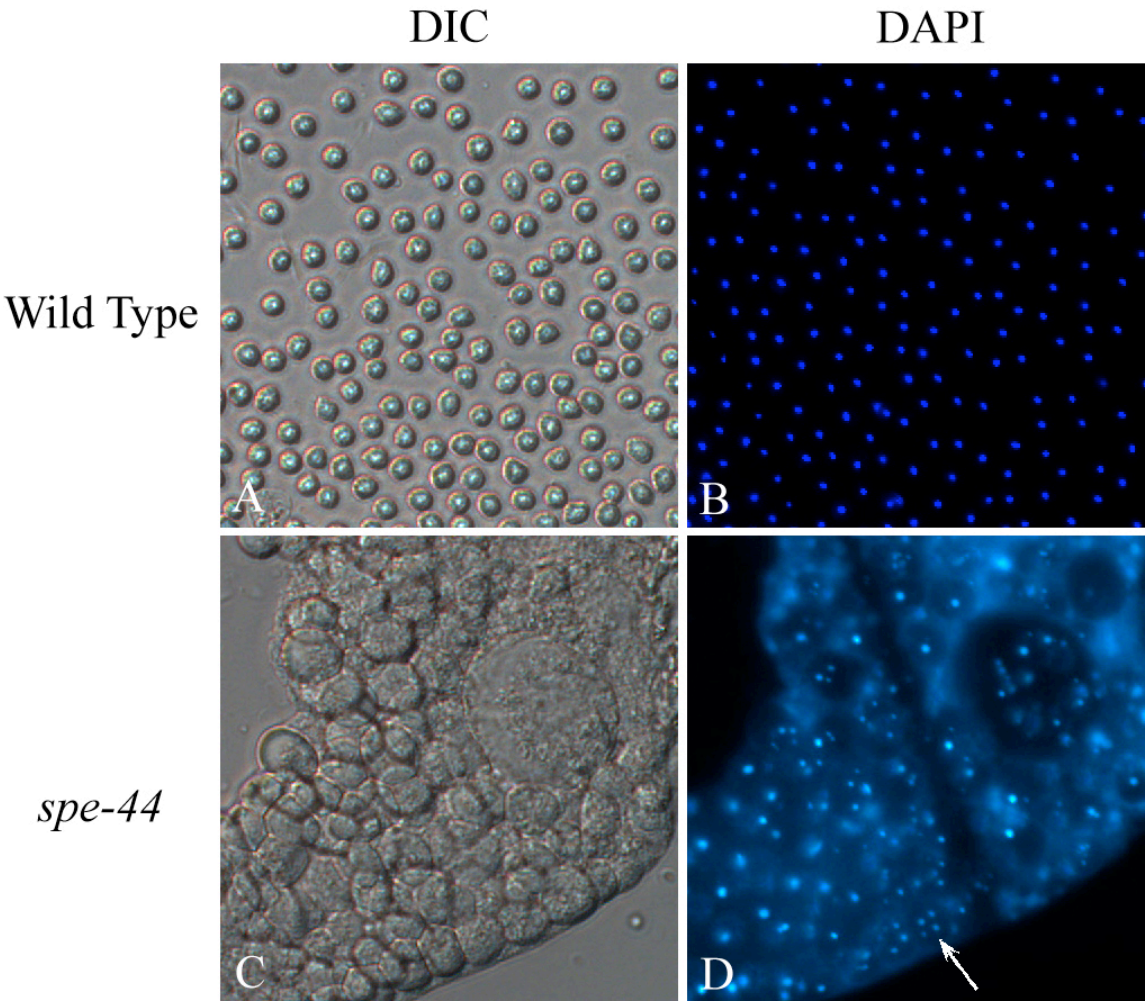

Figure 3-11: *spe-44* terminal spermatocytes with 4 condensed nuclei.

Isolated wild type sperm (A) showing single nucleus each (B). Terminal spermatocytes from *spe-44* male gonads (C) showing four condensed nuclei within the cell (D). 40X magnification.

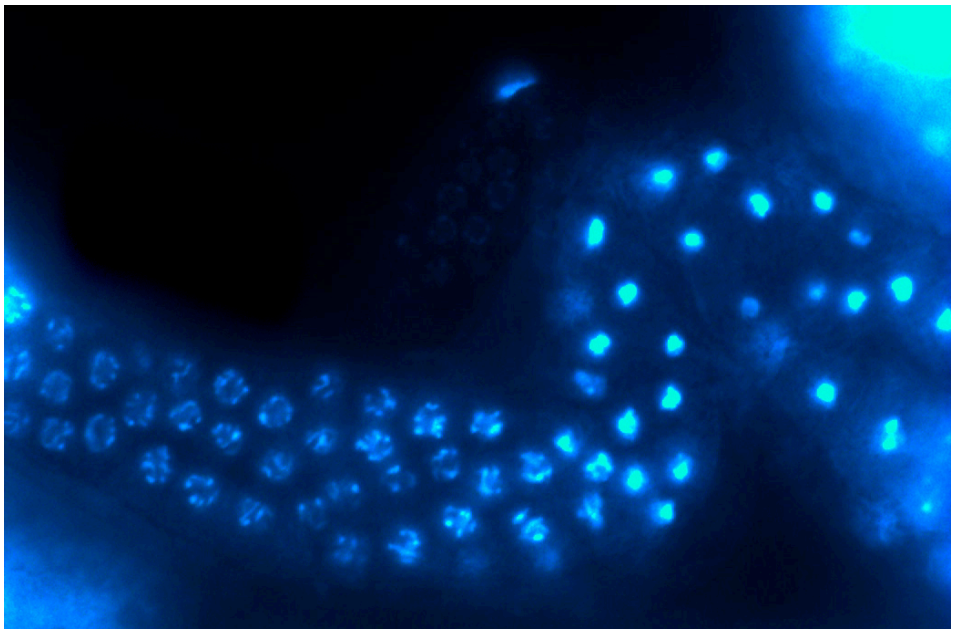

Figure 3-12: Early meiotic progression of *spe-44* germline.

Dissected gonad of *spe-44* adult male stained with DAPI shows normal 'bowl of spaghetti' pattern of pachytene nuclei and condensed nuclei of primary spermatocytes. (100X magnfication)

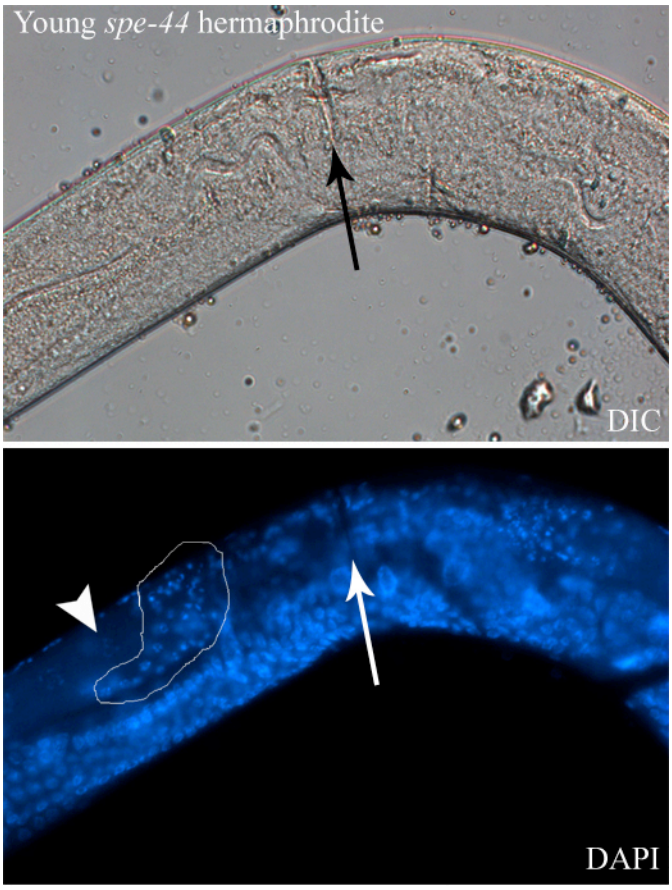

Figure 3-13: Spermatocyte sweep from the *spe-44* young hermaphrodites.
Lower panel shows the oocyte (arrowhead) sweeping terminal spermatocyte cell mass (outlined area) out from the vulval opening (arrow).

3.3.6 Spermatogenic fate is determined in *spe-44(ok1400)* germline

As a putative transcription regulator of sperm gene expression, it is possible that *spe-44* plays a functional role during differentiation of the germline or alternatively, in determining the fate of the early germline (L3 stage) to be spermatogenic. If the second explanation is correct, the spermatocyte-like cells observed in the proximal gonad of the L4 hermaphrodites could be cells undergoing meiosis without a specific fate determined. In wild type hermaphrodites, proximal germline cells are already determined to be sperm by the L4 larval stage. One of the first prominent sperm-specific genes to be expressed is the major sperm protein (MSP). The protein can be detected early in primary spermatocytes with anti-MSP monoclonal antibody. MSP is expressed solely during sperm development; for example, MSP is not detected in *fem-1* loss-of function mutants where the germline is always oogenic (Nance et al., 1999).

Western analysis with anti-MSP antibody on total protein extract from *spe-44/nT1* and *spe-44* adult males showed expression in both the worm strains (Figure 3-14). The total signal intensity in the protein extract from *spe-44* worms is reduced compared to heterozygous *spe-44/nT1* worms. As the germline in *spe-44* does not form terminally differentiated spermatids, the total number of cells with sperm fate is reduced compared to the heterozygous strain. This could lead to reduced signal in Western analysis. Nevertheless, the fate of the *spe-44* germline is already determined to be spermatogenic since MSP is expressed.

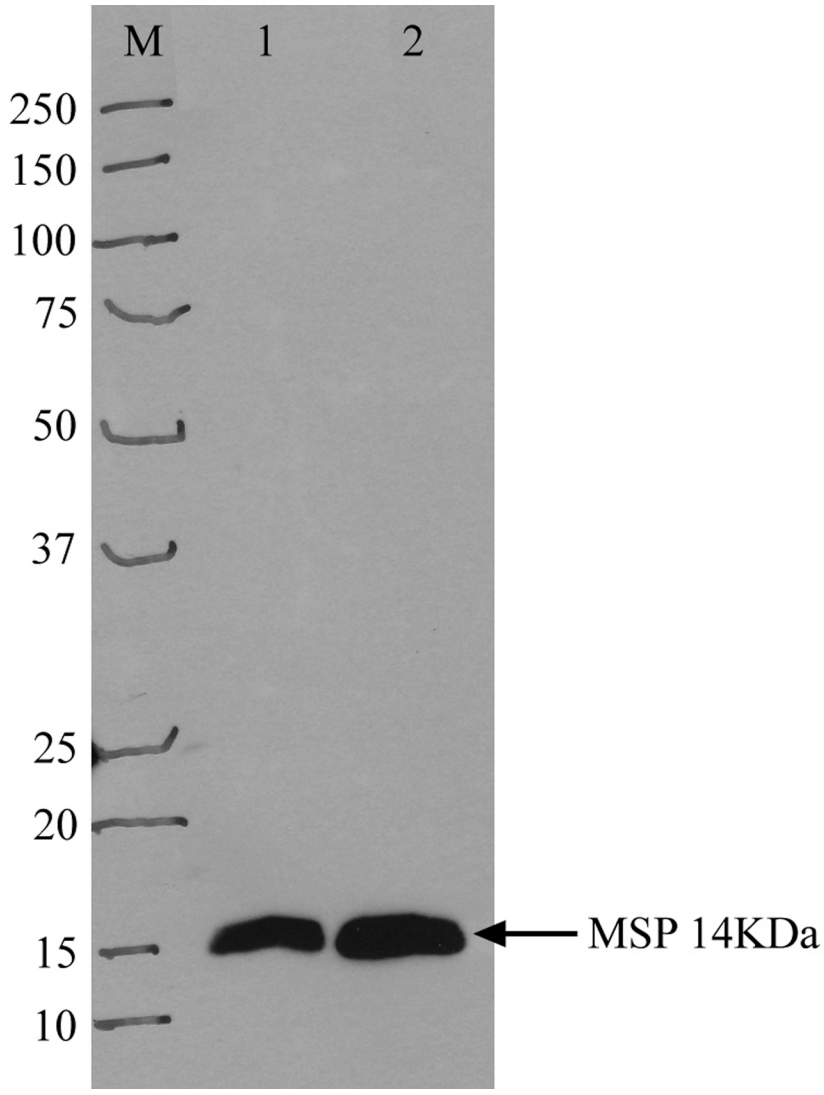

Figure 3-14: **Western analysis of *spe-44* males with Anti-MSP.**

MSP is expressed in both *spe-44*/*nT1* (lane 2) and *spe-44* (lane 1) males. *In vitro* expressed MSP with before and after induction was run as a control (data not shown).

3.3.7 *spe-44* is expressed in pachytene germline

Spermatogenesis is arrested as terminal spermatocytes in *spe-44* mutant worms. According to the hypothesis proposed in the Introduction section, SPE-44 is a putative transcription regulator of sperm gene expression. The observed arrest could be due to reduced or absent expression of downstream targets of *spe-44*, or inappropriate expression if SPE-44 acts as a repressor. If this hypothesis is true, *spe-44* itself should be expressed earlier in the germline during a narrow window of development.

spe-44 mRNA expression was tested by *in situ* hybridization with a *spe-44* cDNA probe on dissected gonads. Gonads from L3, L4 and young adult hermaphrodites of *fem-3(q20)* (which make only sperm) and *fem-1(hc17)* (which make only oocytes) worms were fixed and hybridized with the probe. *fem-3(q20)* gonads from the L3 stage of development show a very strong hybridization signal in the early meiotic germline. The average signal intensity observed in the similar meiotic region in L4 germline is reduced compared to L3 average intensity (Figure 3-15, A-B). The signal is altogether lost in the young adult germline (Figure 3-15C). None of the germlines of *fem-1(hc17)* worms show any hybridization signal (Figure 3-15,D-F). Thus, the oogenic germline does not express *spe-44* during any developmental stages, consistent with the microarray data from Reinke *et al.* (2004).

Higher magnification images of the germline with DAPI show the hybridization signal overlaps nuclei with the "bowl of spaghetti" pattern, which is characteristic of condensed chromosomes within the pachytene stage of prophase I of

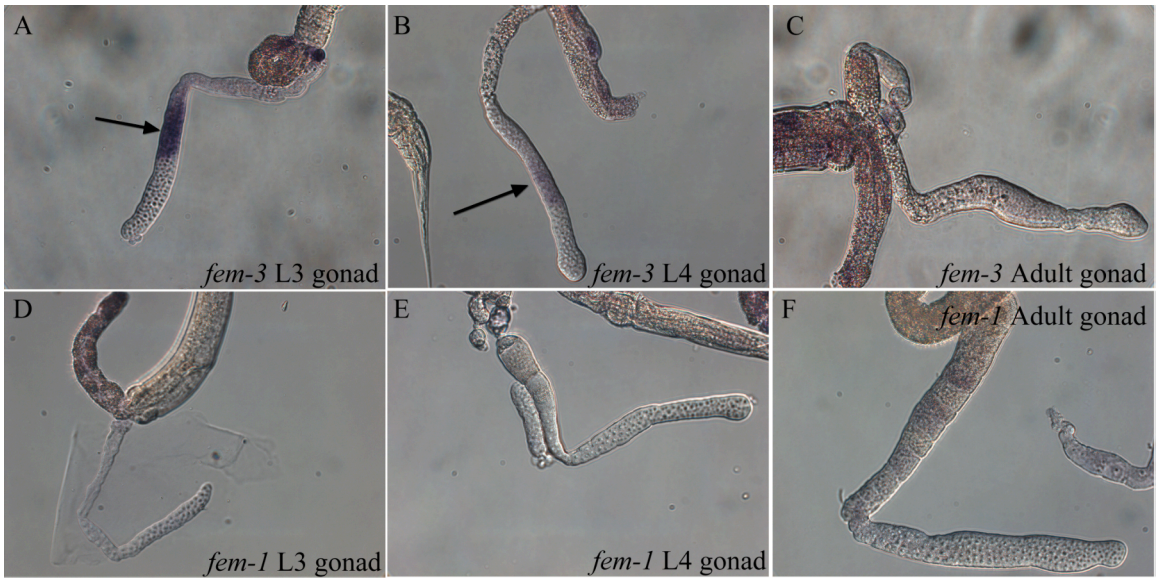

Figure 3-15: *In situ* hybridization on dissected gonads with *spe-44* anti-sense probe. *fem-3(q20)* gonads in L3 (A), L4 (B) and adult (C) stage with successively reduced hybridization signal (black arrows). *fem-1(hc17)* L3 (D), L4 (E) and adult (F) gonad with no hybridization signal.

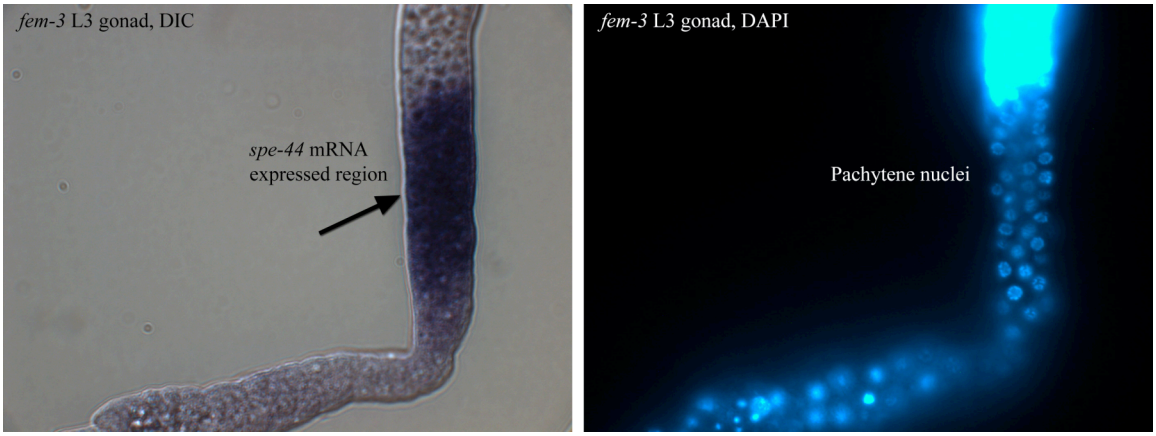

Figure 3-16: Spatial pattern of *spe-44* expression in the *fem-3* adult germ line with respect to cell cycle stage.

The DIC image on the left shows the *spe-44* mRNA expression (arrow) and the right panel is a corresponding DAPI image showing nuclear pattern. The expression is exclusively in pachytene stage of meiosis I.

meiosis I (Figure 3-16). The signal appears as soon as the germline enters meiosis and is expressed in a very brief window during meiosis, temporally and spatially just prior to the specification of spermatogenesis. Although *spe-44* is expressed in the pachytene zone, its function is not necessary until later stages of meiosis, as indicated from the morphological defect.

3.3.7.1 Microinjection rescue of *spe-44* sperm sterility

The wild type *spe-44* gene was cloned with approximately 1kb upstream and 700bp downstream sequence. The construct along with the *rol-6* marker was injected in heterozygous *spe-44(ok1400)dpy-20(e1282)/+* hermaphrodites. Dumpy and rolling worms were picked as transgenic and were screened for fertile hermaphrodites as a rescue of Spe. Two out of seven stably transmitted lines partially rescued the *spe-44(ok1400)* linked sterility, with the total viable progeny count of 62 ± 19 and 50 ± 35, respectively.

3.4 Discussion

C25G4.4 was identified as a putative transcription regulator based on its homology to known transcription factors, and had been shown to be up-regulated during spermatogenesis in *C. elegans* (Reinke *et al.* 2000). The deletion allele of the gene showed the Spe phenotype and hence the gene C25G4.4 was named *spe-44*. Detailed cytological analysis revealed that sperm development is initiated in *spe-44* mutant worms but arrests as terminal spermatocytes. The gene is expressed in a very specific spatial and temporal pattern immediately prior to sperm production.

C25G4.4 was classified as a putative transcription factor based on its homology with proteins containing the SAND domain. In C25G4.4, the domain encompasses amino acids 65-150 and shows 37% identity with the SAND domain in other proteins. Speckled protein 100KDa (Sp100), AIRE-1 (AutoImmune Regulatory-1), NucP41/75 and DEAF-1 (Deformed Epidermal Autoregulatory Factor-1) are the founding members that share the SAND domain. Several proteins that contain this 80 amino acid long SAND domain with the conserved KDWK core sequence are associated with various diseases. AIRE-1 is an autoimmune regulator type 1 protein that when mutated causes various autoimmune syndromes (Gibson et al., 1998; Park et al., 2003). The speckled protein family encodes components of nuclear bodies, which are linked with neurodegenerative disease and acute promyelocytic leukemia (Bloch et al., 1996; Hodges et al., 1998). One of the proteins of this family, Sp110, has been proposed to function as a nuclear hormone receptor transcriptional co-activator (Bloch et al., 2000).

Although the SAND domain does not show any considerable homology to known DNA-binding motifs, its ability to bind to specific DNA sequences and to regulate transcription is well established. The SAND domain in the proteins DEAF-1 (Gross and McGinnis, 1996), NUDR (Nuclear DEAF-1 Related) (Huggenvik et al., 1998), and GMEB (Glucocorticoid Modulatory Element Binding) (Christensen et al., 1999) have been proposed to mediate DNA binding in a sequence-specific manner. The SAND domain of NUDR has been shown to specifically bind to TTCG repeats (Michelson et. al., 1998 and Bottomley et. al., 2001), the SAND domain of GMEB binds ACGT core sequence (Surdo et al., 2003) and AIRE-1 binds ATTGGTTA or TTATTA motifs (Kumar et al., 2001). The SAND domain in NUDR and DEAF-1 bind to the TTCG

signature sequence as a monomer *in vitro* (Bottomley et. al., 2001). It is interesting to note here that the same domain in different proteins shows different binding specificities towards the nucleotide sequence.

Three-dimentional structure of the SAND domain has been resolved for Sp100 using NMR (Bottomley et. al., 2001) and for GMEB with X-ray crystallography (Surdo et. al., 2003). It reveals a novel fold for DNA binding (Wojciak and Clubb, 2001). Known DNA-binding domains contain helix-loop-helix or similar motifs, whereas the SAND domain consists of highly conserved positively charged α-helix with KDWK motif and β-strands. The motif KDWK is essential for DNA binding and single amino acid mutations in the motif abolish DNA binding *in vitro* (Bottomley et. al., 2001, Surdo et. al., 2003). Any mutation in the motif alone eliminates NUDR-dependent transcriptional repression *in vivo* (Bottomley et. al., 2001).

Based on the known role of the SAND domain in transcription regulation, it is highly likely that SPE-44 plays a similar role in *C. elegans.* Expression of *spe-44* is restricted to the germline just prior to the onset of sperm production, suggesting a regulatory role in sperm-specific gene expression. Northern blot analysis of rat NUDR also shows high expression in testicular tissue, specifically in spermatocyte cells (Huggenvik et. al., 1998). Human homolog of NUDR contains a bipartite Nuclear Localization Signal (NLS) as shown in the Figure 3-17, and mutation of the initial residues of the signal sequence eliminates the nuclear localization of hNUDR (Huggenvik et. al., 1998). *spe-44* is also predicted to contain a monopartite NLS (based on the prediction program MultiLoc; Nair et al., 2003), which maps to the exact same

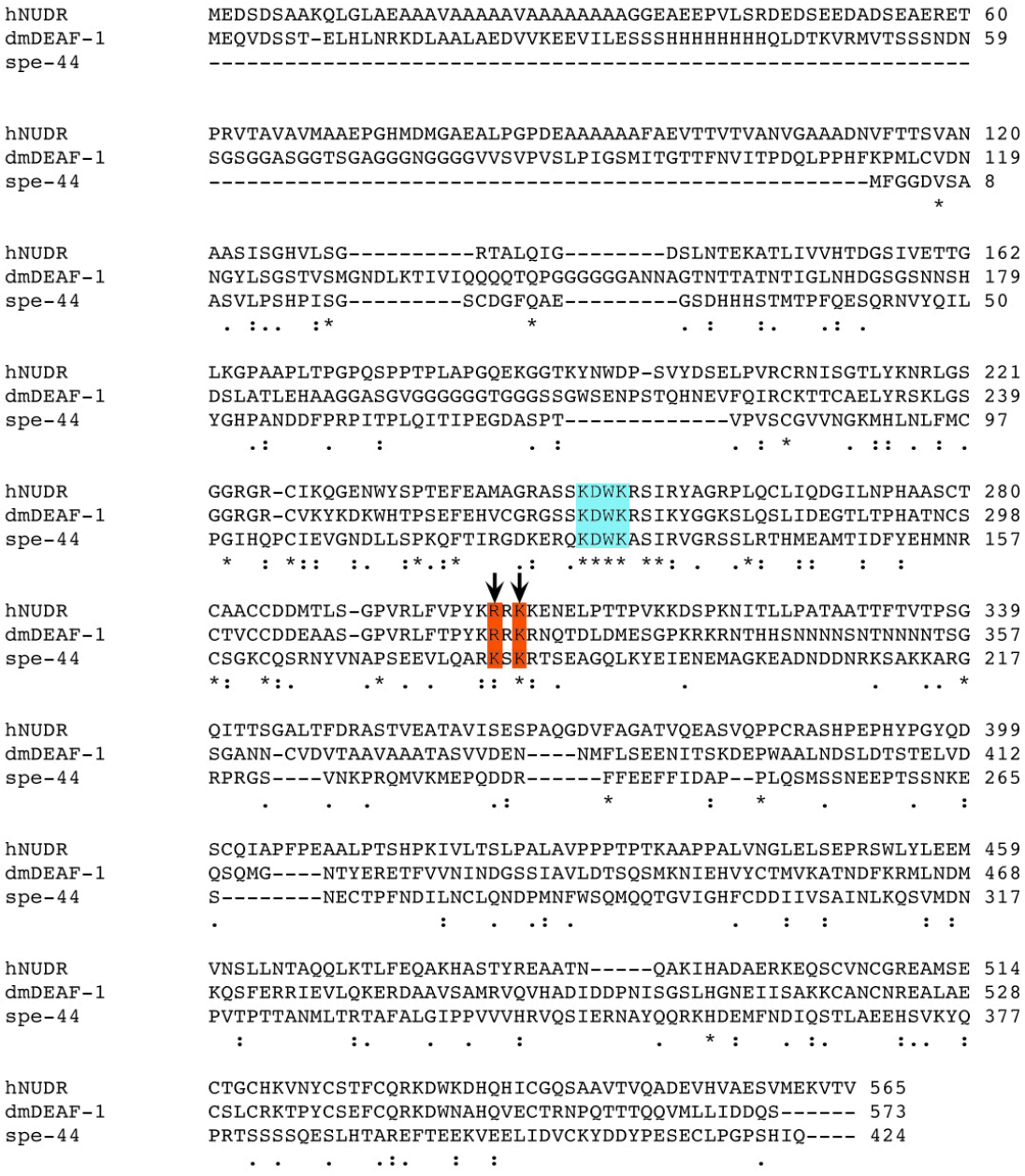

Figure 3-17: CLUSTALW 2.0.5 multiple sequence alignment.

SPE-44 sequence aligned with its homolog hNUDR, which also shows testicular expression in rat testis. The aqua box is the core sequence of SAND domain. The black arrows show the essential amino acids for nuclear localization.

location as that of NUDR (Figure 3-17, arrows), indicating SPE-44 to be a putative nuclear protein. Further, the study presented in this chapter strengthens the hypothesis that *spe-44* is a putative transcription regulator of sperm-specific genes.

Hermaphrodites carrying homozygous deletion allele of C25G4.4 lay unfertilized oocytes giving a classic SPE phenotype; hence the gene assignment, *spe-44*. Cytological analysis of these homozygous worms shows that loss of *spe-44* causes arrest of gamete development during spermatogenesis. Germline proliferation during spermatogenesis is normal until primary spermatocytes are formed. Arrest is observed at the cytokinesis step during meiosis and it specifies the precise window during sperm development where *spe-44* function is essential. Primary spermatocytes initiate meiosis and complete karyokinesis giving four condensed nuclei within the cell (the 'terminal spermatocyte' phenotype). Cytokinesis is either never initiated or not completed in these terminal spermatocytes. In contrast, the oogenic germline is completely unaffected by the loss of *spe-44*. Thus, *spe-44* seems to be essential during spermatid formation but not for oogenic development of the germline.

spe-44 is expressed in the spermatogenic germline just prior to the time when germline starts differentiating into sperm. Germline fate to spermiogenesis is determined prior to the expression of *spe-44*, as complete loss of *spe-44* does not affect MSP expression, a sperm-specific protein. *In situ* hybridization shows strong and uniform expression of *spe-44* in the pachytene zone during the L3 larval stage when the spermatogenic germline transits from the transition zone and enters meiosis. The expression of *spe-44* occurs in very restricted spatial context and it is also temporally transient. L4 germlines show reduced *spe-44* expression and by adulthood, expression

disappeared completely. Rat NUDR also showed a similar pattern of expression that was limited to spermatocyte cells and disappeared in later stages of development (Huggenvik et. al., 1998). Thus, *spe-44* is not essential for sperm fate determination or initiation of meiosis but is required for differentiation of the spermatogenic germline into spermatids.

As mentioned earlier, similar arrest as terminal spermatocytes is observed in five other Spe mutations; *spe-4*, *spe-5*, *spe-39*, *spe-26* and *cpb-1*. The first three proteins are required for the FB-MO morphogenesis and their loss of function affects the asymmetric distribution of FB-MO components during completion of meiosis. *spe-4* encodes a membrane protein that is a member of the presenilin family implicated in Alzheimer's disease onset (L'Hernault and Arduengo, 1992). Null alleles of *spe-4* lead to terminal spermatocyte phenotype due to the defective asymmetric partitioning of the FB-MO organelles. *spe-5* encodes an ortholog of subunit B of the cytoplasmic (V1) domain of vacuolar proton-translocating ATPase and mutations in *spe-5* lead to missegregation of tubulin at the end of the meiotic division leading to terminal spermatocyte arrest (Machaca et. al. 1997). *spe-39* mutants produce terminal spermatocytes that lack MOs; this gene encodes a cytoplasmic protein of unknown homology (Zhu and L'Hernault, 2003).

It is also possible that completion of the asymmetric distribution of cellular components is essential for initiation of cytokinesis after karyokinesis and the lack thereof results in the arrest of cytokinesis. As observed in *spe-26*, a kelch homolog in *C. elegans*, null mutation disrupts the segregation of various components like actin and also arrests the spermatocytes with multiple condensed nuclei (Varkey et. al., 1995).

cpb-1, which encodes a cytoplasmic polyadenylation element binding protein (CPEB), has a more general functional role and is involved in translational control of sperm-specific genes (Luitjens et. al., 2000). The *cpb-1* mutation causes development to stall at the primary spermatocyte stage and they never complete the meiotic divisions, in contrast to the previously described Spe mutations.

All of these five mutant terminal spermatocytes look morphologically similar (Figure 3-18) to the terminal spermatocytes observed in *spe-44*. Although their mechanistic action is required at the same spatial and temporal context, there is no correlation in the molecular nature of these gene products and in their modes of action. It is very tempting to speculate that one or more of these genes could be downstream targets that are transcriptionally regulated through *spe-44*. If this hypothesis is true, the expression of these downstream targets should occur spatially and temporally after *spe-44* expression. The microarray data does show that *spe-4*, *spe-5*, *spe-26* and *cpb-1* are up-regulated specifically during spermatogenesis (Reinke et. al., 2000). The spatial pattern of expression is known for three of these five targets. *spe-39* was shown to be expressed throughout the germline (Zhu et. al., 2003), while *spe-26* mRNA is expressed in spermatocytes and the earlier spermatogonial cells as well (Varkey et. al., 1995). According to their spatial context, *spe-39* seems to be expressed earlier than *spe-44* and is less likely to be a downstream target of *spe-44*, while *spe-26* could be a potential target of *spe-44*.

On the other hand, *cpb-1* mRNA is expressed in both the spermatogenic and oogenic germline. During spermatogenesis, it is expressed just distal to the developing spermatids as the immunohistochemistry data suggests (Luitjens et al., 2000). In the

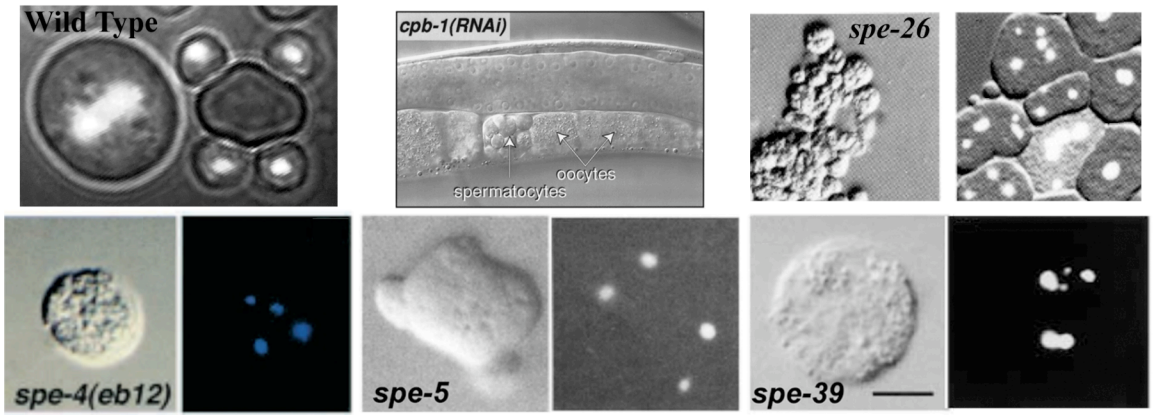

Figure 3-18: **SPE mutations with terminal spermatocyte phenotype.**

Wild type primary spermatocyte with single nucleus (left) and with four budding spermatids (right) showing DAPI stained nuclei. Compared to the aberrations caused by *cpb-1, spe-26, spe4*, *spe-5* and *spe-39* mutations (Luitjens et al., 2000, Varkey et al., 1995, Arduengo et. al., 1998, Machacha et. al., 1997, Zhu et. al., 1997).

germline context, this region immediately follows the pachytene zone where *spe-44* is expressed. Therefore, it is possible for *cpb-1* to be differentially regulated by *spe-44* with or without co-factors during spermatogenesis. *cpb-1* protein controls the translation of the target mRNAs by binding to the poly(A^+) tail of specific mRNAs. The downstream targets of *cpb-1* in the spermatogenic germline are not known. Translation of *spe-44* itself could very well be regulated by *cpb-1* and thereby lead to the terminal spermatocyte phenotype. It will be interesting to see if either gene is regulating the other.

The spatial expression pattern in the germline for the remaining 2 genes, *spe-4* and *spe-5* is not yet known. Quantitative RT-PCR experiments are ongoing to determine their expression levels in the *spe-44(1400)* background to validate if indeed their expression is regulated via *spe-44*.

SPE-44 is a potential transcription factor to regulate sperm-gene expression. In that case, it is likely to be regulating more than these five genes. The limitation of the current work is that not all the targets of SPE-44 are identified. The putative targets of *spe-44* could be uncovered by performing microarray expression analysis on the homozygous *spe-44(ok1400)* and compare the data set with microarray data of *fem-3(q20)* enriched genes. The genes enriched in *fem-3* but missing or downregulated (or up-regulated) in *spe-44* background would be the strong candidates for *spe-44* mediated regulation, either directly or indirectly.

This data set of putative targets could be used for promoter analysis to predict the putative binding site for *spe-44*. The nucleotide sequence present commonly in the promoter region of most or all of the putative targets is likely to be a binding site for SPE-44. This putative binding site could be validated with gel retardation assays. An

alternative approach to find the putative binding sites is CHIP-Chip assay. This approach would need a strong antibody to pull down SPE-44 along with its bound DNA from the nuclear extracts of the spermatogenic germline.

The putative binding sites of SPE-44 could be validated *in vivo* using reporter assays and transgenic rescue experiments. As mentioned in the introduction, about 60 of the sperm-specific genes have been studied in some detail. If any of these genes are revealed to be putative targets of *spe-44*, those could be employed for *in vivo* validation of results. For example, transgenic rescue of sterility of *spe-26* mutants has been demonstrated. The putative promoter of *spe-26* could be mutated to see if it can recapitulate the rescue of sterility caused by *spe-26* after microinjection. This complete study will definitely provide insights about transcriptional regulatory aspects of spermatogenesis in *C. elegans*.

Chapter 4 Discussion

Cellular differentiation into specialized cell types during development is brought about by temporal and spatial regulation of gene expression. Understanding the complexities of gene regulation is key to understanding the development of an organism. As many examples of diseases arise due to mis-regulation of gene expression, studying the underlining mechanisms of gene regulation also helps to uncover the disease principles and can lead towards the cure.

In *C. elegans*, spermatogenesis; the differentiation of a unicellular sperm from a constitutively proliferating germline, provides a good model system to study cell differentiation in a developmental context. This dissertation presents the study of mutations in two distinct genes isolated from screens for spermatogenesis-defective mutations. Both were initially believed to represent alleles of putative transcription factors and thereby thought to control sperm differentiation or a part of the process.

The first allele studied, *uba-1(it129),* was predicted to be an allele of the transcription factor *elt-1* based on the similar phenotypes and map position (refer to Appendices Section A2). *elt-1*, a GATA transcription factor, was known to be expressed and to play a role during spermatogenesis. Detailed genetic analysis and mapping proved *it129* to be an allele of the ubiquitin-activating enzyme (E1) and not a transcription factor. Analysis of *uba-1(it129)* led to the discovery of a novel role for ubiquitination in sperm development and function. It also revealed the role of ubiquitin conjugation in various developmental processes of *C. elegans* as described in Chapter II.

Ubiquitination has been implicated in various roles during spermatogenesis in mammals, including humans (Baarends et al., 1999). The ubiquitin system is intricately linked with DNA repair, regulation of meiotic chromatin, mitochondrial degradation and sperm quality control (Reviewed in Baarends et al., 2000). Mouse and human spermatogonia have been shown to express spermatogenesis-specific E1 isoforms (Kay GF 1991, Mitchell MJ 1992, Zhu H. et al. 2004). The mouse spermatogenesis-specific E1 isoform Ube1y is encoded on the Y chromosome, and deletion of the Ubel1y leads to spermatogenic failure despite expression of Ube1x isoform (Odorisio et al., 1996). The proposed reason for an additional E1-encoding gene devoted for sperm development is that it serves to increase UBE1 production at a time of high demand (Odorisio et al., 1996).

Although a role for ubiquitination during spermatogenesis is already indicated, the *uba-1(it129)* allele in *C. elegans* does not correspond precisely with any of the earlier reported roles for E1. Meiotic progression through spermatogenesis is normal and morphologically normal sperm develop in the mutant worms. These *uba-1(it129)* mutant sperm are sterile as they are incapable of fertilizing oocytes. Recent evidence from sea urchin experiments indicate a role for the ubiquitin-proteasome pathway for penetration through the vitelline layer of the oocyte by the acrosome-reacted spermatozoon (Sawada et al., 2002; Yokota and Sawada, 2007). Drug-induced inhibition of the 26S proteasome inhibited fertilization in these experiments. It is possible that the *uba-1(it129)* mutation impairs sperm-oocyte interaction because of reduced ubiquitination of surface proteins involved in mediating the interaction. It will be interesting to investigate the profile of ubquitin-tagged protein conjugates in wild type and *uba-1(it129)* sperm. A differential

profile could lead us to the proteins involved in sperm-oocyte interactions and help us to understand the ever-complex fertilization phenomenon.

The *uba-1(it129)* mutation affects sperm function during the sperm-oocyte interaction but does not lead to any meiotic aberrations during sperm development as observed for mutations in ubiquitin-conjugation system in other model organisms. One other aspect of *C. elegans* development where ubiquitin conjugation has been implicated to be essential is meiotic progression after fertilization and further embryo development. Many different mutations in the anaphase-promoting complex (APC), a multi-subunit E3 ligase complex led to this discovery. Severe mutations of the APC components lead to metaphase arrest (*Mat* phenotype) during the first meiotic division in the fertilized oocyte (refer to Chapter II). As the ubiquitin-activating enzyme (E1) works upstream of the APC complex, one would expect that impairment of E1 function would lead to a similar phenotype. Instead, *uba-1(it129)* was shown to slow down the meiotic progression rather than arresting it as the Mat phenotype (chapter II, Figure 7). This evidence leads to the conclusion that *uba-1(it129)* is a hypomorph of E1. Some of the other phenotypes manifested by the same allele show drastic aberrations in distinct developmental pathways like larval lethality and male paralysis. Why does a single point mutation in E1 enzyme lead to such diversity in the severity of the defects?

The vast number of E2 and E3s functioning downstream of E1 increase the complexity of the ubiquitin conjugation system. Distinct E3 complexes have been implicated in separate developmental pathways. The interaction between distinct E2-E3 complexes and E1 enzyme could differ in the their respective affinities. As a result, it is possible that different subsets of E2-E3 complexes bind differently to the E1 mutation.

Similar mechanisms are implicated for mutually excusive cell cycle arrest phenotypes manifested by distinct point mutations of E1 in human cell lines (Ayusawa et al., 1992; Jentsch et al., 1991; Zacksenhaus et al., 1990) and antagonistic effects on cell growth caused by distinct mutations in *Drosophila* E1 (Lee et al., 2008).

Recent progress in our understanding of ubiquitin conjugation has revealed increasing complexity of the system as E1-like enzymes known to activate Ubls have been shown to activate ubiquitin as well (Chiu et al., 2007). There are four known ubiquitin-activating enzyme-like proteins predicted in the *C.elegans* genome, but with the emergence of novel ubiquitin-like peptides and their respective E1-like enzymes, it is not unlikely to find more E1-like enzymes encoded in the genome. If similar cross-activity of E1-like enzymes as reported in other organisms exists in *C. elegans* as well, impairment of E1 enzyme itself would not affect the entire ubiquitin-conjugation as severely as one would speculate.

Concentration of free ubiquitin in the cell is critical for cell survival and proper function of the proteasome. How the concentration of free ubiquitin is maintained at appropriate levels (i.e., how ubiquitin homeostasis is maintained) is still not understood. Transcriptional and translational control of the polyubiquitin gene, the rate of free ubiquitin activation, and the rate of deubiquitination from the target proteins all coordinately contribute towards ubiquitin homeostasis. For example, the levels of cellular ubiquitin regulate the cellular abundance of proteasome-associated deubiquitinating enzyme Ubp6; under the conditions of ubiquitin depletion, Ubp6 levels increase (Hanna et al., 2003). In the absence of Ubp6, the half-life of ubiquitin is dramatically reduced and the cells become deficient in free ubiquitin levels (Chernova et al., 2003; Hanna et al.,

2003; Leggett et al., 2002). Ubiquitin-activating enzyme also regulates the free ubiquitin by controlling the rate of activation. In the mammalian cell line containing *ts85* mutation in E1, de novo synthesis of ubiquitin is reduced indicating some feedback mechanism for ubiquitin expression (Finley et al., 1984).

Any deviation from homeostasis is realized as a stress by the cell, which then responds to this stress by altering proteasome subunit composition (Hanna and Finley, 2007). Ubiquitin-dependent upregulation of Ubp6 results in greater loading of proteasomes with Ubp6, presumably resulting in greater efficiency of ubiquitin recycling at the proteasome (Hanna et al., 2003). Opposite to this scenario of ubiquitin depletion, functional impairment of ubiquitin-activating enzyme would lead to increase in the free ubiquitin pool, which also could lead to alteration in the subunit composition of the proteasome. The altered composition of proteasome might change its selectivity for particular E3 complexes and their target proteins, which could lead to inhibition of degradation in a selective manner. Thus, it is possible that the reduced activity of E1 enzyme in the *uba-1(it129)* mutant worms alters ubiquitin homeostasis. Some of the defects observed during development of *uba-1(it129)* mutant worms might be manifested as an indirect effect of the E1 mutation. The differential severity of the phenotypes could reflect the extent of deviation in the proteasomal subunit composition. It will be interesting to monitor the free ubiquitin pool at different developmental stages in wild type and mutant worms and also compare the 26S proteasome composition at those respective stages.

The second mutant studied is a deletion allele of a putative transcription factor with a SAND domain, *spe-44*. It is required for sperm differentiation, as the deletion

arrests spermatogenesis during cytokinesis after completion of meiotic karyokinesis. This terminal spermatocyte phenotype manifested by the *spe-44* deletion has also been reported for five different *spe* genes as discussed in Chapter III. None of these five genes encode a transcription factor. *spe-44* and these genes could be part of the same regulatory cascade as depletion of any of the genes leads to the arrest at the same developmental point during sperm differentiation. The expression of one or more of these genes could very well be regulated by *spe-44*, along with additional putative targets for *spe-44*. Microarray expression analysis in the *spe-44* deletion background would reveal the network of players involved in post-meiotic differentiation of *C. elegans* sperm.

How *spe-44* itself is regulated is an important question. The expression analysis showed transient expression of *spe-44* during the spermatogenic phase of the germline in a very narrow spatial window (Figure 3-14 and 3-15). To achieve this transient spatio-temporal expression, *spe-44* has to be under tight regulatory control.

microRNAs (miRNAs) could be regulating the depletion of *spe-44* mRNA observed in the late meiotic spermatogenic germline. miRNAs are single-stranded RNA molecules with approximately 21 or 22 nucleotides. They encode sequences complementary to the sites in the 3' untranslated region (UTR) of their target mRNAs. They function as inhibitory regulators of mRNAs either by decreasing target messenger RNA levels or by directly inhibiting their translation (Reviewed by Boyd, 2008). miRNAs are also proposed to destabilize the target mRNA via deadenylation of the poly-A tail (Standart and Jackson, 2007; Wu L et. al., 2006). Registry of annotated miRNA targets predicts three miRNAs (cel-miR-34, cel-miR-251 and cel-miR-272) with complimentary sequence in the *spe-44* 5' UTR (http://microrna.sanger.ac.uk/cgi-

bin/targets/v5/detail_view.pl?transcript_id=C25G4.4). The rapid depletion of *spe-44* mRNA observed in the germline at pachytene exit could be brought about by one or more of these miRNAs, although further investigation is necessary to validate these predictions.

Spermatogenic fate in the male and hermaphrodite germline is determined by *fog-3*, a member of Tob family of transcription cofactors, in conjunction with *fog-1*, which is a homolog of the cytoplasmic polyadenylation element binding protein (Chen P et al., 2000, Luitjens et al., 2000, Jin et al., 2001). Sperm fate determination is under direct control of the sex-determination pathway transcription factor TRA-1, as both *fog-1* and *fog-3* promoters contain multiple TRA-1 binding sites (Chen and Ellis, 2000; Jin et al., 2001) and *fog-3* expression has been experimentally shown to be under direct control of TRA-1 (Chen P et al., 2000).

FOG-1 protein is expressed from early L3 through the mid-L4 larval stage and disappears from spermatogenic precursors prior to expression of an early sperm-differentiation marker, SP56 (Lamont and Kimble, 2007). The extent and duration of *fog-1* directly determines the total number of sperm in the hermaphrodite germline (Lamont and Kimble, 2007). FOG-1 encodes a CPEB homolog, which binds to regulatory elements in the 3' untranslated region of target mRNAs and can either activate or repress their translation as demonstrated for *Xenopus* homolog (Richter, 2000). It could function as a sperm specification factor by initiating the expression of transcription factors such as *spe-44* and *elt-1*, which are essential for further differentiation of the sperm. It will be interesting to search for CPEB binding regulatory elements (CPEs) in *spe-44* UTRs.

Along with the expression initiation, suppression of the expression of *spe-44* after mid-L4 stage and post-pachytene germline has to be regulated. According the mRNA expression analysis, *spe-44* expression ceases during mid-L4 stage, when the germline switches the fate from spermatogenesis to oogenesis. During the fate switch, sperm-fate-determining factors like *fog-1* and *fog-3* are also downregulated. If *spe-44* is under direct or indirect control of these factors, one would expect that *spe-44* expression also will go down at the same time. Another possibility is that, as the germline switches the fate to oogenesis, transcription regulators needed for further specification and differentiation will be expressed in the meiotic germline. Analogous to antagonistic actions between the sub-networks of transcription factors in C-blastomere lineage specifications (Refer to Chapter I; section X), these oogenic transcription regulators could continuously shut down the expression of *spe-44* and other sperm-specific regulators.

A few details of the two ends of the regulatory cascade from determination of sperm fate till differentiation of functional spermatozoa have been characterized. As explained earlier, *fog-3* and *fog-1* are known factors required to specify the sperm fate. Many different genes have been identified at the end of the cascade, which play a role in sperm activation and functional aspects of spermatozoa (as reviewed in L'Hernault, 2005). The link between these two ends of the pathway is still missing. The transcription factors revealed from the microarray experiments (Reinke et al., 2004) are potential factors to initiate the expression of the downstream effectors and themselves could be under *fog-3* and *fog-1* control, either directly or indirectly. The experiments proposed above to understand the regulation of *spe-44* expression and the downstream targets of SPE-44 could provide insights for this missing link.

Chapter 5 Appendices

5.1 Western analysis of *uba-1(it129)* worms to detect ubiquitin-activating enzyme expression and ubiquitination of proteins.

5.1.1 Introduction

uba-1 encodes ubiquitin-activating enzyme (E1) in *C. elegans* (refer to Chapter II). It is the first enzyme in ubiquitin-conjugation pathway, which leads to poly-ubiquitination of target proteins. The allele $it129^{ts}$ encodes a point mutation in *uba-1*. The mutant protein is functional at permissive temperature, but at the restrictive temperature the mutation renders various developmental defects in *C. elegans*. To detect if the E1 protein levels are altered at the restrictive temperature, I performed Western analysis using anti-E1 antibody. Wild type *uba-1* cDNA was cloned in protein expression vector pET28a and *in vitro* protein induction was attempted to purify E1 protein to use as a positive control in the Western analysis.

Various developmental defects observed in $it129^{ts}$ mutant worms like embryonic lethality, sperm-specific sterility, male tail aberrations are more likely to be affected through independent E3 ubiquitin-ligases (please refer to chapter II discussion section). Since the E1 function is essential at the apex of the ubiquitin-conjugation function i.e. prior to all the E3 action, various defects in $it129^{ts}$ allele could be due to overall reduction in ubiquitin-conjugation. To test this hypothesis, I performed Western analysis with anti-ubiquitin antibody on total protein extracts from wild type and *uba-1(*$it129^{ts}$*)*worms.

Ubiquitination levels in sperm protein extracts were also analyzed by anti-ubiquitin Western as *it129*^{ts} mutation affects sperm function.

SP56 antibody was generated in Dr. Samuel Ward's lab against total sperm isolated from wild type *C. elegans* males (Ward et al., 1986). It was shown to recognize multiple bands up to 8 from total sperm protein extracts. Our speculation is that this antibody could be recognizing ubiquitin epitope from the sperm proteins. The staining pattern of this SP56 antibody was compared with anti-ubiquitin staining pattern for total sperm protein. The hybridoma culture supernatant of the SP56 antibody was a generous gift of Dr. Steven L'Hernault.

The methods and results for all these Western experiments are discussed in the following sections.

5.1.2 *uba-1* cDNA cloning and *in vitro* protein induction.

5.1.2.1 Methods

uba-1 cDNA was PCR amplified from cDNA pool extracted from *fem-1(hc17)* and *fem-3(q20)* worms. 3342 bp fragment was amplified using sense primer with NheI site CTA**GCTAGC**ATGACTACCATCCTTGAG and anti-sense primer with BamHI site CGC**GGATCC**TTAGAAAGAGTAGCG. The fragment was cloned into pET28a between NheI and BamHI. Selected clones were sequenced to confirm the correct coding sequence. The plasmid clone was transformed in *E. coli*; strain BL21(DE3). The expressed protein is predicted to be 1113 amino acids from the *uba-1* cDNA plus 19 amino acids from vector including 6 histidines. The approximate size of the expressed protein is 126 KDa.

One colony of pET28a:*uba-1*cDNA was grown in LB-kanamycin overnight culture at 37^0C. Culture was diluted to OD_{600nm}=0.05 and split in two batches of triplicates of 5 ml. One batch was grown at 37^0C and second was at room temperature. Both the batches were induced with 0.5 mM, 1 mM and 2 mM IPTG at OD_{600nm}=0.5. Samples were collected as 300 µl before induction (T_0) and at 1 hour after induction (T_1) and then 100 µl at every 3 hours (T_2 to T_6). Final sample of 100 µl was collected after overnight induction.

Collected samples were pelleted at 5000 g and the pellet was boiled with 50 µl 1X sample buffer (100 mM Tris-HCl, pH 6.8, 2% Sodium Dodecyl Sulfate (SDS), 20% Glycerol, 0.2% Bromophenol Blue, 2–10% β-mercaptoethanol). 20 µl of each sample was loaded on 4-20% SDS-PAGE gel along with NEB broad-range protein marker (P7702; 2-212 KDa).

5.1.2.2 Results

Wild type *uba-1* was expressed from pET28a bacterial vector (Novagen) for *in vitro* purification. Induction of a protein of molecular weight of 126 KDa was observed within 1 hour when induced with 2 mM IPTG and grown at 37^0C and in all the overnight grown cultures at room temperature with 0.5 mM, 1 mM and 2 mM IPTG. Protein band at 126 KDa was absent in uninduced (T_0) samples. Refer to Figure 5-1.

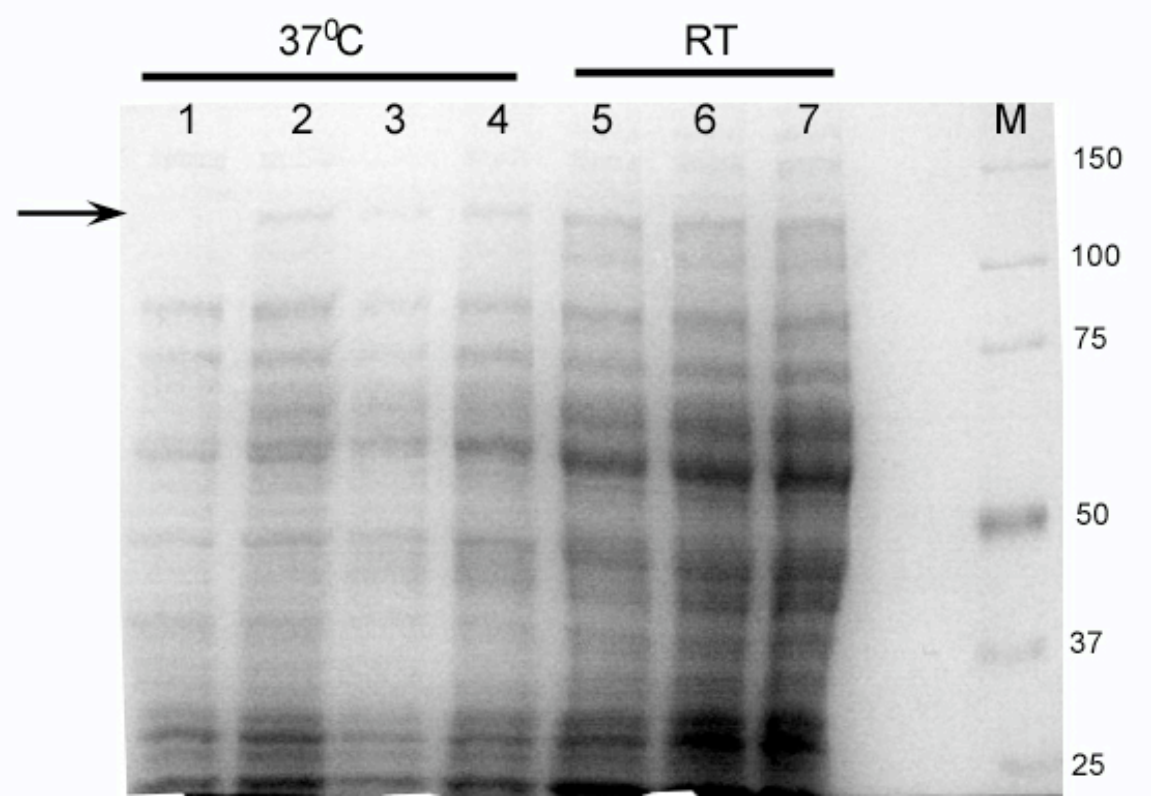

Figure 5-1: Coomassie gel with crude protein extract from bacterial pellet expressing Ce-UBA-1.

Lanes 1-4, bacterial protein extracts induced with 2 mM IPTG at 0 hr (lane 1), 1 hr (lane 2), 6 hr (lane 3) and overnight induction point. Lanes 3-7, bacterial extracts after overnight induction with 0.5 mM, 1 mM and 2 mM IPTG. Lane M is the protein marker indicated with the size standards on the right. The arrow indicates the induced E1 protein at approximately 126 KDa size.

Although the E1 protein band of expected size was observed after IPTG induction, the expression level needs to be improved to be able to purify E1. Trials are ongoing currently to improve the expression using different growth media. Since the pure protein was not obtained, it was not included in the following Western analysis. Instead, total cell extract from a human cancer cell line was included as a positive control.

5.1.3 Western blot analysis with anti-E1 (ubiquitin-activating enzyme) antibody.

5.1.3.1 Methods

5.1.3.1.1 Total protein preparation from adult worms

Synchronized populations of worm strains were raised at appropriate temperature (15^0C or 25^0C) in 25cm peptone plates with NA22 bacteria. Worms were washed with M9 and pelleted in a tight pellet of 100μl in homogenization buffer (15 mM Hepes pH7.5, 10 mM KCl, 1.5 mM $MgCl_2$, 0.1 mM EDTA, 0.5 mM EGTA, 44 mM Sucrose) with 1μl of 1M DTT and 3μl of protease inhibitor mix (1 μg Pepstatin, 1 μg Leupeptin, 4 μg Aproteinin and 10 μM MG132-26S proteasome inhibitor). The pellet was frozen at -80^0. The pellet was homogenized before it was completely thawed using handheld homogenizer with additional 1 μl of 1M DTT and 3 μl of protease inhibitor mix for about 40 seconds until it was thick slurry. The slurry was boiled for 10 minutes with equal volume of 2X sample buffer (4%SDS, 100 mM Tris-Cl pH 6.8, 20% glycerol). Then it was passed through 26G syringe for 2-3 times and centrifuged at 10,000 g for 10 minutes.

The supernatant was stored at -80^{0}C. Samples were loaded with 1 µl of 1M DTT and 1 µl of 10X Bromo-phenol blue solution.

5.1.3.1.2 Total protein preparation from isolated sperm

This protocol was adopted from the one developed in Dr. Ward's lab (Klass, M.R et al. 1981). Large synchronized populations of worms enriched for males (Him strain) were grown till young adulthood at appropriate temperature. Worms were rinsed with M9 buffer twice and left in 5 ml volume of M9 buffer. These worms were passed through sterilized 35 µm mesh screens into 15 cm containing M9 for about 30 minutes. The males being smaller in diameter pass through the mesh. The flowthrough with males was concentrated by centrifugation at 2000 rpm with 2 minutes spin. The males were grown for additional 24 hours on bacteria to maximize sperm production.

Purified males were rinsed three times in PSM (10 mg/ml polyvinylpyrrolidone, 45 mM choline chloride, 25 mM KCl, 10 mM HEPES (K), pH 7.3, 0.1% glucose, 1 mM $MgSO_4$, 1 µg/µl leupeptin, 1 µg/µl pepstatin A, 5 µg/µl aprotinin). A plain, sterile microscope slide was placed into 10 cm glass petri dish (sterile) and up to 500 µl male suspension was dispensed onto the slide. The slurry was chopped with sterile razor blade for five minutes, using slicing motion. The slide and the razor were rinsed with 5 ml of PSM into 15 ml centrifuge tube. The volume was dispensed onto the surface of sterile 10µm screen and rinsed twice with 5 to 10 ml PSM. 10 ml aliquots of the flow through were carefully underlaid with 3 ml 10% (v/v) Percoll in PSM in 15 ml centrifuge tubes with Pasteur pipette. The interface was gently mixed by stirring the pipette tip. The tubes were centrifuged at 500 g for 10 minutes and supernatant was aspirated gently. The

sperm pellet was resuspended in 2 ml PSM and was washed twice at 750 g for 3 minutes. Total sperm present in the solution were counted using hematocytometer. The pellet was either frozen at -80^{0}C or resuspended in 1X SDS sample buffer to give 5 μg/μl total protein concentration (3 x 10^7 sperm ≡ 480 μg of protein).

5.1.3.1.3 Total protein isolation from human cell line ChaGo-K-1 (ATCC# HTB-168)

Total protein from human lung cancer cell line was isolated to use as positive control for the Anti-E1 Western. One flask of confluent culture was a generous gift from Dr. Turko, it washed with 2ml of 1X PBS containing protease inhibitor mix. 1 ml volume was sonicated 3 times at 40% with smallest tip using Branson Sonifier-450. The sample was centrifuged at 120K g for 3 minutes at 4^{0}C. The supernatant and the pellet were frozen at -80^{0}C. 150 μl supernatant was used to precipitate protein using chloroform/methanol precipitation method. Protein concentration was 0.57 μg/μl as estimated by Bradford method.

5.1.3.1.4 Western Transfer

After running the SDS-PAGE gel for protein separation, the gel was equilibrated with 1X transfer buffer (25 mM Tris, 192 mM Glycine, 0.1% SDS) with 20% methanol. PVDF membrane was activated in 100% methanol, washed with water and was equilibrated with 1X transfer buffer for 20 minutes. The gel and the PVDF membrane were sandwiched between 2 sheets of 3MM Whatman papers soaked in 1X transfer buffer. The entire assembly was sandwiched in a cassette between 2 sponges soaked in

1X transfer buffer and the cassette was immersed in the Hoefer tank containing 1.5 liters of 1X transfer buffer keeping the PVDF membrane towards the anode side. The transfer was carried out at 100V for 70 minutes. After transfer, the membrane was blocked in 5% milk (nonfat powdered milk) in TBST (20 mM Tris pH 8, 150 mM NaCl, 0.05% Tween-20) for 1hr at room temperature. The membrane was washed in TBST for 3 times at 15 minutes interval. It was then incubated overnight at 4^0C with mouse monoclonal Anti-E1 (Sigma #E3152) at 1:500 dilution in 5% milk-TBST. The next morning, the membrane was washed and then incubated with HRP conjugated Anti-mouse IgG_1 (Stressgen # SAB-100) 1:2000 diluted in 5% milk-TBST for 1 hr at room temperature. The membrane was washed 3 times with TBST and then developed using PIERCE Supersignal substrate (# 34077). It was then exposed to X-ray film in the dark for 1 to 40 minutes. The film was developed using AFP imaging system.

5.1.3.2 Results

5.1.3.2.1 *uba-1* protein expression in wild type and *it129^{ts}* worms.

To determine if expression level of E1 was affected by the *it129^{ts}* mutation, Western analysis was performed on total protein extracts of wild type and mutant males raised at 25^0C. Human ubiquitin-activating enzyme (E1) was detected at appropriate 117KDa position on the blot (Figure 5-2). Although the predicted size of *C. elegans* ubiquitin-activating enzyme (E1) is 124 KDa, multiple bands were observed in worm protein samples at 100 KDa, 150 KDa and between 150 KDa and 250 KDa. The band sizes observed above 120 KDa could be isoforms of worm E1 as shown for E1 from mammalian system (Cook and Chock, 1992). The Expressed

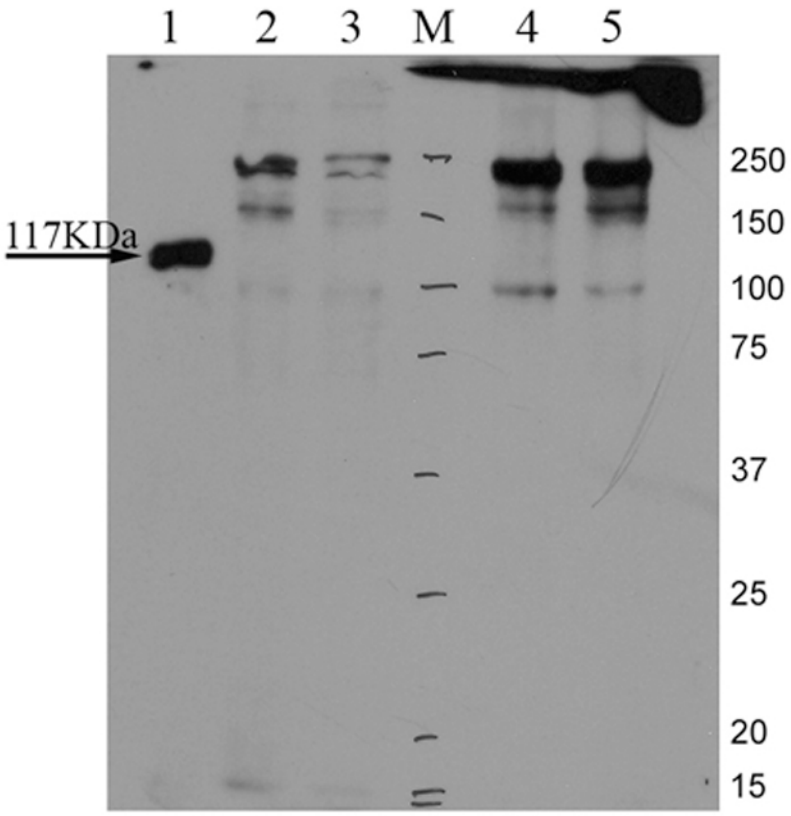

Figure 5-2: Western analysis of total protein from wild type and *uba-1(it129^{ts})* worms with Anti-E1.

10% SDS-PAGE gel was run with the following protein extracts. Lane 1) 0.6 µl Cha-Go cell extract, 2) 10 µg of extract from *fem-1(hc17)* adult hermaphrodites (produce only oocytes), 3) 10 µg of extract from *fem-3*(*q20)* adult hermaphrodites (produce only sperm), 4) 10 µg of extract from *him-5(e1490)* and *uba-1(it129^{ts})him-5(e1490)* adult males grown at 25^{0}C and M) the protein marker Biorad # 161-0373 (15-250 KDa) as indicated on the right side.

Sequence Tag (EST) database for *C. elegans* gene annotations also predicts six different transcripts from the *uba-1* gene. The protein extracts from adult male worms show a difference in the band size at around 150 KDa and 250 KDa compared to adult hermaphrodite protein extracts indicating differential transcripts or post-translational modifications of E1 in males and hermaphrodites.

Confirmatory experiments like MS-MS analysis need to be to done to conclude the identity the protein bands recognized by anti-E1 antibody to be E1. If the protein bands recognized are indeed of E1, the protein expression level is elevated in $it129^{ts}$ males compared to wild type males, whereas mutant hermaphrodites show equivalent expression of UBA-1. This could possibly be the cause for sever sex-specific phenotypes manifested in *uba-1(*$it129^{ts}$*)* males.

5.1.3.2.2 *uba-1* protein expression in wild type sperm.

uba-1($it129^{ts}$*)* worms produced morphologically normal but functionally impaired sperm (refer to chapter II). To detect if E1 is expressed in sperm tissue as well, Anti-E1 Western was performed on the total protein extracted from isolated sperm. The sperm protein extract, even at 30 μg concentration, did not show any distinct E1 band at expected size (Figure 5-3). There is a faint band in between size standard 150KDa and 250KDa in 6 μl sample lane. Either E1 is not expressed in sperm cells or not to the level enough to detect within the limits of Western analysis. The extraneous bands detected at 37 KDa and 70 KDa could be non-specific or degradation products of E1.

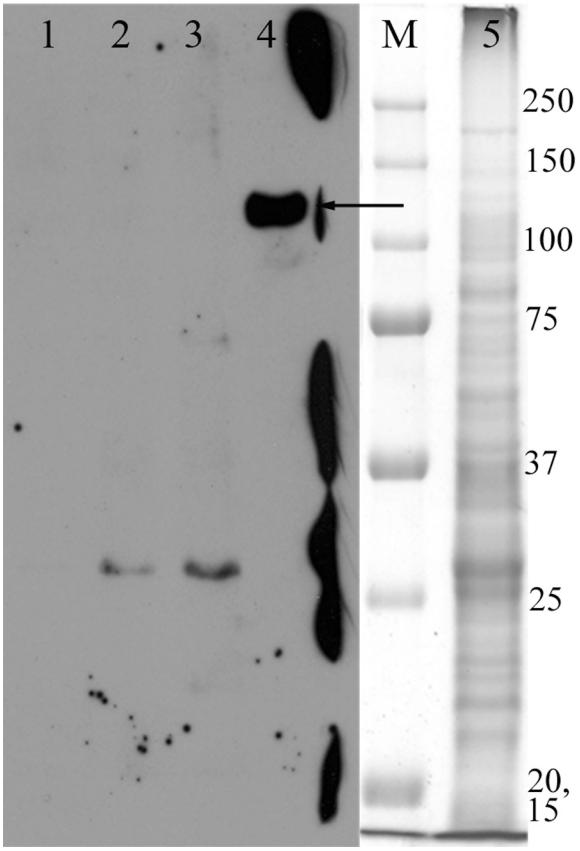

Figure 5-3: Western analysis of total protein from isolated sperm for E1.

10% SDS-PAGE gel was run with the following samples. Lanes 1-4, Western blot with anti-E1 antibody (1:500 dilution) exposed for 45 minutes. Lane 1-3) 5 µg; 20 µg; 30 µg of sperm protein sample isolated from *him-5(e1490)* adult males grown at 25^0C. Lane 4) 0.6 µl Cha-Go cell protein extract. Lane M) The protein marker Biorad # 161-0373 (10-250KDa). Lanes 5) Coomassie stained gel with 20 µg of total sperm protein from *him-5(e1490)* adult males.

Spermatids are formed during spermatogenesis by asymmetric distribution of the components between four haploid spermatids and a residual body. The components non-essential for spermiogeneis and sperm function are packaged in the residual body. It is possible that the proteins are loaded in the budding spermatids as ubiquitinated form, so that E1 does not need to be packaged in the spermatids. In such scenario, we would not detect any E1 in the Western analysis of total sperm protein.

5.1.4 Western analysis to detect ubiquitination levels in wild type and *it129^{ts}* mutant worms.

5.1.4.1 Methods

All the procedures were carried out as described in the section 5.1.3.1. Blocked PVDF membrane was incubated overnight at 4^0C with mouse monoclonal Anti-Ubiquitin (Stressgen # SPA-203) at 1:500 dilution in 5% milk-TBST. The secondary antibody used was HRP conjugated Anti-mouse IgG_1 (Stressgen # SAB-100) at 1:2000 dilution in 5% milk-TBST.

5.1.4.2 Results

5.1.4.2.1 Anti-ubiquitin Western on serial protein concentrations to determine the sensitivity of the antibody.

Serial concentrations of protein extracts from different tissues were tested with anti-ubiquitin antibody. Ubiquitin-conjugation as polyubiquitin or monoubiquitin tag is an essential post-translational modification of proteins. The list of proteins regulated by this modification is ever increasing. Multiple protein bands were detected from both the

sperm and *fem-3* adult worm samples indicating multiple ubiquitinated proteins as expected (Figure 5-4).

Ubiquitin is expressed as a precursor polyubiquitin peptide from the polyubiquitin. The *C. elegans* genome has one polyubiquitin locus, *ubq-1* (Graham et al., 1989). It encodes 11 tandem repeats of ubiquitin as an 838 amino acid peptide (Gonczy et al., 2000; Piano et al., 2000). Protein band detected at around 75 KDa could be an unprocessed protein product from the poly-ubiquitin gene.

5.1.4.2.2 Comparative analysis of ubiquitination levels between wild type and *it129^{ts}* worms.

This Western analysis was performed to compare the status of ubiquitination of proteins in *uba-1(it129^{ts})* mutant, which is predicted to encode a functionally impaired ubiquitin-activating enzyme, with wild type worms. Multiple proteins were recognized as ubiquitinated on the blot in all of the protein samples (Figure 5-5). The sperm protein and adult mixed population for hermaphrodites and males protein extract from *uba-1(it129^{ts})* genetic background do show reduced signal compared to wild type protein extract. This could be a direct result of reduced ubiquitination. The ubiquitination signal in adult *uba-1(it129^{ts})* males is either not reduced dramatically or the blot is overexposed to make any statement. Although there are few differences in the band pattern observed compared to *him-5(e1490)* males.

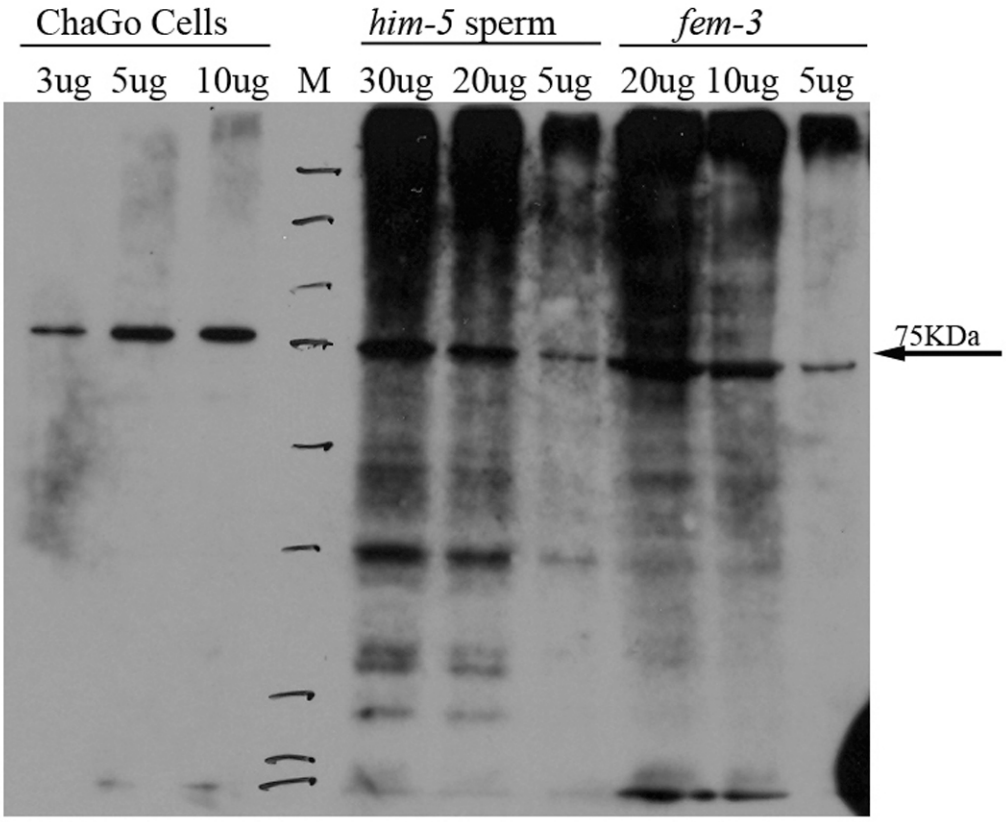

Figure 5-4: Standardization of Western analysis with anti-ubiquitin antibody.
10% SDS-PAGE gel was run with the following samples. 5 µl; 10 µl; 20 µl Cha-Go cell protein extract, 30 µg; 20 µg; 6 µg of protein extract from *him-5(e1490)* male sperm, 20 µg; 10 µg; 5 µg of protein extract from *fem-3*(*q20)* adult hermaphrodites producing only sperm and the protein marker (Lane-M) Biorad # 161-0373 (10-250KDa).

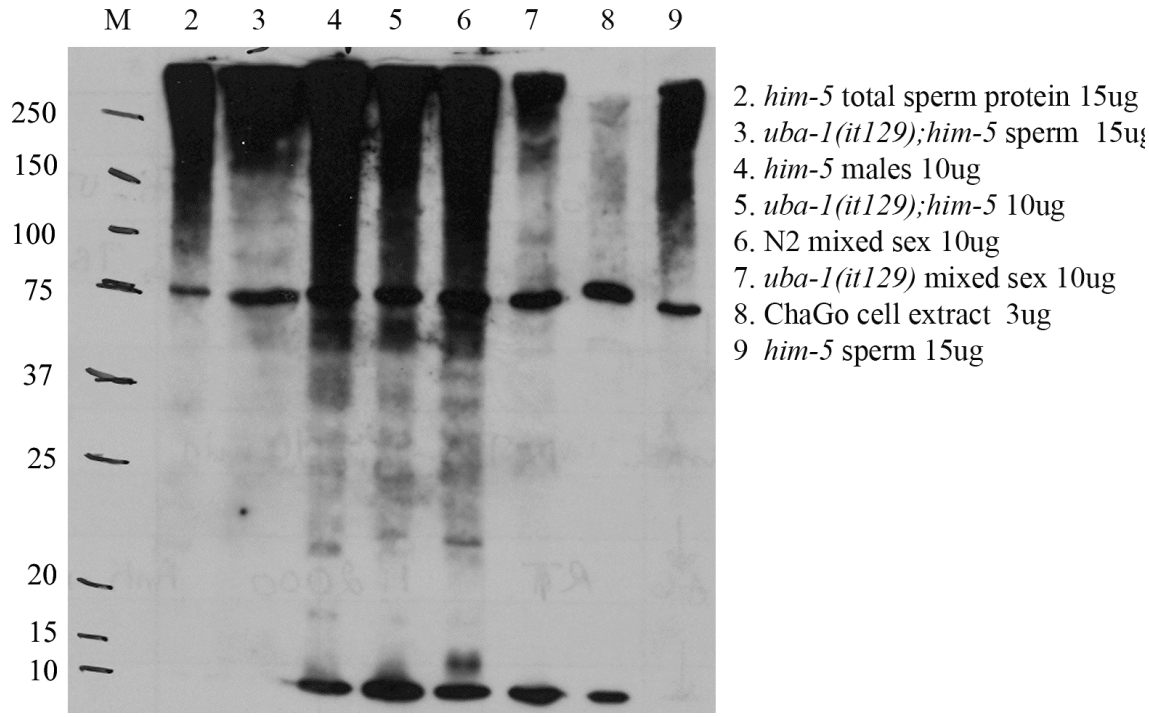

Figure 5-5: Western analysis with anti-ubiquitin antibody on protein extracts from adult worms and isolated sperm.

10% SDS-PAGE gel was run with 10 µl Cha-Go cell protein extract (lane-8), 15 µg of *him-5(e1490)* sperm protein (lane 2) and *uba-1(it129^{ts})him-5(e1490)* sperm protein (lane 3), 5 µl of total protein isolated from *him-5(e1490)* (lane 4) and *uba-1(it129^{ts})him-5(e1490)* adult males (lane 5) grown at 25^{0}C, 5 µl of total protein isolated from N2 (lane 6) and *uba-1(it129^{ts})* (lane 7) adult populations containing hermaphrodites and males both and the protein marker Biorad # 161-0373 (lane M). The blot was exposed for 2 minutes.

5.1.5 Western blot analysis with SP56 antibody

5.1.5.1 Methods

10% SDS-PAGE gel was run with the following samples at 25mA for 90 minutes. Triplicates of 6μl sperm protein sample (conc. 5 μg/μl) isolated from *him-5(e1490)* and the protein marker Biorad # 161-0373 (10-250KDa). Western analysis was performed as described in section 5.1.3.1 with 1:10, 1:100 and 1:200 dilutions of SP56 antibody in 5% milk-TBST.

5.1.5.2 Results

Monoclonal antibody SP56, recognizes 8 sperm-specific epitopes (Figure 5-6). It is very unusual for any anti-body to recognize more than one epitope, but SP56 has been shown to recognize a post-translational modification of the subset of sperm proteins (Ward et al. 1986). We speculate this post-translational modification to be poly- or mono-ubiquitination of sperm proteins. But the signal pattern observed here for SP56 does not overlap with the pattern observed in anti-ubiquitin Western analysis of the same sperm protein extract (Compare Figure 5-6 with Figure 5-5, lane 2). Based on the band pattern, it is less likely that SP56 recognizes the ubiquitin epitope.

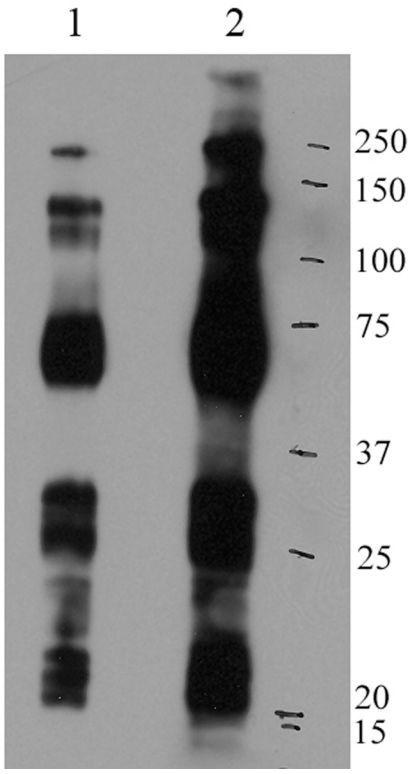

Figure 5-6: Western analysis with SP56 antibody on sperm protein extract.
25 μg of total sperm protein from *him-5(e1490)* adult males blotted with 1:200 (lane 1) and 1:100 (lane 2) dilution of SP56 antibody.

5.2 Genetic interaction between *elt-1(zu180)* and *uba-1(it129^{ts})*

5.2.1 Introduction

In *C. elegans*, *elt-1* encodes a GATA transcription factor. It has been shown to play an essential role during embryogenesis to specify hypodermal fate and also for the maintenance of hypodermal seam cells in later life (Smith et al., 2005). The allele *zu180,* whose molecular nature is not known, leads to embryonic lethality when homozygous. Various novel phenotypes were observed in worms treated with *elt-1* RNAi apart from the embryonic lethality (Smith J.A. et. al. 2005). L1/L2 larvae hatched from RNAi treated embryos die as lumpy-dumpy larvae. Treated P0 hermaphrodites burst their vulva in adulthood. Overexpression of *elt-1* in transgenic animals makes hermaphrodites hypermotile and eventually leads to paralysis.

All these phenotypes overlap with the range of phenotypes observed with *it129^{ts}* (refer to chapter II). Also, based on *elt-1* RNAi on wild type males as described in section 5.2.2, treated males showed similar tail aberrations as seen in homozygous *it129^{ts}* males. On the genetic map of *C. elegans*, both the alleles *it129^{ts}* and *elt-1(zu180)* are placed very close to each other on chromosome IV. Prior to the identification of *it129^{ts}* as an allele of uba-1, this data led to the speculation that *it129^{ts}* could be a temperature-sensitive allele of *elt-1* and phenocopies the stage-specific RNAi phenotypes of *elt-1*.

I performed non-complementation analysis to test the allelism of *it129^{ts}* with *elt-1* using the *zu180* allele. The *elt-1* mutation did complement all of the phenotypes of *it129^{ts}*, indicating that allele *it129^{ts}* is encoded in a different gene than *elt-1*. During the course of this study, genetic interaction between these two alleles was observed. The next

few sections will discuss the nature of the genetic interaction, novel observations made for *zu180* allele and *elt-1* mRNA expression in the germline.

5.2.2 *elt-1* RNAi on early larval males leads to developmental defects in their tail organs.

5.2.2.1 Methods

RNAi construct (pHS482) was generated by cloning an *elt-1* cDNA fragment into pPD129.36 between inverted T7 promoters using BamHI and XhoI sites. The cDNA was amplified from *fem-3* cDNA pool using primers HES-209 (AAAGGATCCAGGAAAACATGGACTACG) and HES-210 (AAAGTCGACGGAATGTTTGAAATGAG). The clone was then transformed in *E. coli* strain HT115.

Synchronized populations of N2 (wild type) hermaphrodites and males were grown until L2-L3. Sets of 20 hermaphrodites or males were shifted to NGM plates expressing *elt-1* RNAi construct or control HT115 strain in triplicates. The worms were maintained on RNAi plates until late adulthood and the worms were examined for the phenotypes.

5.2.2.2 Results

elt-1 RNAi on hermaphrodites reproduced all the previously reported phenotypes like F1 embryonic lethality, lumpy-dumpy F1 larvae and vulval bursting in P0 (treated) hermaphrodites (Smith et al., 2005). None of these phenotypes were observed in the hermaphrodites treated with control RNAi, confirming the specificity of *elt-1* RNAi.

elt-1 RNAi was performed on males to check for possible novel phenotypes. The males treated with *elt-1* RNAi did show aberrations in the tail development. The tail tip, cuticular fan and the sensory rays are reduced in size compared to wild type male tail at the equivalent life stage as shown in Figure 5-7. The posterior body portion in *elt-1* RNAi treated males show an increased number of vacuoles compared to control-treated wild type males. Thus, loss of *elt-1* in males affects the same organs of the tail as in $it129^{ts}$, although the severity of the defect is different.

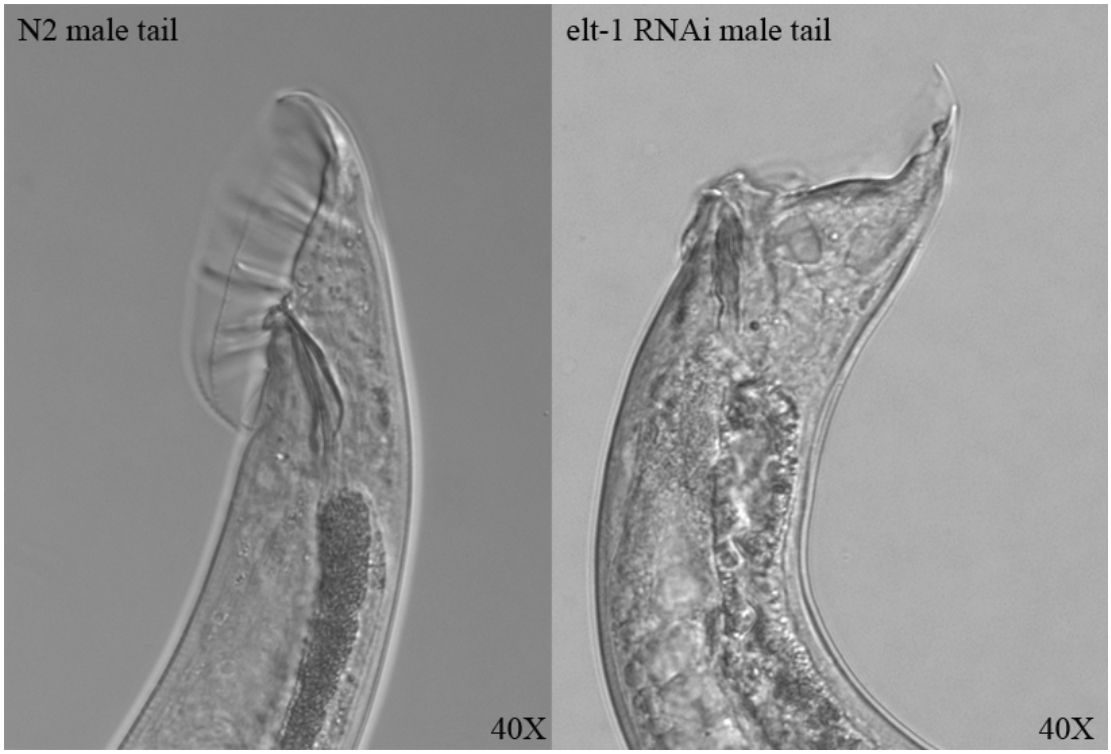

Figure 5-7: Comparison of male tail structures between wild type and *elt-1* RNAi treated wild type males.

The tail of *elt-1* RNAi treated male shows reduced cuticular fan and no sensory rays as compared to the wild type tail.

5.2.3 *elt-1 (zu180)* homozygous strain behaves differently at 15^0C and 25^0C.

The allele *zu180* is maintained as balanced lines in strains JJ398 (*unc-24(e138) daf-14(m77)/elt-1(zu180) dpy-20(e1282)* IV) and JJ1129 (*elt-1(zu180) unc-43(e408)/unc-24(e138) dpy-20(e1282)* IV). Both the strains produce reduced proportion of homozygous *elt-1* progeny. The reduction in the proportion is severe at 25^0C than at 15^0C (Table 5-1). At 25^0C, though, both the strains only lay 6-13 dead embryos per 147 average total progeny (4-9%). Proportion of the surviving F1 progeny is not altered in case of both the strains. This indicates that the higher temperature has some effect on the quality of the oocytes and/or sperm carrying *elt-1(zu180)* allele, making the homozygous *elt-1* embryos disappear from the pool of the F1 progeny.

Strain JJ1129: *elt-1unc-43*/*unc-24daf-14*			
selfed progeny	Expected	Observed	
		15^0C	25^0C
elt-1unc-43 (dead eggs)	25%	28±1.2 (14%)	6±4.2 (4%)
Parental (wild type)	50%	131±24.6 (65%)	88±21.7 (62%)
unc-24daf-14	25%	43±5.1 (21%)	39±9.6 (27%)
Total progeny		202±14.2	143±22.5

Table 5-1: Proportion of genotypes in the F1 progeny from the strain carrying *elt-1(zu180).*

Strains carrying *elt-1(zu180)* allele show anomalous bevavior at 25^0C. The heterozygous strains throw only 4% dead embryos insead of 25% (expected) of total progeny, representing homozygous *elt-1(zu180)* worms.

5.2.4 *in situ* hybridization to check *elt-1* mRNA expression pattern in sperm producing germline.

5.2.4.1 Methods

N2 hermaphrodites and males, *fem-3(q20)* and *fem-1(hc17)* worm populations were bleached and hatched on NGM plates overnight at 15^0C. The hatched L1 larvae were shifted to NGM plates with food at 25^0C until the appropriate stage. *fem-3(q20)* hermaphrodites produce only sperm while *fem-1(hc17)* produce only oocytes at 25^0C

5.2.4.1.1 Worm dissections

Synchronized populations of worm strains were obtained at L4 or adult stage. The worms were collected in PBS with 0.25 mM leavamisole. About 200-300 worms were dissected with a 20-gauge needle to extrude the gonad arms and then collected in sterile 3ml glass culture tube with the conical bottom.

5.2.4.1.2 ssDNA probe synthesis

elt-1 cDNA was amplified (1.3 kb fragment) from the clone pHS482 using anti-sense primer HES-395 (AAAAAGCTTGTCGACGGAATGTCTTGAAATGAGGAG) and sense primer HES-398 (AAAAAGCTTCTCGAGCAGGAAAACATGGACTACG). Using this cDNA as a template, single stand was linearly amplified using either 3' anti-sense or 5' sense primer with a DIG-labeled mix according to the instructions given in PCR DIG probe synthesis kit (Roche, Cat. No. 11636090910). Amplified ssDNA was run on a denaturing agarose gel to confirm the size and presence of a single band. ssDNA

was then precipitated with 0.2 M NaCl and ethanol and resuspended in 250 µl hybridization buffer. The probe was boiled for 1hr and stored at –20^{0}C until use.

The probe concentration was determined by dot-blotting on to a nitrocellulose membrane along with a marker of known concentration. The probe was detected using colorimetric assay with alkaline phosphatase-conjugated anti-DIG antibody and NBT/BCIP substrate. 1:5000 dilution of both the sense and anti-sense probes showed equivalent staining as 10 pg of a control DIG labeled fragment. Prior to use, each probe was diluted 1:2 with the hybridization buffer and boiled for 5 minutes.

5.2.4.1.3 Gonad fixation and hybridization:

In situ hybridization was carried out according to the protocol by Min-Ho Lee and Tim Schedl (http://www.wormbook.org/toc_wormmethods.html) with minor modifications. After fixation, the gonads were treated with Proteinase K for 1hr at the concentration of 100 µg/ml of PBT. Hybridization with the DIG labeled ssDNA probe was carried out at 48^{0}C for 36 hrs. Subsequent washes were also carried out at 48^{0}C. After blocking with BSA, the DIG probe was detected by colorimetric assay; Alkaline Phosphatase conjugated anti-DIG antibody and NBT/BCIP substrate. The gonads were incubated overnight at 4^{0}C with 1:2500 diluted Alkaline Phosphatase conjugated to anti-DIG antibody and the staining was done at room temperature for 2 hrs with NBT/BCIP and 100 ng DAPI in staining solution. Finally, gonads were mounted on an agar pad in PBS with 100 ng DAPI and the images were taken with Olympus BX51 microscope at 40X under DIC and DAPI filter.

5.2.4.2 Results

About 5% of the *elt-1* RNAi treated L2/L3 hermaphrodites lay unfertilized oocytes after reaching adulthood. Unfertilized oocytes is a characteristic of the Spe (Sperm-specific sterility) phenotype in *C. elegans*. Also, *elt-1* is reported to be overexpressed in the sperm-producing germline (Reinke et al., 2000). This information points towards a sperm-specific role of *elt-1*. If it does play functional role in spermatogenesis, it should be expressed in the germline during sperm development.

Based on the signal pattern of the DIG-labeled anti-sense probe, *elt-1* is indeed expressed in the meiotic region of spermatogenic germline (Figure 5-8). *fem-3(q20)* hermaphrodites produce sperm throughout their life and express *elt-1* in meiotic germline at both L4 and adult stages. *fem-1(hc17)* adult hermaphrodites, which produce only oocytes, did not show any expression in the meiotic germline. N2 hermaphrodites during L4 larval stage and N2 males also show *elt-1* expression in the meiotic region of the gonad (data not shown). The oocytes and sperm show non-specific staining with both sense and anti-sense probes.

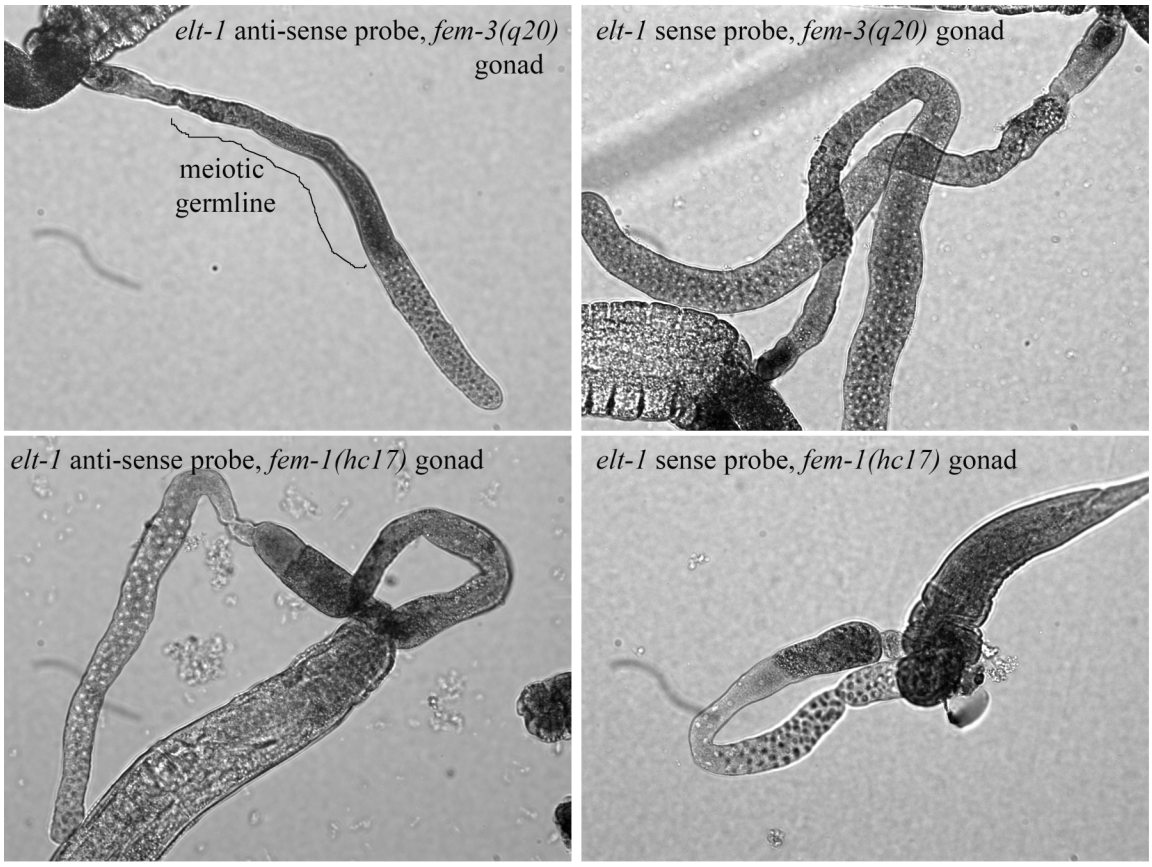

Figure 5-8: *In situ* hybridization to detect *elt-1* expression in the germlines

DIC images of the gonads showing anti-sense and sense *elt-1* probe hybridization at 40X magnification in *fem-1* and *fem-3* dissected gonads. Anti-sense probe showed signal only in the *fem-3* gonads (top left) during sperm differentiation phase.

5.2.5 Complementation test between *elt-1(zu180)* and *it129^{ts}*.

5.2.5.1 Methods

The complementation analysis was done between two alleles, *elt-1(zu180)* and *it129^{ts}*, as described in the following figure (Figure 5-9).

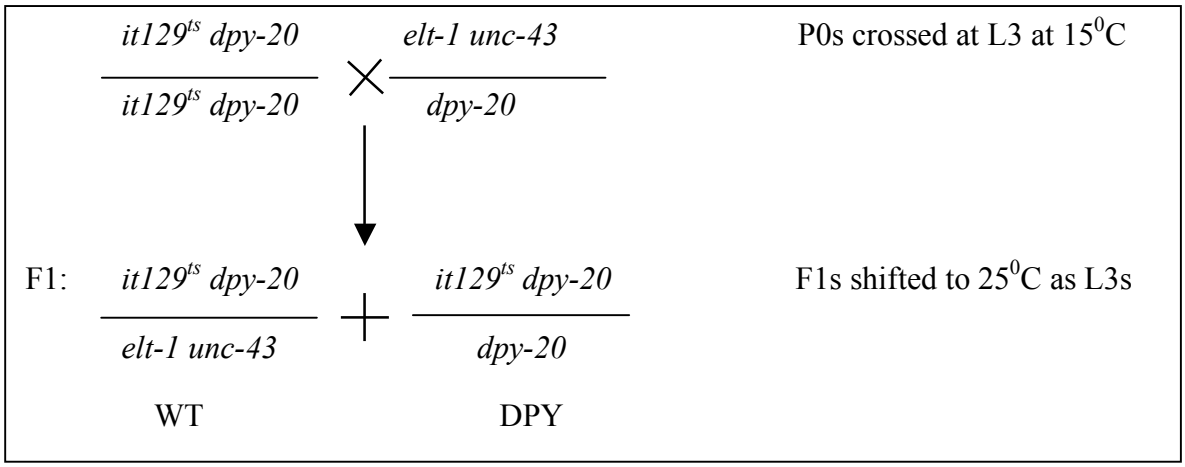

Figure 5-9: Strategy used to generate heterozygous *elt-1(zu180)* over *(it129^{ts})* worms.

5.2.5.2 Results

F1 progeny from the cross as described in Figure 5-9 is expected to give 50% wild type and 50% dumpy worms. Both wild type and dumpy worms were observed in the progeny with 1:1 ratio of hermaphrodites to males. All of the heterozygous *it129^{ts}*/*elt-1(zu180)* tested (20 hermaphrodites from each cross) laid viable progeny. Both the alleles complement each other for embryonic lethality and sperm-specific sterility. Thus, *it129^{ts}* is not an allele of *elt-1(zu180)*. As described in chapter II, *it129^{ts}* allele encodes a point mutation in *uba-1* (ubiquitin-activating enzyme) gene.

25% of the total progeny from the cross (Figure 5-9) was recorded as dead embryos. A few of the non-dumpy F1 hermaphrodites which are heterozygous for both, *it129^{ts}* and *elt-1(zu180)* alleles, showed partial male like tail development ("intersex" phenotype as it will be referred to hereafter) as shown in Figure 5-10. The 'intersex' phenotype is observed at low penetrance but persists in the hermaphrodites throughout their life. Thus, *elt-1* and *it129^{ts}* show genetic interaction in the double heterozygous condition. Additional experiments were undertaken to further characterize the interaction.

5.2.6 *elt-1* RNAi or wild type *elt-1* genomic region microinjection in *uba-1(it129^{ts})* hermaphrodites leads to 'intersex' phenotype.

5.2.6.1 Methods

elt-1 RNAi was performed on *it129^{ts}* L2 hermaphrodites grown at 15^{0}C as described in 5.2.2.1 and the adult hermaphrodites were scored for 'intersex' phenotype. The *elt-1* gene was also introduced into *uba-1(it129^{ts})* strain by micro-injection.

Genomic region of 10Kb ecoding *elt-1* gene was PCR amplified from wild type genomic DNA and was purified by precipitating with potassium acetate and ethanol. Injection mix was prepared with 100 ng *elt-1* PCR DNA, 450 ng of EcoRI digested pRF4 (*rol-6* transgenic marker) and 200 ng of PuvII digested wild type genomic DNA to the final concentration of 156 ng/µl. The mix was injected in homozygous *it129^{ts}* hermaphrodites. The hermaphrodites and the progeny were maintained at 15^{0}C. Transgenic lines were isolated based on the roller phenotype conferred by *rol-6* marker.

5.2.6.2 Results

By performing *elt-1* RNAi on *it129^{ts}* worms at 25^{0}C, *elt-1* activity was reduced in the *uba-1* mutant background where both (*uba-1* and *elt-1*) the gene functions are reduced. The intersex phenotype was reproduced in the F1 hermaphrodites at low frequency. About 2 in 30 hermaphrodites had intersex tail. The tail retraction persisted throughout the life as seen in the double heterozygous *it129^{ts}/elt-1(zu180)* hermaphrodites.

More frequent (10 in 30 transgenic worms) but transient intersex phenotype was observed in *it129^{ts}* transgenic hermaphrodites expressing *elt-1* transgene. It is possible that overexpression of *elt-1* mRNA in the transgenic lines is leading to co-suppression of *elt-1* (Ketting and Plasterk, 2000). During co-suppression, overexpressed transcript of the gene from the transgene leads to (as speculated, small RNAs mediated) degradation of itself along with the native transcript from the homologous gene. As a result, the

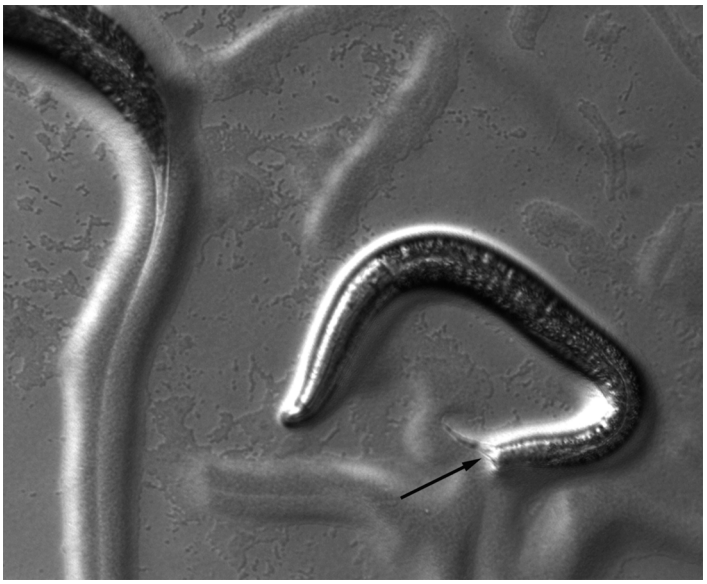

Figure 5-10: Intersex phenotype in transgenic *uba-1(it129^{ts})* hermaphrodites carrying *elt-1* transgene.

Arow indicates the male like developing tale in the hermaprhodite soma of L3 stage. The intersex tale is transient as normal hermaphrodite tale appears by adulthood (top left of the image).

stransgenic lines have reduced or no expression of *elt-1* in *it129*^{ts} mutant background, creating similar phenotype as observed in *it129*^{ts}/ *elt-1* double heterozygotes. It is also likely that ELT-1 itself is targeted for ubiquitin-mediated degradation, which is inhibited in the *uba-1* mutant background leading to observed abnormalities.

Male tail is specialized organ for copulatory functions performed by the male. The development of the tail is acheived by the retraction of the cells in the tail region of the male during L4 larval stage. This retraction does not occur in hermaphrodites as a result the hermaphrodite tail develops with a tapering end. In 'intersex' hermaphrodites where expression of both the genes; *elt-1* and *uba-1* is reduced, the tail retraction is possibly activated in hermaphrodites during larval stages giving rise to L4 male tail structure. Where as, in the transgenic worms, co-suppression could occur transiently leading to transient 'intersex' phenotype.

BIBLIOGRAPHY

Al-Hakim, A. K., Zagorska, A., Chapman, L., Deak, M., Peggie, M., and Alessi, D. R. (2008). Control of AMPK-related kinases by USP9X and atypical Lys(29)/Lys(33)-linked polyubiquitin chains. Biochem J *411*, 249-260.

Ardley, H. C., and Robinson, P. A. (2004). The role of ubiquitin-protein ligases in neurodegenerative disease. Neurodegener Dis *1*, 71-87.

Argon, Y., and Ward, S. (1980). Caenorhabditis elegans fertilization-defective mutants with abnormal sperm. Genetics *96*, 413-433.

Ayusawa, D., Kaneda, S., Itoh, Y., Yasuda, H., Murakami, Y., Sugasawa, K., Hanaoka, F., and Seno, T. (1992). Complementation by a cloned human ubiquitin-activating enzyme E1 of the S-phase-arrested mouse FM3A cell mutant with thermolabile E1. Cell Struct Funct *17*, 113-122.

Baarends, W. M., Hoogerbrugge, J. W., Roest, H. P., Ooms, M., Vreeburg, J., Hoeijmakers, J. H., and Grootegoed, J. A. (1999a). Histone ubiquitination and chromatin remodeling in mouse spermatogenesis. Dev Biol *207*, 322-333.

Baarends, W. M., Roest, H. P., and Grootegoed, J. A. (1999b). The ubiquitin system in gametogenesis. Mol Cell Endocrinol *151*, 5-16.

Baarends, W. M., van der Laan, R., and Grootegoed, J. A. (2000). Specific aspects of the ubiquitin system in spermatogenesis. J Endocrinol Invest *23*, 597-604.

Baird, S. E., and Ellazar, S. A. (1999). TGFbeta-like signaling and spicule development in Caenorhabditis elegans. Dev Biol *212*, 93-100.

Barton, M. K., and Kimble, J. (1990). fog-1, a regulatory gene required for specification of spermatogenesis in the germ line of Caenorhabditis elegans. Genetics *125*, 29-39.

Barton, M. K., Schedl, T. B., and Kimble, J. (1987). Gain-of-function mutations of fem-3, a sex-determination gene in Caenorhabditis elegans. Genetics *115*, 107-119.

Batchelder, C., Dunn, M. A., Choy, B., Suh, Y., Cassie, C., Shim, E. Y., Shin, T. H., Mello, C., Seydoux, G., and Blackwell, T. K. (1999). Transcriptional repression by the Caenorhabditis elegans germ-line protein PIE-1. Genes Dev *13*, 202-212.

Baugh, L. R., Hill, A. A., Claggett, J. M., Hill-Harfe, K., Wen, J. C., Slonim, D. K., Brown, E. L., and Hunter, C. P. (2005). The homeodomain protein PAL-1 specifies a lineage-specific regulatory network in the C. elegans embryo. Development *132*, 1843-1854.

Baugh, L. R., Hill, A. A., Slonim, D. K., Brown, E. L., and Hunter, C. P. (2003). Composition and dynamics of the Caenorhabditis elegans early embryonic transcriptome. Development *130*, 889-900.

Beanan, M. J., and Strome, S. (1992). Characterization of a germ-line proliferation mutation in C. elegans. Development *116*, 755-766.

Ben-Saadon, R., Zaaroor, D., Ziv, T., and Ciechanover, A. (2006). The polycomb protein Ring1B generates self atypical mixed ubiquitin chains required for its in vitro histone H2A ligase activity. Mol Cell *24*, 701-711.

Berry, L. W., Westlund, B., and Schedl, T. (1997). Germ-line tumor formation caused by activation of glp-1, a Caenorhabditis elegans member of the Notch family of receptors. Development *124*, 925-936.

Bloch, D. B., de la Monte, S. M., Guigaouri, P., Filippov, A., and Bloch, K. D. (1996). Identification and characterization of a leukocyte-specific component of the nuclear body. J Biol Chem *271*, 29198-29204.

Bloch, D. B., Nakajima, A., Gulick, T., Chiche, J. D., Orth, D., de La Monte, S. M., and Bloch, K. D. (2000). Sp110 localizes to the PML-Sp100 nuclear body and may function as a nuclear hormone receptor transcriptional coactivator. Mol Cell Biol *20*, 6138-6146.

Bosu, D. R., and Kipreos, E. T. (2008). Cullin-RING ubiquitin ligases: global regulation and activation cycles. Cell Div *3*, 7.

Bottomley, M. J., Collard, M. W., Huggenvik, J. I., Liu, Z., Gibson, T. J., and Sattler, M. (2001). The SAND domain structure defines a novel DNA-binding fold in transcriptional regulation. Nat Struct Biol *8*, 626-633.

Bourbon, H. M., Aguilera, A., Ansari, A. Z., Asturias, F. J., Berk, A. J., Bjorklund, S., Blackwell, T. K., Borggrefe, T., Carey, M., Carlson, M.*, et al.* (2004). A unified nomenclature for protein subunits of mediator complexes linking transcriptional regulators to RNA polymerase II. Mol Cell *14*, 553-557.

Bowerman, B., Draper, B. W., Mello, C. C., and Priess, J. R. (1993). The maternal gene skn-1 encodes a protein that is distributed unequally in early C. elegans embryos. Cell *74*, 443-452.

Bowerman, B., Eaton, B. A., and Priess, J. R. (1992). skn-1, a maternally expressed gene required to specify the fate of ventral blastomeres in the early C. elegans embryo. Cell *68*, 1061-1075.

Bowerman, B., and Kurz, T. (2006). Degrade to create: developmental requirements for ubiquitin-mediated proteolysis during early C. elegans embryogenesis. Development *133*, 773-784.

Boyd, S. D. (2008). Everything you wanted to know about small RNA but were afraid to ask. Lab Invest *88*, 569-578.

Brenner, S. (1974). The genetics of Caenorhabditis elegans. Genetics *77*, 71-94.

Buonomo, S. B., Clyne, R. K., Fuchs, J., Loidl, J., Uhlmann, F., and Nasmyth, K. (2000). Disjunction of homologous chromosomes in meiosis I depends on proteolytic cleavage of the meiotic cohesin Rec8 by separin. Cell *103*, 387-398.

Campbell, S. L., Khosravi-Far, R., Rossman, K. L., Clark, G. J., and Der, C. J. (1998). Increasing complexity of Ras signaling. Oncogene *17*, 1395-1413.

Catic, A., and Ploegh, H. L. (2005). Ubiquitin--conserved protein or selfish gene? Trends Biochem Sci *30*, 600-604.

Chan, N. L., and Hill, C. P. (2001). Defining polyubiquitin chain topology. Nat Struct Biol *8*, 650-652.

Chasnov, J. R., So, W. K., Chan, C. M., and Chow, K. L. (2007). The species, sex, and stage specificity of a Caenorhabditis sex pheromone. Proc Natl Acad Sci U S A *104*, 6730-6735.

Chastagner, P., Israel, A., and Brou, C. (2006). Itch/AIP4 mediates Deltex degradation through the formation of K29-linked polyubiquitin chains. EMBO Rep *7*, 1147-1153.

Chatterjee, I., Richmond, A., Putiri, E., Shakes, D. C., and Singson, A. (2005). The Caenorhabditis elegans spe-38 gene encodes a novel four-pass integral membrane protein required for sperm function at fertilization. Development *132*, 2795-2808.

Checchi, P. M., and Kelly, W. G. (2006). emb-4 is a conserved gene required for efficient germline-specific chromatin remodeling during Caenorhabditis elegans embryogenesis. Genetics *174*, 1895-1906.

Chen, P., and Ellis, R. E. (2000). TRA-1A regulates transcription of fog-3, which controls germ cell fate in C. elegans. Development *127*, 3119-3129.

Chernova, T. A., Allen, K. D., Wesoloski, L. M., Shanks, J. R., Chernoff, Y. O., and Wilkinson, K. D. (2003). Pleiotropic effects of Ubp6 loss on drug sensitivities and yeast prion are due to depletion of the free ubiquitin pool. J Biol Chem *278*, 52102-52115.

Chiu, Y. H., Sun, Q., and Chen, Z. J. (2007). E1-L2 activates both ubiquitin and FAT10. Mol Cell *27*, 1014-1023.

Christensen, J., Cotmore, S. F., and Tattersall, P. (1999). Two new members of the emerging KDWK family of combinatorial transcription modulators bind as a heterodimer to flexibly spaced PuCGPy half-sites. Mol Cell Biol, 7741-7750.

Ciechanover, A., Elias, S., Heller, H., and Hershko, A. (1982). "Covalent affinity" purification of ubiquitin-activating enzyme. J Biol Chem *257*, 2537-2542.

Ciechanover, A., Finley, D., and Varshavsky, A. (1984). Ubiquitin dependence of selective protein degradation demonstrated in the mammalian cell cycle mutant ts85. Cell *37*, 57-66.

Ciechanover, A., Finley, D., and Varshavsky, A. (1985). Mammalian cell cycle mutant defective in intracellular protein degradation and ubiquitin-protein conjugation. Prog Clin Biol Res *180*, 17-31.

Ciechanover, A., and Schwartz, A. L. (1989). The ubiquitin-dependent proteolytic pathway: specificity of recognition of the proteolytic substrates. Revis Biol Celular *20*, 217-234.

Cohen-Fix, O., Peters, J. M., Kirschner, M. W., and Koshland, D. (1996). Anaphase initiation in Saccharomyces cerevisiae is controlled by the APC-dependent degradation of the anaphase inhibitor Pds1p. Genes Dev *10*, 3081-3093.

Conradt, B., and Horvitz, H. R. (1998). The C. elegans protein EGL-1 is required for programmed cell death and interacts with the Bcl-2-like protein CED-9. Cell *93*, 519-529.

Conradt, B., and Horvitz, H. R. (1999). The TRA-1A sex determination protein of C. elegans regulates sexually dimorphic cell deaths by repressing the egl-1 cell death activator gene. Cell *98*, 317-327.

Cook, J. C., and Chock, P. B. (1992). Isoforms of mammalian ubiquitin-activating enzyme. J Biol Chem *267*, 24315-24321.

Cook, J. C., and Chock, P. B. (1995). Phosphorylation of ubiquitin-activating enzyme in cultured cells. Proc Natl Acad Sci U S A *92*, 3454-3457.

Davis, E. S., Wille, L., Chestnut, B. A., Sadler, P. L., Shakes, D. C., and Golden, A. (2002). Multiple subunits of the Caenorhabditis elegans anaphase-promoting complex are required for chromosome segregation during meiosis I. Genetics *160*, 805-813.

Del Rio-Albrechtsen, T., Kiontke, K., Chiou, S. Y., and Fitch, D. H. (2006). Novel gain-of-function alleles demonstrate a role for the heterochronic gene lin-41 in C. elegans male tail tip morphogenesis. Dev Biol *297*, 74-86.

DeRenzo, C., Reese, K. J., and Seydoux, G. (2003). Exclusion of germ plasm proteins from somatic lineages by cullin-dependent degradation. Nature *424*, 685-689.

Ding, M., Chao, D., Wang, G., and Shen, K. (2007). Spatial regulation of an E3 ubiquitin ligase directs selective synapse elimination. Science *317*, 947-951.

Draper, B. W., Mello, C. C., Bowerman, B., Hardin, J., and Priess, J. R. (1996). MEX-3 is a KH domain protein that regulates blastomere identity in early C. elegans embryos. Cell *87*, 205-216.

Dupuy, D., Bertin, N., Hidalgo, C. A., Venkatesan, K., Tu, D., Lee, D., Rosenberg, J., Svrzikapa, N., Blanc, A., Carnec, A.*, et al.* (2007). Genome-scale analysis of in vivo spatiotemporal promoter activity in Caenorhabditis elegans. Nat Biotechnol *25*, 663-668.

Eletr, Z. M., Huang, D. T., Duda, D. M., Schulman, B. A., and Kuhlman, B. (2005). E2 conjugating enzymes must disengage from their E1 enzymes before E3-dependent ubiquitin and ubiquitin-like transfer. Nat Struct Mol Biol *12*, 933-934.

Ellis, R. E., and Kimble, J. (1995). The fog-3 gene and regulation of cell fate in the germ line of Caenorhabditis elegans. Genetics *139*, 561-577.

Finley, D., Ciechanover, A., and Varshavsky, A. (1984). Thermolability of ubiquitin-activating enzyme from the mammalian cell cycle mutant ts85. Cell *37*, 43-55.

Ford, L. P., Bagga, P. S., and Wilusz, J. (1997). The poly(A) tail inhibits the assembly of a 3'-to-5' exonuclease in an in vitro RNA stability system. Mol Cell Biol, 398-406.

Francis, R., Barton, M. K., Kimble, J., and Schedl, T. (1995). gld-1, a tumor suppressor gene required for oocyte development in Caenorhabditis elegans. Genetics *139*, 579-606.

Fraser, A. G., Kamath, R. S., Zipperlen, P., Martinez-Campos, M., Sohrmann, M., and Ahringer, J. (2000). Functional genomic analysis of C. elegans chromosome I by systematic RNA interference. Nature *408*, 325-330.

Frazier, T., Shakes, D., Hota, U., and Boyd, L. (2004). Caenorhabditis elegans UBC-2 functions with the anaphase-promoting complex but also has other activities. J Cell Sci *117*, 5427-5435.

Fukushige, T., Brodigan, T. M., Schriefer, L. A., Waterston, R. H., and Krause, M. (2006). Defining the transcriptional redundancy of early bodywall muscle development in C. elegans: evidence for a unified theory of animal muscle development. Genes Dev *20*, 3395-3406.

Funabiki, H., Yamano, H., Kumada, K., Nagao, K., Hunt, T., and Yanagida, M. (1996). Cut2 proteolysis required for sister-chromatid seperation in fission yeast. Nature *381*, 438-441.

Furuta, T., Tuck, S., Kirchner, J., Koch, B., Auty, R., Kitagawa, R., Rose, A. M., and Greenstein, D. (2000). EMB-30: an APC4 homologue required for metaphase-to-anaphase transitions during meiosis and mitosis in Caenorhabditis elegans. Mol Biol Cell *11*, 1401-1419.

Geetha, T., Kenchappa, R. S., Wooten, M. W., and Carter, B. D. (2005). TRAF6-mediated ubiquitination regulates nuclear translocation of NRIF, the p75 receptor interactor. Embo J *24*, 3859-3868.

Ghaboosi, N., and Deshaies, R. J. (2007). A conditional yeast E1 mutant blocks the ubiquitin-proteasome pathway and reveals a role for ubiquitin conjugates in targeting Rad23 to the proteasome. Mol Biol Cell *18*, 1953-1963.

Ghosh, D., and Seydoux, G. (2008). Inhibition of transcription by the Caenorhabditis elegans germline protein PIE-1: genetic evidence for distinct mechanisms targeting initiation and elongation. Genetics *178*, 235-243.

Gibson, T. J., Ramu, C., Gemund, C., and Aasland, R. (1998). The APECED polyglandular autoimmune syndrome protein, AIRE-1, contains the SAND domain and is probably a transcription factor. Trends Biochem Sci *23*, 242-244.

Gilleard, J. S., and McGhee, J. D. (2001). Activation of hypodermal differentiation in the Caenorhabditis elegans embryo by GATA transcription factors ELT-1 and ELT-3. Mol Cell Biol *21*, 2533-2544.

Gilleard, J. S., Shafi, Y., Barry, J. D., and McGhee, J. D. (1999). ELT-3: A Caenorhabditis elegans GATA factor expressed in the embryonic epidermis during morphogenesis. Dev Biol *208*, 265-280.

Gladden, J. M., and Meyer, B. J. (2007). A ONECUT Homeodomain Protein Communicates X Chromosome Dose to Specify Caenorhabditis elegans Sexual Fate by Repressing a Sex Switch Gene. Genetics *177*, 1621-1637.

Golden, A., Sadler, P. L., Wallenfang, M. R., Schumacher, J. M., Hamill, D. R., Bates, G., Bowerman, B., Seydoux, G., and Shakes, D. C. (2000). Metaphase to anaphase (mat) transition-defective mutants in Caenorhabditis elegans. J Cell Biol *151*, 1469-1482.

Gonczy, P., and Rose, L. S. Asymmetric cell division and axis formation in the embryo, In WormBook, T. C. e. R. Community, ed. (WormBook).

Graham, R. W., Jones, D., and Candido, E. P. (1989). UbiA, the major polyubiquitin locus in Caenorhabditis elegans, has unusual structural features and is constitutively expressed. Mol Cell Biol *9*, 268-277.

Gross, C. T., and McGinnis, W. (1996). DEAF-1, a novel protein that binds an essential region in a Deformed response element. EMBO J *15*, 1961-1970.

Guardavaccaro, D., Kudo, Y., Boulaire, J., Barchi, M., Busino, L., Donzelli, M., Margottin-Goguet, F., Jackson, P. K., Yamasaki, L., and Pagano, M. (2003). Control of meiotic and mitotic progression by the F box protein beta-Trcp1 in vivo. Dev Cell *4*, 799-812.

Gudgen, M., Chandrasekaran, A., Frazier, T., and Boyd, L. (2004). Interactions within the ubiquitin pathway of Caenorhabditis elegans. Biochem Biophys Res Commun *325*, 479-486.

Guedes, S., and Priess, J. R. (1997). The C. elegans MEX-1 protein is present in germline blastomeres and is a P granule component. Development *124*, 731-739.

Haas, A. L., and Rose, I. A. (1982). The mechanism of ubiquitin activating enzyme. A kinetic and equilibrium analysis. J Biol Chem *257*, 10329-10337.

Haglund, K., and Dikic, I. (2005). Ubiquitylation and cell signaling. Embo J *24*, 3353-3359.

Haglund, K., Sigismund, S., Polo, S., Szymkiewicz, I., Di Fiore, P. P., and Dikic, I. (2003). Multiple monoubiquitination of RTKs is sufficient for their endocytosis and degradation. Nat Cell Biol *5*, 461-466.

Handley-Gearhart, P. M., Stephen, A. G., Trausch-Azar, J. S., Ciechanover, A., and Schwartz, A. L. (1994). Human ubiquitin-activating enzyme, E1. Indication of potential nuclear and cytoplasmic subpopulations using epitope-tagged cDNA constructs. J Biol Chem *269*, 33171-33178.

Hanna, J., and Finley, D. (2007). A proteasome for all occasions. FEBS Lett *581*, 2854-2861.

Hanna, J., Leggett, D. S., and Finley, D. (2003). Ubiquitin depletion as a key mediator of toxicity by translational inhibitors. Mol Cell Biol *23*, 9251-9261.

Hanna, J., Meides, A., Zhang, D. P., and Finley, D. (2007). A ubiquitin stress response induces altered proteasome composition. Cell *129*, 747-759.

Hansen, D., and Pilgrim, D. (1999). Sex and the single worm: sex determination in the nematode C. elegans. Mech Dev *83*, 3-15.

Hatfield, P. M., Callis, J., and Vierstra, R. D. (1990). Cloning of ubiquitin activating enzyme from wheat and expression of a functional protein in Escherichia coli. J Biol Chem *265*, 15813-15817.

Hatfield, P. M., Gosink, M. M., Carpenter, T. B., and Vierstra, R. D. (1997). The ubiquitin-activating enzyme (E1) gene family in Arabidopsis thaliana. Plant J *11*, 213-226.

Hatfield, P. M., and Vierstra, R. D. (1992). Multiple forms of ubiquitin-activating enzyme E1 from wheat. Identification of an essential cysteine by in vitro mutagenesis. J Biol Chem *267*, 14799-14803.

Hershko, A. (1991). The ubiquitin pathway for protein degradation. Trends Biochem Sci *16*, 265-268.

Hershko, A., Heller, H., Elias, S., and Ciechanover, A. (1983). Components of ubiquitin-protein ligase system. Resolution, affinity purification, and role in protein breakdown. J Biol Chem *258*, 8206-8214.

Hicke, L. (2001). Protein regulation by monoubiquitin. Nat Rev Mol Cell Biol *2*, 195-201.

Hicke, L., Schubert, H. L., and Hill, C. P. (2005). Ubiquitin-binding domains. Nat Rev Mol Cell Biol *6*, 610-621.

Hill, K. L., and L'Hernault, S. W. (2001). Analyses of reproductive interactions that occur after heterospecific matings within the genus Caenorhabditis. Dev Biol *232*, 105-114.

Hirsh, D., Oppenheim, D., and Klass, M. (1976). Development of the reproductive system of Caenorhabditis elegans. Dev Biol *49*, 200-219.

Hirsh, D., and Vanderslice, R. (1976). Temperature-sensitive developmental mutants of Caenorhabditis elegans. Dev Biol *49*, 220-235.

Hochstrasser, M. (2000). Evolution and function of ubiquitin-like protein-conjugation systems. Nat Cell Biol *2*, E153-157.

Hodges, M., Tissot, C., Howe, K., Grimwade, D., and Freemont, P. S. (1998). Structure, organization, and dynamics of promyelocytic leukemia protein nuclear bodies. Am J Hum Genet *63*, 297-304.

Hodgkin, J. (1986). Sex determination in the nematode C. elegans: analysis of tra-3 suppressors and characterization of fem genes. Genetics *114*, 15-52.

Hodgkin, J. (1987). A genetic analysis of the sex-determining gene, tra-1, in the nematode Caenorhabditis elegans. Genes Dev *1*, 731-745.

Hodgkin, J., Horvitz, H. R., and Brenner, S. (1979). Nondisjunction Mutants of the Nematode CAENORHABDITIS ELEGANS. Genetics *91*, 67-94.

Hodgkin, J. A., and Brenner, S. (1977). Mutations causing transformation of sexual phenotype in the nematode Caenorhabditis elegans. Genetics *86*, 275-287.

Hoppe, T., Cassata, G., Barral, J. M., Springer, W., Hutagalung, A. H., Epstein, H. F., and Baumeister, R. (2004). Regulation of the myosin-directed chaperone UNC-45 by a novel E3/E4-multiubiquitylation complex in C. elegans. Cell *118*, 337-349.

Howard, R. A., Sharma, P., Hajjar, C., Caldwell, K. A., Caldwell, G. A., du Breuil, R., Moore, R., and Boyd, L. (2007). Ubiquitin conjugating enzymes participate in polyglutamine protein aggregation. BMC Cell Biol *8*, 32.

Huang, D. T., Paydar, A., Zhuang, M., Waddell, M. B., Holton, J. M., and Schulman, B. A. (2005). Structural basis for recruitment of Ubc12 by an E2 binding domain in NEDD8's E1. Mol Cell *17*, 341-350.

Huggenvik, J. I., Michelson, R. J., Collard, M. W., Ziemba, A. J., Gurley, P., and Mowen, K. A. (1998). Characterization of a nuclear deformed epidermal autoregulatory factor-1 (DEAF-1)-related (NUDR) transcriptional regulator protein. Mol Endocrinol, 1619-1639.

Hunter, C. P., and Kenyon, C. (1996). Spatial and temporal controls target pal-1 blastomere-specification activity to a single blastomere lineage in C. elegans embryos. Cell *87*, 217-226.

Hunter, C. P., and Wood, W. B. (1992). Evidence from mosaic analysis of the masculinizing gene her-1 for cell interactions in C. elegans sex determination. Nature *355*, 551-555.

Ichimura, Y., Kirisako, T., Takao, T., Satomi, Y., Shimonishi, Y., Ishihara, N., Mizushima, N., Tanida, I., Kominami, E., Ohsumi, M.*, et al.* (2000). A ubiquitin-like system mediates protein lipidation. Nature *408*, 488-492.

Itoh, S., and ten Dijke, P. (2007). Negative regulation of TGF-beta receptor/Smad signal transduction. Curr Opin Cell Biol *19*, 176-184.

Jackson, P. K., Eldridge, A. G., Freed, E., Furstenthal, L., Hsu, J. Y., Kaiser, B. K., and Reimann, J. D. (2000). The lore of the RINGs: substrate recognition and catalysis by ubiquitin ligases. Trends Cell Biol *10*, 429-439.

Jager, S., Schwartz, H. T., Horvitz, H. R., and Conradt, B. (2004). The Caenorhabditis elegans F-box protein SEL-10 promotes female development and may target FEM-1 and FEM-3 for degradation by the proteasome. Proc Natl Acad Sci U S A *101*, 12549-12554.

Jentsch, S. (1992). The ubiquitin-conjugation system. Annu Rev Genet *26*, 179-207.

Jentsch, S., and Pyrowolakis, G. (2000). Ubiquitin and its kin: how close are the family ties? Trends Cell Biol *10*, 335-342.

Jentsch, S., Seufert, W., and Hauser, H. P. (1991). Genetic analysis of the ubiquitin system. Biochim Biophys Acta *1089*, 127-139.

Jiang, M., Ryu, J., Kiraly, M., Duke, K., Reinke, V., and Kim, S. K. (2001). Genome-wide analysis of developmental and sex-regulated gene expression profiles in Caenorhabditis elegans. Proc Natl Acad Sci U S A *98*, 218-223.

Jin, S. W., Arno, N., Cohen, A., Shah, A., Xu, Q., Chen, N., and Ellis, R. E. (2001). In Caenorhabditis elegans, the RNA-binding domains of the cytoplasmic polyadenylation element binding protein FOG-1 are needed to regulate germ cell fates. Genetics *159*, 1617-1630.

Johnson, E. S. (2004). Protein modification by SUMO. Annu Rev Biochem *73*, 355-382.

Johnston, S. C., Riddle, S. M., Cohen, R. E., and Hill, C. P. (1999). Structural basis for the specificity of ubiquitin C-terminal hydrolases. Embo J *18*, 3877-3887.

Jones, D., and Candido, E. P. (1993). Novel ubiquitin-like ribosomal protein fusion genes from the nematodes Caenorhabditis elegans and Caenorhabditis briggsae. J Biol Chem *268*, 19545-19551.

Jones, D., Crowe, E., Stevens, T. A., and Candido, E. P. (2002). Functional and phylogenetic analysis of the ubiquitylation system in Caenorhabditis elegans: ubiquitin-conjugating enzymes, ubiquitin-activating enzymes, and ubiquitin-like proteins. Genome Biol *3*, RESEARCH0002.

Jones, S. J., Riddle, D. L., Pouzyrev, A. T., Velculescu, V. E., Hillier, L., Eddy, S. R., Stricklin, S. L., Baillie, D. L., Waterston, R., and Marra, M. A. (2001). Changes in

gene expression associated with developmental arrest and longevity in Caenorhabditis elegans. Genome Res *11*, 1346-1352.

Juo, P., and Kaplan, J. M. (2004). The anaphase-promoting complex regulates the abundance of GLR-1 glutamate receptors in the ventral nerve cord of C. elegans. Curr Biol *14*, 2057-2062.

Kaiser, P., Flick, K., Wittenberg, C., and Reed, S. I. (2000). Regulation of transcription by ubiquitination without proteolysis: Cdc34/SCF(Met30)-mediated inactivation of the transcription factor Met4. Cell *102*, 303-314.

Kamath, R. S., Fraser, A. G., Dong, Y., Poulin, G., Durbin, R., Gotta, M., Kanapin, A., Le Bot, N., Moreno, S., Sohrmann, M.*, et al.* (2003). Systematic functional analysis of the Caenorhabditis elegans genome using RNAi. Nature *421*, 231-237.

Kawakami, T., Chiba, T., Suzuki, T., Iwai, K., Yamanaka, K., Minato, N., Suzuki, H., Shimbara, N., Hidaka, Y., Osaka, F.*, et al.* (2001). NEDD8 recruits E2-ubiquitin to SCF E3 ligase. Embo J *20*, 4003-4012.

Kay, G. F., Ashworth, A., Penny, G. D., Dunlop, M., Swift, S., Brockdorff, N., and Rastan, S. (1991). A candidate spermatogenesis gene on the mouse Y chromosome is homologous to ubiquitin-activating enzyme E1. Nature *354*, 486-489.

Kee, Y., and Huibregtse, J. M. (2007). Regulation of catalytic activities of HECT ubiquitin ligases. Biochem Biophys Res Commun *354*, 329-333.

Kelleher, J. F., Mandell, M. A., Moulder, G., Hill, K. L., L'Hernault, S. W., Barstead, R., and Titus, M. A. (2000). Myosin VI is required for asymmetric segregation of cellular components during C. elegans spermatogenesis. Curr Biol *10*, 1489-1496.

Kemphues, K. J., Wolf, N., Wood, W. B., and Hirsh, D. (1986). Two loci required for cytoplasmic organization in early embryos of Caenorhabditis elegans. Dev Biol *113*, 449-460.

Kerscher, O., Felberbaum, R., and Hochstrasser, M. (2006). Modification of proteins by ubiquitin and ubiquitin-like proteins. Annu Rev Cell Dev Biol *22*, 159-180.

Ketting, R. F., and Plasterk, R. H. (2000). A genetic link between co-suppression and RNA interference in C. elegans. Nature *404*, 296-298.

Kim, E. Y., Ridgway, L. D., Zou, S., Chiu, Y. H., and Dryer, S. E. (2007a). Alternatively spliced C-terminal domains regulate the surface expression of large conductance calcium-activated potassium channels. Neuroscience *146*, 1652-1661.

Kim, H. T., Kim, K. P., Lledias, F., Kisselev, A. F., Scaglione, K. M., Skowyra, D., Gygi, S. P., and Goldberg, A. L. (2007b). Certain pairs of ubiquitin-conjugating enzymes (E2s) and ubiquitin-protein ligases (E3s) synthesize nondegradable forked ubiquitin chains containing all possible isopeptide linkages. J Biol Chem *282*, 17375-17386.

Kim, M. O., Chawla, P., Overland, R. P., Xia, E., Sadri-Vakili, G., and Cha, J. H. (2008). Altered histone monoubiquitylation mediated by mutant huntingtin induces transcriptional dysregulation. J Neurosci *28*, 3947-3957.

Kim, S. K., Lund, J., Kiraly, M., Duke, K., Jiang, M., Stuart, J. M., Eizinger, A., Wylie, B. N., and Davidson, G. S. (2001). A gene expression map for Caenorhabditis elegans. Science *293*, 2087-2092.

Kim, V. N. (2005). Small RNAs: classification, biogenesis, and function. Mol Cells *19*, 1-15.

Kimble, J. (1988). Genetic control of sex determination in the germ line of Caenorhabditis elegans. Philos Trans R Soc Lond B Biol Sci *322*, 11-18.

Kipreos, E. T. Ubiquitin-mediated pathways in C. elegans, In WormBook, T. C. e. R. Community, ed. (WormBook).

Kitagawa, R., Law, E., Tang, L., and Rose, A. M. (2002). The Cdc20 homolog, FZY-1, and its interacting protein, IFY-1, are required for proper chromosome segregation in Caenorhabditis elegans. Curr Biol *12*, 2118-2123.

Kosinski, M., McDonald, K., Schwartz, J., Yamamoto, I., and Greenstein, D. (2005). C. elegans sperm bud vesicles to deliver a meiotic maturation signal to distant oocytes. Development *132*, 3357-3369.

Krause, M., Harrison, S. W., Xu, S. Q., Chen, L., and Fire, A. (1994). Elements regulating cell- and stage-specific expression of the C. elegans MyoD family homolog hlh-1. Dev Biol *166*, 133-148.

Kroft, T. L., Gleason, E. J., and L'Hernault, S. W. (2005). The spe-42 gene is required for sperm-egg interactions during C. elegans fertilization and encodes a sperm-specific transmembrane protein. Dev Biol *286*, 169-181.

Kulka, R. G., Raboy, B., Schuster, R., Parag, H. A., Diamond, G., Ciechanover, A., and Marcus, M. (1988). A Chinese hamster cell cycle mutant arrested at G2 phase has a temperature-sensitive ubiquitin-activating enzyme, E1. J Biol Chem *263*, 15726-15731.

Kumar, P. G., Laloraya, M., Wang, C. Y., Ruan, Q. G., Davoodi-Semiromi, A., Kao, K. J., and She, J. X. (2001). The autoimmune regulator (AIRE) is a DNA-binding protein. J Biol Chem *276*, 41357-41364.

L'Hernault, S. W. Spermatogenesis, In WormBook, T. C. e. R. Community, ed. (WormBook).

L'Hernault, S. W., and Arduengo, P. M. (1992). Mutation of a putative sperm membrane protein in Caenorhabditis elegans prevents sperm differentiation but not its associated meiotic divisions. J Cell Biol *119*, 55-68.

L'Hernault, S. W., Shakes, D. C., and Ward, S. (1988). Developmental genetics of chromosome I spermatogenesis-defective mutants in the nematode Caenorhabditis elegans. Genetics *120*, 435-452.

Labouesse, M., Hartwieg, E., and Horvitz, H. R. (1996). The Caenorhabditis elegans LIN-26 protein is required to specify and/or maintain all non-neuronal ectodermal cell fates. Development *122*, 2579-2588.

Lamitina, S. T., and L'Hernault, S. W. (2002). Dominant mutations in the Caenorhabditis elegans Myt1 ortholog wee-1.3 reveal a novel domain that controls M-phase entry during spermatogenesis. Development *129*, 5009-5018.

Lamont, L. B., and Kimble, J. (2007). Developmental expression of FOG-1/CPEB protein and its control in the Caenorhabditis elegans hermaphrodite germ line. Dev Dyn *236*, 871-879.

LaMunyon, C. W., and Ward, S. (1998). Larger sperm outcompete smaller sperm in the nematode Caenorhabditis elegans. Proc Biol Sci *265*, 1997-2002.

Lee, M.-H., and Schedl, T. RNA in situ hybridization of dissected gonads, In WormBook, T. C. e. R. Community, ed. (WormBook).

Lee, T. I., and Young, R. A. (1998). Regulation of gene expression by TBP-associated proteins. Genes Dev *12*, 1398-1408.

Lee, T. V., Ding, T., Chen, Z., Rajendran, V., Scherr, H., Lackey, M., Bolduc, C., and Bergmann, A. (2008). The E1 ubiquitin-activating enzyme Uba1 in Drosophila controls apoptosis autonomously and tissue growth non-autonomously. Development *135*, 43-52.

Leggett, D. S., Hanna, J., Borodovsky, A., Crosas, B., Schmidt, M., Baker, R. T., Walz, T., Ploegh, H., and Finley, D. (2002). Multiple associated proteins regulate proteasome structure and function. Mol Cell *10*, 495-507.

Li, W., and Ye, Y. (2008). Polyubiquitin chains: functions, structures, and mechanisms. Cell Mol Life Sci.

Liao, E. H., Hung, W., Abrams, B., and Zhen, M. (2004). An SCF-like ubiquitin ligase complex that controls presynaptic differentiation. Nature *430*, 345-350.

Lin, R. (2003). A gain-of-function mutation in oma-1, a C. elegans gene required for oocyte maturation, results in delayed degradation of maternal proteins and embryonic lethality. Dev Biol *258*, 226-239.

Liu, J., Vasudevan, S., and Kipreos, E. T. (2004). CUL-2 and ZYG-11 promote meiotic anaphase II and the proper placement of the anterior-posterior axis in C. elegans. Development *131*, 3513-3525.

Lois, L. M., and Lima, C. D. (2005). Structures of the SUMO E1 provide mechanistic insights into SUMO activation and E2 recruitment to E1. Embo J *24*, 439-451.

Luitjens, C., Gallegos, M., Kraemer, B., Kimble, J., and Wickens, M. (2000). CPEB proteins control two key steps in spermatogenesis in C. elegans. Genes Dev *14*, 2596-2609.

Luz, J. G., Hassig, C. A., Pickle, C., Godzik, A., Meyer, B. J., and Wilson, I. A. (2003). XOL-1, primary determinant of sexual fate in C. elegans, is a GHMP kinase family member and a structural prototype for a class of developmental regulators. Genes Dev *17*, 977-990.

Machaca, K., DeFelice, L. J., and L'Hernault, S. W. (1996). A novel chloride channel localizes to Caenorhabditis elegans spermatids and chloride channel blockers induce spermatid differentiation. Dev Biol *176*, 1-16.

Madl, J. E., and Herman, R. K. (1979). Polyploids and sex determination in Caenorhabditis elegans. Genetics *93*, 393-402.

Maduro, M. F., Meneghini, M. D., Bowerman, B., Broitman-Maduro, G., and Rothman, J. H. (2001). Restriction of mesendoderm to a single blastomere by the combined action of SKN-1 and a GSK-3beta homolog is mediated by MED-1 and -2 in C. elegans. Mol Cell *7*, 475-485.

Martinho, R. G., Kunwar, P. S., Casanova, J., and Lehmann, R. (2004). A noncoding RNA is required for the repression of RNApolII-dependent transcription in primordial germ cells. Curr Biol *14*, 159-165.

McGrath, J. P., Jentsch, S., and Varshavsky, A. (1991). UBA 1: an essential yeast gene encoding ubiquitin-activating enzyme. Embo J *10*, 227-236.

McKay, J. P., Raizen, D. M., Gottschalk, A., Schafer, W. R., and Avery, L. (2004). eat-2 and eat-18 are required for nicotinic neurotransmission in the Caenorhabditis elegans pharynx. Genetics *166*, 161-169.

Mehta, N., Loria, P. M., and Hobert, O. (2004). A genetic screen for neurite outgrowth mutants in Caenorhabditis elegans reveals a new function for the F-box ubiquitin ligase component LIN-23. Genetics *166*, 1253-1267.

Mello, C. C., Kramer, J. M., Stinchcomb, D., and Ambros, V. (1991). Efficient gene transfer in C.elegans: extrachromosomal maintenance and integration of transforming sequences. Embo J *10*, 3959-3970.

Mello, C. C., Schubert, C., Draper, B., Zhang, W., Lobel, R., and Priess, J. R. (1996). The PIE-1 protein and germline specification in C. elegans embryos. Nature *382*, 710-712.

Miranda, T. B., and Jones, P. A. (2007). DNA methylation: the nuts and bolts of repression. J Cell Physiol *213*, 384-390.

Mitchell, M. J., Woods, D. R., Wilcox, S. A., Graves, J. A., and Bishop, C. E. (1992). Marsupial Y chromosome encodes a homologue of the mouse Y-linked candidate spermatogenesis gene Ube1y. Nature *359*, 528-531.

Morokuma, Y., Nakamura, N., Kato, A., Notoya, M., Yamamoto, Y., Sakai, Y., Fukuda, H., Yamashina, S., Hirata, Y., and Hirose, S. (2007). MARCH-XI, a novel transmembrane ubiquitin ligase implicated in ubiquitin-dependent protein sorting in developing spermatids. J Biol Chem *282*, 24806-24815.

Nair, R., Carter, P., and Rost, B. (2003). NLSdb: database of nuclear localization signals. Nucleic Acids Res *31*, 397-399.

Nakayama, K. I., and Nakayama, K. (2006). Ubiquitin ligases: cell-cycle control and cancer. Nat Rev Cancer *6*, 369-381.

Nasmyth, K., Peters, J. M., and Uhlmann, F. (2000). Splitting the chromosome: cutting the ties that bind sister chromatids. Science *288*, 1379-1385.

Nelson, G. A., Lew, K. K., and Ward, S. (1978). Intersex, a temperature-sensitive mutant of the nematode Caenorhabditis elegans. Dev Biol *66*, 386-409.

Nelson, G. A., and Ward, S. (1980). Vesicle fusion, pseudopod extension and amoeboid motility are induced in nematode spermatids by the ionophore monensin. Cell *19*, 457-464.

Nenoi, M., Ichimura, S., and Mita, K. (2000). Interspecific comparison in the frequency of concerted evolution at the polyubiquitin gene locus. J Mol Evol *51*, 161-165.

Odorisio, T., Mahadevaiah, S. K., McCarrey, J. R., and Burgoyne, P. S. (1996). Transcriptional analysis of the candidate spermatogenesis gene Ube1y and of the closely related Ube1x shows that they are coexpressed in spermatogonia and spermatids but are repressed in pachytene spermatocytes. Dev Biol *180*, 336-343.

Okazaki, K., Okayama, H., and Niwa, O. (2000). The polyubiquitin gene is essential for meiosis in fission yeast. Exp Cell Res *254*, 143-152.

Ozkaynak, E., Finley, D., and Varshavsky, A. (1984). The yeast ubiquitin gene: head-to-tail repeats encoding a polyubiquitin precursor protein. Nature *312*, 663-666.

Page, B. D., Diede, S. J., Tenlen, J. R., and Ferguson, E. L. (2007). EEL-1, a Hect E3 ubiquitin ligase, controls asymmetry and persistence of the SKN-1 transcription factor in the early C. elegans embryo. Development *134*, 2303-2314.

Page, B. D., Zhang, W., Steward, K., Blumenthal, T., and Priess, J. R. (1997). ELT-1, a GATA-like transcription factor, is required for epidermal cell fates in Caenorhabditis elegans embryos. Genes Dev *11*, 1651-1661.

Park, Y., Moon, Y., and Chung, H. Y. (2003). AIRE-1 (autoimmune regulator type 1) as a regulator of the thymic induction of negative selection. Ann N Y Acad Sci *1005*, 431-435.

Perry, M. D., Li, W., Trent, C., Robertson, B., Fire, A., Hageman, J. M., and Wood, W. B. (1993). Molecular characterization of the her-1 gene suggests a direct role in cell signaling during Caenorhabditis elegans sex determination. Genes Dev *7*, 216-228.

Petroski, M. D., and Deshaies, R. J. (2005). Function and regulation of cullin-RING ubiquitin ligases. Nat Rev Mol Cell Biol *6*, 9-20.

Pickart, C. M., and Rose, I. A. (1985). Functional heterogeneity of ubiquitin carrier proteins. J Biol Chem *260*, 1573-1581.

Pintard, L., Willis, J. H., Willems, A., Johnson, J. L., Srayko, M., Kurz, T., Glaser, S., Mains, P. E., Tyers, M., Bowerman, B., and Peter, M. (2003). The BTB protein MEL-26 is a substrate-specific adaptor of the CUL-3 ubiquitin-ligase. Nature *425*, 311-316.

Pique, M., Lopez, J. M., Foissac, S., Guigo, R., and Mendez, R. (2008). A combinatorial code for CPE-mediated translational control. Cell *132*, 434-448.

Powell, J. R., Jow, M. M., and Meyer, B. J. (2005). The T-box transcription factor SEA-1 is an autosomal element of the X:A signal that determines C. elegans sex. Dev Cell *9*, 339-349.

Rappleye, C. A., Tagawa, A., Lyczak, R., Bowerman, B., and Aroian, R. V. (2002). The anaphase-promoting complex and separin are required for embryonic anterior-posterior axis formation. Dev Cell *2*, 195-206.

Rechsteiner, M. (1987). Ubiquitin-mediated pathways for intracellular proteolysis. Annu Rev Cell Biol *3*, 1-30.

Reece-Hoyes, J. S., Deplancke, B., Shingles, J., Grove, C. A., Hope, I. A., and Walhout, A. J. (2005). A compendium of Caenorhabditis elegans regulatory transcription factors: a resource for mapping transcription regulatory networks. Genome Biol *6*, R110.

Reinke, V., Gil, I. S., Ward, S., and Kazmer, K. (2004). Genome-wide germline-enriched and sex-biased expression profiles in Caenorhabditis elegans. Development *131*, 311-323.

Reinke, V., Smith, H. E., Nance, J., Wang, J., Van Doren, C., Begley, R., Jones, S. J., Davis, E. B., Scherer, S., Ward, S., and Kim, S. K. (2000). A global profile of germline gene expression in C. elegans. Mol Cell *6*, 605-616.

Reiss, Y., Heller, H., and Hershko, A. (1989). Binding sites of ubiquitin-protein ligase. Binding of ubiquitin-protein conjugates and of ubiquitin-carrier protein. J Biol Chem *264*, 10378-10383.

Richter, J. D. (2007). CPEB: a life in translation. Trends Biochem Sci *32*, 279-285.

Roberts, T. M., Pavalko, F. M., and Ward, S. (1986). Membrane and cytoplasmic proteins are transported in the same organelle complex during nematode spermatogenesis. J Cell Biol *102*, 1787-1796.

Roberts, T. M., and Ward, S. (1982). Centripetal flow of pseudopodial surface components could propel the amoeboid movement of Caenorhabditis elegans spermatozoa. J Cell Biol *92*, 132-138.

Ross, J. M., Kalis, A. K., Murphy, M. W., and Zarkower, D. (2005). The DM domain protein MAB-3 promotes sex-specific neurogenesis in C. elegans by regulating bHLH proteins. Dev Cell *8*, 881-892.

Roy, P. J., Stuart, J. M., Lund, J., and Kim, S. K. (2002). Chromosomal clustering of muscle-expressed genes in Caenorhabditis elegans. Nature *418*, 975-979.

Salvat, C., Acquaviva, C., Scheffner, M., Robbins, I., Piechaczyk, M., and Jariel-Encontre, I. (2000). Molecular characterization of the thermosensitive E1 ubiquitin-activating enzyme cell mutant A31N-ts20. Requirements upon different levels of E1 for the ubiquitination/degradation of the various protein substrates in vivo. Eur J Biochem *267*, 3712-3722.

Sasagawa, Y., Yamanaka, K., and Ogura, T. (2007). ER E3 ubiquitin ligase HRD-1 and its specific partner chaperone BiP play important roles in ERAD and developmental growth in Caenorhabditis elegans. Genes Cells *12*, 1063-1073.

Savage, C., Das, P., Finelli, A. L., Townsend, S. R., Sun, C. Y., Baird, S. E., and Padgett, R. W. (1996). Caenorhabditis elegans genes sma-2, sma-3, and sma-4 define a conserved family of transforming growth factor beta pathway components. Proc Natl Acad Sci U S A *93*, 790-794.

Sawada, H., Sakai, N., Abe, Y., Tanaka, E., Takahashi, Y., Fujino, J., Kodama, E., Takizawa, S., and Yokosawa, H. (2002). Extracellular ubiquitination and proteasome-mediated degradation of the ascidian sperm receptor. Proc Natl Acad Sci U S A *99*, 1223-1228.

Schaefer, H., and Rongo, C. (2006). KEL-8 is a substrate receptor for CUL3-dependent ubiquitin ligase that regulates synaptic glutamate receptor turnover. Mol Biol Cell *17*, 1250-1260.

Scheffner, M., Nuber, U., and Huibregtse, J. M. (1995). Protein ubiquitination involving an E1-E2-E3 enzyme ubiquitin thioester cascade. Nature *373*, 81-83.

Scheffner, M., Smith, S., and Jentsch, S. (1998). The ubiquitin-conjugation system. (New York: Plenum Press).

Schnell, J. D., and Hicke, L. (2003). Non-traditional functions of ubiquitin and ubiquitin-binding proteins. J Biol Chem *278*, 35857-35860.

Schvarzstein, M., and Spence, A. M. (2006). The C. elegans sex-determining GLI protein TRA-1A is regulated by sex-specific proteolysis. Dev Cell *11*, 733-740.

Schwartz, D. C., and Hochstrasser, M. (2003). A superfamily of protein tags: ubiquitin, SUMO and related modifiers. Trends Biochem Sci *28*, 321-328.

Schwartz, H. T., and Horvitz, H. R. (2007). The C. elegans protein CEH-30 protects male-specific neurons from apoptosis independently of the Bcl-2 homolog CED-9. Genes Dev *21*, 3181-3194.

Segal, S. P., Graves, L. E., Verheyden, J., and Goodwin, E. B. (2001). RNA-Regulated TRA-1 nuclear export controls sexual fate. Dev Cell *1*, 539-551.

Setoyama, D., Yamashita, M., and Sagata, N. (2007). Mechanism of degradation of CPEB during Xenopus oocyte maturation. Proc Natl Acad Sci U S A *104*, 18001-18006.

Seydoux, G., and Braun, R. E. (2006). Pathway to totipotency: lessons from germ cells. Cell *127*, 891-904.

Seydoux, G., and Dunn, M. A. (1997). Transcriptionally repressed germ cells lack a subpopulation of phosphorylated RNA polymerase II in early embryos of Caenorhabditis elegans and Drosophila melanogaster. Development *124*, 2191-2201.

Seydoux, G., and Fire, A. (1994). Soma-germline asymmetry in the distributions of embryonic RNAs in Caenorhabditis elegans. Development *120*, 2823-2834.

Seydoux, G., Mello, C. C., Pettitt, J., Wood, W. B., Priess, J. R., and Fire, A. (1996). Repression of gene expression in the embryonic germ lineage of C. elegans. Nature *382*, 713-716.

Shakes, D. C., Sadler, P. L., Schumacher, J. M., Abdolrasulnia, M., and Golden, A. (2003). Developmental defects observed in hypomorphic anaphase-promoting complex mutants are linked to cell cycle abnormalities. Development *130*, 1605-1620.

Shakes, D. C., and Ward, S. (1989a). Initiation of spermiogenesis in C. elegans: a pharmacological and genetic analysis. Dev Biol *134*, 189-200.

Shakes, D. C., and Ward, S. (1989b). Mutations that disrupt the morphogenesis and localization of a sperm-specific organelle in Caenorhabditis elegans. Dev Biol *134*, 307-316.

Shen, M. M., and Hodgkin, J. (1988). mab-3, a gene required for sex-specific yolk protein expression and a male-specific lineage in C. elegans. Cell *54*, 1019-1031.

Shimada, M., Kanematsu, K., Tanaka, K., Yokosawa, H., and Kawahara, H. (2006). Proteasomal ubiquitin receptor RPN-10 controls sex determination in Caenorhabditis elegans. Mol Biol Cell *17*, 5356-5371.

Siepmann, T. J., Bohnsack, R. N., Tokgoz, Z., Baboshina, O. V., and Haas, A. L. (2003). Protein interactions within the N-end rule ubiquitin ligation pathway. J Biol Chem *278*, 9448-9457.

Singson, A., Hill, K. L., and L'Hernault, S. W. (1999). Sperm competition in the absence of fertilization in Caenorhabditis elegans. Genetics *152*, 201-208.

Slack, F. J., Basson, M., Liu, Z., Ambros, V., Horvitz, H. R., and Ruvkun, G. (2000). The lin-41 RBCC gene acts in the C. elegans heterochronic pathway between the let-7 regulatory RNA and the LIN-29 transcription factor. Mol Cell *5*, 659-669.

Smith, J. A., McGarr, P., and Gilleard, J. S. (2005). The Caenorhabditis elegans GATA factor elt-1 is essential for differentiation and maintenance of hypodermal seam cells and for normal locomotion. J Cell Sci *118*, 5709-5719.

Snee, M., Benz, D., Jen, J., and Macdonald, P. M. (2008). Two distinct domains of Bruno bind specifically to the oskar mRNA. RNA Biol *5*.

Sonneville, R., and Gonczy, P. (2004). Zyg-11 and cul-2 regulate progression through meiosis II and polarity establishment in C. elegans. Development *131*, 3527-3543.

Sonnichsen, B., Koski, L. B., Walsh, A., Marschall, P., Neumann, B., Brehm, M., Alleaume, A. M., Artelt, J., Bettencourt, P., Cassin, E.*, et al.* (2005). Full-genome RNAi profiling of early embryogenesis in Caenorhabditis elegans. Nature *434*, 462-469.

Soustelle, L., Roy, N., Ragone, G., and Giangrande, A. (2008). Control of gcm RNA stability is necessary for proper glial cell fate acquisition. Mol Cell Neurosci *37*, 657-662.

Standart, N., and Jackson, R. J. (2007). MicroRNAs repress translation of m7Gppp-capped target mRNAs in vitro by inhibiting initiation and promoting deadenylation. Genes Dev *21*, 1975-1982.

Starostina, N. G., Lim, J. M., Schvarzstein, M., Wells, L., Spence, A. M., and Kipreos, E. T. (2007). A CUL-2 ubiquitin ligase containing three FEM proteins degrades TRA-1 to regulate C. elegans sex determination. Dev Cell *13*, 127-139.

Stephen, A. G., Trausch-Azar, J. S., Ciechanover, A., and Schwartz, A. L. (1996). The ubiquitin-activating enzyme E1 is phosphorylated and localized to the nucleus in a cell cycle-dependent manner. J Biol Chem *271*, 15608-15614.

Stephen, A. G., Trausch-Azar, J. S., Handley-Gearhart, P. M., Ciechanover, A., and Schwartz, A. L. (1997). Identification of a region within the ubiquitin-activating enzyme required for nuclear targeting and phosphorylation. J Biol Chem *272*, 10895-10903.

Subramanian, L., Benson, M. D., and Iniguez-Lluhi, J. A. (2003). A synergy control motif within the attenuator domain of CCAAT/enhancer-binding protein alpha inhibits transcriptional synergy through its PIASy-enhanced modification by SUMO-1 or SUMO-3. J Biol Chem *278*, 9134-9141.

Sulston, J. E., and Horvitz, H. R. (1977). Post-embryonic cell lineages of the nematode, Caenorhabditis elegans. Dev Biol *56*, 110-156.

Sulston, J. E., Schierenberg, E., White, J. G., and Thomson, J. N. (1983). The embryonic cell lineage of the nematode Caenorhabditis elegans. Dev Biol *100*, 64-119.

Sung, P., Berleth, E., Pickart, C., Prakash, S., and Prakash, L. (1991). Yeast RAD6 encoded ubiquitin conjugating enzyme mediates protein degradation dependent on the N-end-recognizing E3 enzyme. Embo J *10*, 2187-2193.

Surdo, P. L., Bottomley, M. J., Sattler, M., and Scheffzek, K. (2003). Crystal structure and nuclear magnetic resonance analyses of the SAND domain from glucocorticoid modulatory element binding protein-1 reveals deoxyribonucleic acid and zinc binding regions. Mol Endocrinol *17*, 1283-1295.

Sutovsky, P., Moreno, R., Ramalho-Santos, J., Dominko, T., Thompson, W. E., and Schatten, G. (2001). A putative, ubiquitin-dependent mechanism for the recognition and elimination of defective spermatozoa in the mammalian epididymis. J Cell Sci *114*, 1665-1675.

Suzuki, Y., Yandell, M. D., Roy, P. J., Krishna, S., Savage-Dunn, C., Ross, R. M., Padgett, R. W., and Wood, W. B. (1999). A BMP homolog acts as a dose-dependent regulator of body size and male tail patterning in Caenorhabditis elegans. Development *126*, 241-250.

Swanson, R., and Hochstrasser, M. (2000). A viable ubiquitin-activating enzyme mutant for evaluating ubiquitin system function in Saccharomyces cerevisiae. FEBS Lett *477*, 193-198.

Tenenhaus, C., Schubert, C., and Seydoux, G. (1998). Genetic requirements for PIE-1 localization and inhibition of gene expression in the embryonic germ lineage of Caenorhabditis elegans. Dev Biol *200*, 212-224.

Teng, F. Y., and Tang, B. L. (2005). APC/C regulation of axonal growth and synaptic functions in postmitotic neurons: the Liprin-alpha connection. Cell Mol Life Sci *62*, 1571-1578.

Tenlen, J. R., Schisa, J. A., Diede, S. J., and Page, B. D. (2006). Reduced dosage of pos-1 suppresses Mex mutants and reveals complex interactions among CCCH zinc-finger proteins during Caenorhabditis elegans embryogenesis. Genetics *174*, 1933-1945.

Thrower, J. S., Hoffman, L., Rechsteiner, M., and Pickart, C. M. (2000). Recognition of the polyubiquitin proteolytic signal. Embo J *19*, 94-102.

Timmons, L., and Fire, A. (1998). Specific interference by ingested dsRNA. Nature *395*, 854.

Trausch, J. S., Grenfell, S. J., Handley-Gearhart, P. M., Ciechanover, A., and Schwartz, A. L. (1993). Immunofluorescent localization of the ubiquitin-activating enzyme, E1, to the nucleus and cytoskeleton. Am J Physiol *264*, C93-102.

Varkey, J. P., Muhlrad, P. J., Minniti, A. N., Do, B., and Ward, S. (1995). The Caenorhabditis elegans spe-26 gene is necessary to form spermatids and encodes a protein similar to the actin-associated proteins kelch and scruin. Genes Dev *9*, 1074-1086.

Vermeirssen, V., Barrasa, M. I., Hidalgo, C. A., Babon, J. A., Sequerra, R., Doucette-Stamm, L., Barabasi, A. L., and Walhout, A. J. (2007). Transcription factor modularity in a gene-centered C. elegans core neuronal protein-DNA interaction network. Genome Res *17*, 1061-1071.

Walden, H., Podgorski, M. S., and Schulman, B. A. (2003). Insights into the ubiquitin transfer cascade from the structure of the activating enzyme for NEDD8. Nature *422*, 330-334.

Walker, A. K., Boag, P. R., and Blackwell, T. K. (2007). Transcription reactivation steps stimulated by oocyte maturation in C. elegans. Dev Biol *304*, 382-393.

Ward, S., Argon, Y., and Nelson, G. A. (1981). Sperm morphogenesis in wild-type and fertilization-defective mutants of Caenorhabditis elegans. J Cell Biol *91*, 26-44.

Ward, S., and Carrel, J. S. (1979). Fertilization and sperm competition in the nematode Caenorhabditis elegans. Dev Biol *73*, 304-321.

Ward, S., Hogan, E., and Nelson, G. A. (1983). The initiation of spermiogenesis in the nematode Caenorhabditis elegans. Dev Biol *98*, 70-79.

Ward, S., and Klass, M. (1982). The location of the major protein in Caenorhabditis elegans sperm and spermatocytes. Dev Biol *92*, 203-208.

Ward, S., Roberts, T. M., Strome, S., Pavalko, F. M., and Hogan, E. (1986). Monoclonal antibodies that recognize a polypeptide antigenic determinant shared by multiple Caenorhabditis elegans sperm-specific proteins. J Cell Biol *102*, 1778-1786.

Weissman, A. M. (2001). Themes and variations on ubiquitylation. Nat Rev Mol Cell Biol *2*, 169-178.

Wiborg, O., Pedersen, M. S., Wind, A., Berglund, L. E., Marcker, K. A., and Vuust, J. (1985). The human ubiquitin multigene family: some genes contain multiple directly repeated ubiquitin coding sequences. Embo J *4*, 755-759.

Wicks, S. R., Yeh, R. T., Gish, W. R., Waterston, R. H., and Plasterk, R. H. (2001). Rapid gene mapping in Caenorhabditis elegans using a high density polymorphism map. Nat Genet *28*, 160-164.

Williamson, A., and Lehmann, R. (1996). Germ cell development in Drosophila. Annu Rev Cell Dev Biol *12*, 365-391.

Wojciak, J. M., and Clubb, R. T. (2001). Finding the function buried in SAND. Nat Struct Biol *8*, 568-570.

Wolf, N., Hirsh, D., and McIntosh, J. R. (1978). Spermatogenesis in males of the free-living nematode, Caenorhabditis elegans. J Ultrastruct Res *63*, 155-169.

Xu, L., Wei, Y., Reboul, J., Vaglio, P., Shin, T. H., Vidal, M., Elledge, S. J., and Harper, J. W. (2003). BTB proteins are substrate-specific adaptors in an SCF-like modular ubiquitin ligase containing CUL-3. Nature *425*, 316-321.

Xu, X. Z., and Sternberg, P. W. (2003). A C. elegans sperm TRP protein required for sperm-egg interactions during fertilization. Cell *114*, 285-297.

Yanai, I., Baugh, L. R., Smith, J. J., Roehrig, C., Shen-Orr, S. S., Claggett, J. M., Hill, A. A., Slonim, D. K., and Hunter, C. P. (2008). Pairing of competitive and topologically distinct regulatory modules enhances patterned gene expression. Mol Syst Biol *4*, 163.

Yang, F., Vought, B. W., Satterlee, J. S., Walker, A. K., Jim Sun, Z. Y., Watts, J. L., DeBeaumont, R., Saito, R. M., Hyberts, S. G., Yang, S.*, et al.* (2006). An

ARC/Mediator subunit required for SREBP control of cholesterol and lipid homeostasis. Nature *442*, 700-704.

Yi, W., Ross, J. M., and Zarkower, D. (2000). Mab-3 is a direct tra-1 target gene regulating diverse aspects of C. elegans male sexual development and behavior. Development *127*, 4469-4480.

Yokota, N., and Sawada, H. (2007). Sperm proteasomes are responsible for the acrosome reaction and sperm penetration of the vitelline envelope during fertilization of the sea urchin Pseudocentrotus depressus. Dev Biol *308*, 222-231.

Zacksenhaus, E., Sheinin, R., and Wang, H. S. (1990). Localization of the human A1S9 gene complementing the ts A1S9 mouse L-cell defect in DNA replication and cell cycle progression to Xp11.2----p11.4. Cytogenet Cell Genet *53*, 20-22.

Zarkower, D. Somatic sex determination, In WormBook, T. C. e. R. Community, ed. (WormBook).

Zarkower, D., and Hodgkin, J. (1992). Molecular analysis of the C. elegans sex-determining gene tra-1: a gene encoding two zinc finger proteins. Cell *70*, 237-249.

Zhang, F., Barboric, M., Blackwell, T. K., and Peterlin, B. M. (2003). A model of repression: CTD analogs and PIE-1 inhibit transcriptional elongation by P-TEFb. Genes Dev *17*, 748-758.

Zhao, C., Beaudenon, S. L., Kelley, M. L., Waddell, M. B., Yuan, W., Schulman, B. A., Huibregtse, J. M., and Krug, R. M. (2004). The UbcH8 ubiquitin E2 enzyme is also the E2 enzyme for ISG15, an IFN-alpha/beta-induced ubiquitin-like protein. Proc Natl Acad Sci U S A *101*, 7578-7582.

Zhu, G. D., and L'Hernault, S. W. (2003). The Caenorhabditis elegans spe-39 gene is required for intracellular membrane reorganization during spermatogenesis. Genetics *165*, 145-157.

Zhu, H., Zhou, Z. M., Huo, R., Huang, X. Y., Lu, L., Lin, M., Wang, L. R., Zhou, Y. D., Li, J. M., and Sha, J. H. (2004). Identification and characteristics of a novel E1 like gene nUBE1L in human testis. Acta Biochim Biophys Sin (Shanghai) *36*, 227-234.